

LOAN DOCUMENT

PHOTOGRAPH THIS SHEET

DTIC ACCESSION NUMBER

LEVEL

INVENTORY

WL-TR-96-2095

DOCUMENT IDENTIFICATION

DISTRIBUTION STATEMENT A

Approved for public release
Distribution Unlimited

DISTRIBUTION STATEMENT

ACCESSIONED BY	GRAN	<input checked="" type="checkbox"/>
NTIS	GRAN	<input type="checkbox"/>
DTIC	TRAC	<input type="checkbox"/>
UNANNOUNCED		
JUSTIFICATION		
<hr/>		
<hr/>		
<hr/>		
BY		
DISTRIBUTION/		
AVAILABILITY CODES		
DISTRIBUTION	AVAILABILITY AND/OR SPECIAL	
<hr/>	<hr/>	<hr/>
A-1	<hr/>	<hr/>

DISTRIBUTION STAMP

DATA OWNERSHIP TRANSFERRED

H
A
N
D
L
E

W
I
T
H

C
A
R
E

DATE ACCESSIONED

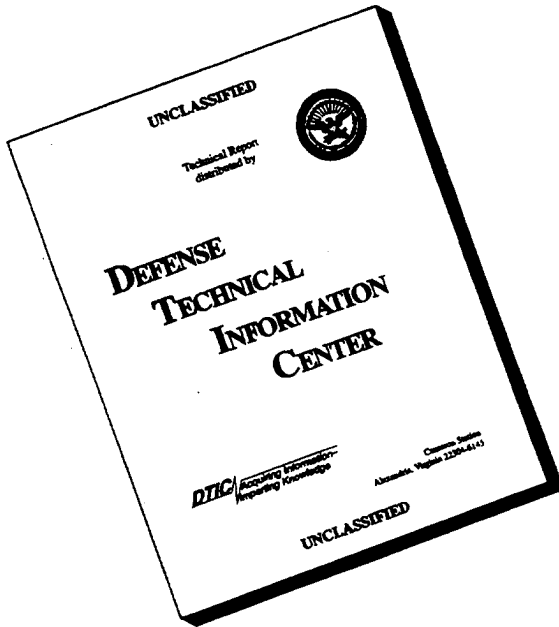
DATE RETURNED

DATE RECEIVED IN DTIC

REGISTERED OR CERTIFIED NUMBER

PHOTOGRAPH THIS SHEET AND RETURN TO DTIC-FDAC

DISCLAIMER NOTICE



**THIS DOCUMENT IS BEST
QUALITY AVAILABLE. THE
COPY FURNISHED TO DTIC
CONTAINED A SIGNIFICANT
NUMBER OF PAGES WHICH DO
NOT REPRODUCE LEGIBLY.**

WL-TR-96-2095

**AERO-THERMAL CASCADE TUNNEL
FLOW QUALITY: TURBULENCE
GENERATION AND PREDICTION**



**John Duncan
Kristin Petersen**

29 NOVEMBER 1995

FINAL REPORT 1 NOVEMBER 1995--9 JULY 1996

Approved for public release; distribution unlimited

**AERO PROPULSION & POWER DIRECTORATE
WRIGHT LABORATORY
AIR FORCE MATERIEL COMMAND
WRIGHT-PATTERSON AIR FORCE BASE, OH 45433-7650**

This paper is declared a work of the U.S. Government and as such is not subject to copyright protection in the United States

REPORT DOCUMENTATION PAGE

Form Approved
OMB No. 0704-0188

Public reporting burden for this collection of information is estimated to average 1 hour per response, including the time for reviewing instructions, searching existing data sources, gathering and maintaining the data needed, and completing and reviewing the collection of information. Send comments regarding this burden estimate or any other aspect of this collection of information, including suggestions for reducing this burden, to Washington Headquarters Services, Directorate for Information Operations and Reports, 1215 Jefferson Davis Highway, Suite 1204, Arlington, VA 22202-4302, and to the Office of Management and Budget, Paperwork Reduction Project (0704-0188), Washington, DC 20503.

1. AGENCY USE ONLY (Leave blank)			2. REPORT DATE 29 November 1995		3. REPORT TYPE AND DATES COVERED Final 1 Nov 95 - 9 Jul 96		
4. TITLE AND SUBTITLE Aero-Thermal Cascade Tunnel Flow Quality: Turbulence Generation and Prediction			5. FUNDING NUMBERS PE 61102F JON 2307S315				
6. AUTHOR(S) John Duncan, Kristin Petersen							
7. PERFORMING ORGANIZATION NAME(S) AND ADDRESS(ES) Aero Propulsion & Power Directorate Wright Laboratory Air Force Materiel Command Wright-Patterson Air Force Base, OH 45433-7650			8. PERFORMING ORGANIZATION REPORT NUMBER				
9. SPONSORING/MONITORING AGENCY NAME(S) AND ADDRESS(ES) Aero Propulsion & Power Directorate Wright Laboratory Air Force Materiel Command Wright-Patterson Air Force Base, OH 45433-7650 POC: Richard B Rivir, WL/POTT, 513-255-5132			10. SPONSORING/MONITORING AGENCY REPORT NUMBER WL-TR-96-2095				
11. SUPPLEMENTARY NOTES							
12a. DISTRIBUTION / AVAILABILITY STATEMENT APPROVED FOR PUBLIC RELEASE; DISTRIBUTION IS UNLIMITED				12b. DISTRIBUTION CODE			
13. ABSTRACT (Maximum 200 words) Turbine blade temperatures in modern turbine engines are the limiting factor in the advancement of aircraft propulsion today. One reason for the blades' thermal stress failure has to do with the traverse effects of turbulent flow over the blades--the more turbulence in the flow, the greater the heat transfer to the blade. Of concern here are both freestream and boundary layer turbulence. Therefore, the focus of much research today is on studying turbine blade models with post-burner turbulent flow conditions in order to design and build blades around the predicted failure levels and coordinates. The focus of this paper is on the generation of the turbulence characteristics which will be necessary for use in cascade wind tunnel facilities. Methods of turbulence generation and turbulence trends are analyzed with the main parameter being turbulence intensity variation with both lateral and streamwise location. The results presented here are a complete turbulent flow field description for a turbulence generation method, supporting the "air off" grid configuration as ready for use and research while demanding revision of the "air on" high turbulence generation method.							
14. SUBJECT TERMS					15. NUMBER OF PAGES 94		
					16. PRICE CODE		
17. SECURITY CLASSIFICATION OF REPORT UNCLASSIFIED		18. SECURITY CLASSIFICATION OF THIS PAGE UNCLASSIFIED		19. SECURITY CLASSIFICATION OF ABSTRACT UNCLASSIFIED		20. LIMITATION OF ABSTRACT SAR	

GENERAL INSTRUCTIONS FOR COMPLETING SF 298

The Report Documentation Page (RDP) is used in announcing and cataloging reports. It is important that this information be consistent with the rest of the report, particularly the cover and title page. Instructions for filling in each block of the form follow. It is important to stay *within the lines* to meet optical scanning requirements.

Block 1. Agency Use Only (Leave blank).

Block 2. Report Date. Full publication date including day, month, and year, if available (e.g. 1 Jan 88). Must cite at least the year.

Block 3. Type of Report and Dates Covered.

State whether report is interim, final, etc. If applicable, enter inclusive report dates (e.g. 10 Jun 87 - 30 Jun 88).

Block 4. Title and Subtitle. A title is taken from the part of the report that provides the most meaningful and complete information. When a report is prepared in more than one volume, repeat the primary title, add volume number, and include subtitle for the specific volume. On classified documents enter the title classification in parentheses.

Block 5. Funding Numbers. To include contract and grant numbers; may include program element number(s), project number(s), task number(s), and work unit number(s). Use the following labels:

C - Contract	PR - Project
G - Grant	TA - Task
PE - Program Element	WU - Work Unit
	Accession No.

Block 6. Author(s). Name(s) of person(s) responsible for writing the report, performing the research, or credited with the content of the report. If editor or compiler, this should follow the name(s).

Block 7. Performing Organization Name(s) and Address(es). Self-explanatory.

Block 8. Performing Organization Report Number. Enter the unique alphanumeric report number(s) assigned by the organization performing the report.

Block 9. Sponsoring/Monitoring Agency Name(s) and Address(es). Self-explanatory.

Block 10. Sponsoring/Monitoring Agency Report Number. (If known)

Block 11. Supplementary Notes. Enter information not included elsewhere such as: Prepared in cooperation with...; Trans. of...; To be published in.... When a report is revised, include a statement whether the new report supersedes or supplements the older report.

Block 12a. Distribution/Availability Statement.

Denotes public availability or limitations. Cite any availability to the public. Enter additional limitations or special markings in all capitals (e.g. NOFORN, REL, ITAR).

DOD - See DoDD 5230.24, "Distribution Statements on Technical Documents."

DOE - See authorities.

NASA - See Handbook NHB 2200.2.

NTIS - Leave blank.

Block 12b. Distribution Code.

DOD - Leave blank.

DOE - Enter DOE distribution categories from the Standard Distribution for Unclassified Scientific and Technical Reports.

NASA - Leave blank.

NTIS - Leave blank.

Block 13. Abstract. Include a brief (*Maximum 200 words*) factual summary of the most significant information contained in the report.

Block 14. Subject Terms. Keywords or phrases identifying major subjects in the report.

Block 15. Number of Pages. Enter the total number of pages.

Block 16. Price Code. Enter appropriate price code (*NTIS only*).

Blocks 17. - 19. Security Classifications. Self-explanatory. Enter U.S. Security Classification in accordance with U.S. Security Regulations (i.e., UNCLASSIFIED). If form contains classified information, stamp classification on the top and bottom of the page.

Block 20. Limitation of Abstract. This block must be completed to assign a limitation to the abstract. Enter either UL (unlimited) or SAR (same as report). An entry in this block is necessary if the abstract is to be limited. If blank, the abstract is assumed to be unlimited.

Objective:

This research experimentally characterizes turbulent flow produced with an upstream turbulence generation grid in the USAF Academy Aero-thermal Cascade Facility. A full characterization of flow quality in this case consists of (a) planar velocity and turbulence intensity mapping, and (b) streamwise variations in turbulence intensity and length scales. In application, a desired flow quality, for subsequent turbulent flow heat transfer experiments, can be reproduced based on the computational data trends and tunnel/grid specific flow variations detailed here. Results from the current experiments will also help in the improvement of turbulence grid design and as a comparison for existing turbulent flow CFD codes and equations, such as the linear Roach correlation for turbulence intensity and decay rate.

All flow quality relationships are analyzed with respect to whether or not the grid air jets (pressurized air injected from the grid points across the freestream flow) are on or off, and using both mean and centerline values where appropriate.

Background:

The research done here will contribute to a better knowledge of how to generate and predict turbulence. The conditions researched here, based on Reynolds number similarity ($Re \approx 10^4$), allows direct application of the results in modeling low pressure (3rd-4th stage) turbine blades which are typically around 10-20% turbulence intensity. More importantly, the turbulence is directly related to the heat transfer coefficient of the blades, based on an understanding of basic thermodynamics and quantified by the equation:

$$h = \frac{q}{(T_{srr} - T_{surf})}$$

Heat transfer coefficient, h , (dependent on T_{surf}) changes, however, based on turbulence. The prerequisite, then, is adequate turbulent flow test conditions. Turbulence vortex intensities and their decay rates, and macroscopic length scales will be the main interest in the turbulence characterization. These parameters are the most helpful in visualizing the strength (energy) and size of the eddies present in the flow. Variation in these parameters is dependent primarily on distance from the turbulence

	UCDavis	USAF Academy
Operation	Open Loop	Closed Loop
Axial Chord (B_x)	0.171 m	0.166 m
Blade Pitch (p)	.159 m	.196 m
Pitch/Axial Chord	.93	1.18
Span/Axial Chord	3.56	3.97
Inlet Camber Angle	44°	46.5°
Exit Camber Angle	26°	23.5°
Air Inlet Angle (B_z)	44.7°	49°
Air Exit Angle (B_z)	26°	23.5°
Grid	Perpendicular to free-stream	Parallel to cascade
Turbulence (clean,grid)	1% 10%	.5% 9%
Re (clean,grid)	144,000 134,000	110,000 110,000

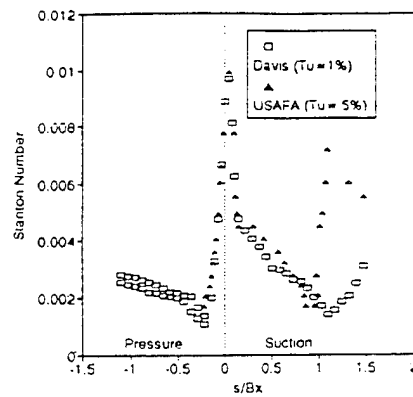


FIGURE 6. UCDAVIS ($Re=144K$) AND USAFA ($Re=110K$) RESULTS AT LOW TURBULENCE

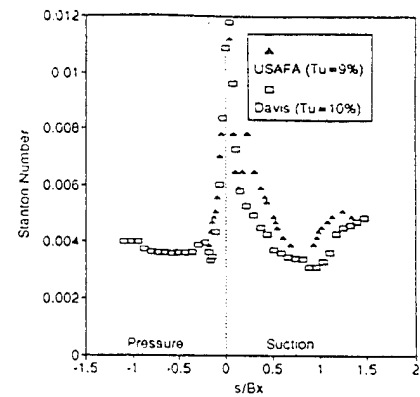


FIGURE 7. UCDAVIS ($Re=134K$) AND USAFA ($Re=110K$) RESULTS AT HIGHER TURBULENCE

Figure 1. USAFA and UCDavis Turbulent Flow Results Comparison

(Taken from Baughn, et al, "An Experimental Investigation of Heat Transfer, Transition, and Separation on Turbine Blades at Low Reynolds Number and High Turbulence Intensity")

Cascade tunnel results have sometimes been scrutinized for the inability of the tunnel to model rotational flow, spanwise flow, and sequential blade array effects characteristic of a rotating turbine spool. However, the analysis done in the above cascade experiments showed that both sets of data compared favorably to actual rotational data (Baughn 13).

Expected Results/Theory:

The data collected will allow two things to be done. The first is to characterize turbulent flow at various x, y , and z positions away from the grid. This, in turn, will allow predictions concerning such things as the point turbulence intensities, vortex decay rates, turbulence length scales,

correlation factors from statistics software become the means of deducing the length scale. The equation used for the macro length scale is:

$$\Omega = \bar{u} \int_0^{\infty} R(t) dt$$

where the integral is just the area under the correlation curve as the correlation factor R goes from 1 to 0.

Microscopic length scales can be described as those smaller eddies "peeling off" of the major eddy due to shear boundary layer effects between the eddy flow and freestream flow. These micro length scales are the means by which the macro length scale loses energy to the surrounding flow. They can be visualized as minor vortices within a major vortex. The micro length scale is a less descriptive parameter than the macro scale in the scope of this study, but is useful because of its dependence on and description of turbulence eddy and surrounding flow energy difference, not solely a function of the turbulence generation method itself. The equation for microscopic length scale is

$$\lambda = \sqrt{\frac{[-2\bar{u}^2]}{[\partial^2 R / \partial t^2]_{t=0}}}$$

where the denominator can be represented as

$$[\partial^2 R / \partial t^2]_{t=0} = \frac{R_{t=1} + R_{t=-1} - 2R_{t=0}}{\Delta t^2}$$

In words, the micro scale can be mathematically represented according to the slope of the correlation curve at time=0 (Essentially, the initial correlation or macro length scale decay rate).

Other data reduction calculations performed by spreadsheet from HP raw data include Pitot tube velocity from total and static pressures from the incompressible Bernoulli equation,

$$V = \sqrt{\frac{2T_s R \Delta P}{Patm}}$$

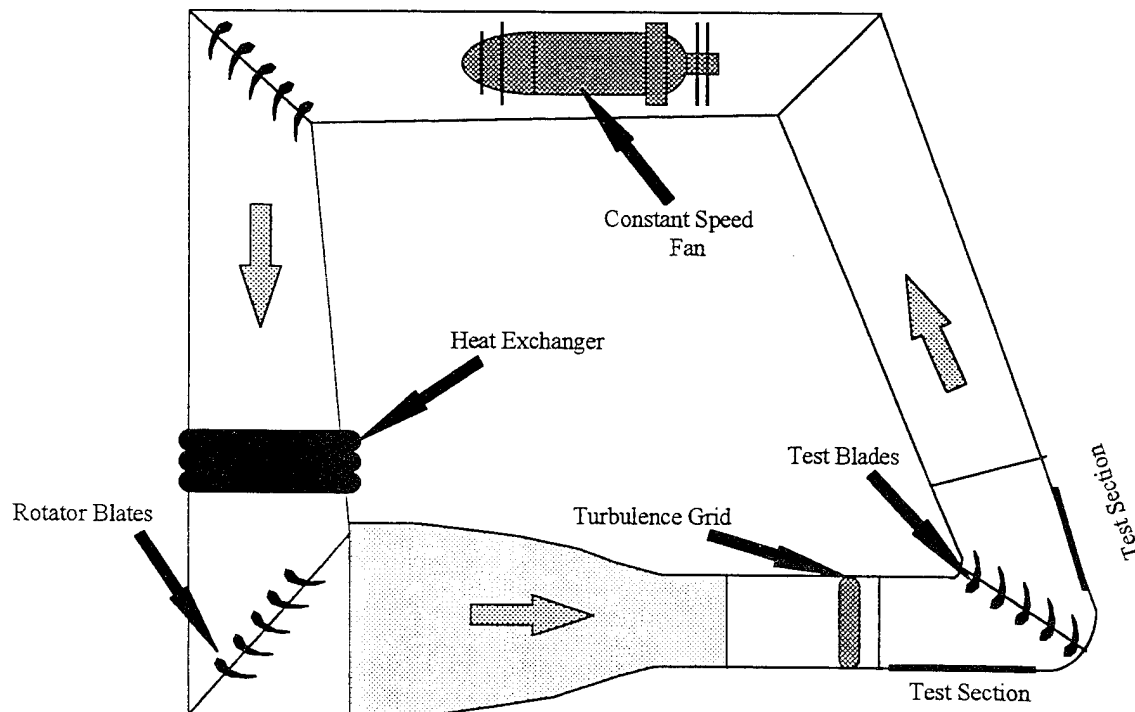
and constant resistance hot wire velocity from voltage difference

$$V = C_0 + C_1(e_o - e) + C_2(e_o - e)^2 + C_3(e_o - e)^3 + C_4(e_o - e)^4.$$

Setup:

The theory behind a Cascade Wind Tunnel is that it simulates flow over an array of turbine blades. This is accomplished by turning the flow through an angle of 105° as it passes through the test section (see Figure 2 below). Therefore, the supposed result is that each blade sees the same flow qualities, changing direction with the camber of the blade, void of interference from neighboring blades. Turbulence can be produced by a grid (see Figure 5 below) perpendicular to the flow which can supplementally inject pressurized air across the steady streamline flow. These air jets produce a significant increase in the turbulence levels from those obtained with the grid obstruction alone- more characteristic of post-combustion levels. The turbulent flow then enters the array of blades at a 43.3 degree angle, the distance downstream from the grid being the main determinant of turbulence intensity. The flow then leaves the blade aligned in a trailing edge alignment due to the "bent" test section (more accurate from a modeling perspective in simulating arrays of repeating blades). The behavior of turbulence and heat transfer in such a model is significantly different from that obtained in "straight" wind tunnels.

The following diagrams show various key aspects of the experimental setup.



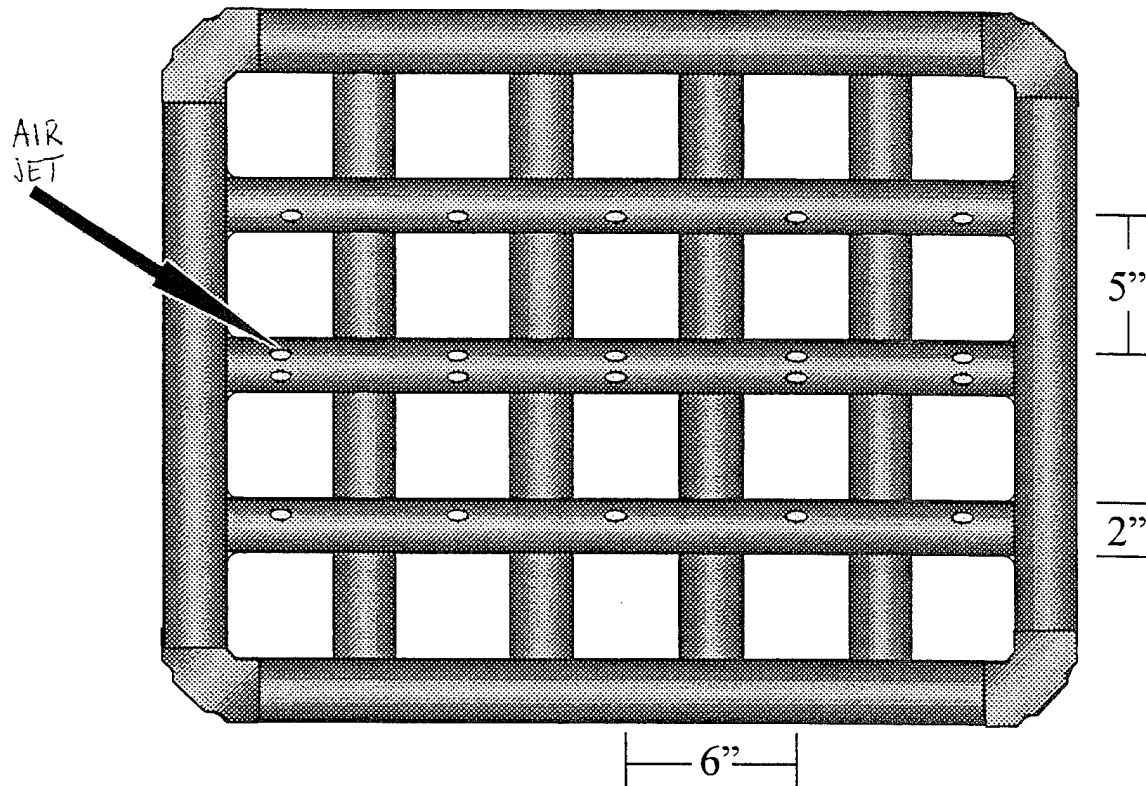


Figure 5. Turbulence Generation Grid

Setup values consistent for each traverse run were a 7500 Hz sampling rate (used both as individual data and for time averaged values), grid air pressure of 57 psi, traverse steps of 2", and traverse placement of 22.5" from the leading edge line of the array. The array itself consisted of five 6.5" spaced scaled-up Langston turbine blades.

Calibration:

The majority of equipment used was already calibrated prior to the beginning of the flow quality study, and was seen to be so by preliminary verification runs of the facility. A digital pressure transducer calibrated by the USAFA PMEL facility was used as the secondary standard in a manometry based pitot-static system. Based on the output of this system, the general fourth-order equation (mentioned above) for dynamic hot-wire voltage measurements was supplied with the appropriate constants (listed in Appendix J). However, due to a since changed bias in the system as evidenced in early pitot-hot wire comparisons, the hot wire was thereafter statically calibrated following each run by manually adjusting the velocity conversion e_0 (the "no flow"

length scales according to eddy flow energy. Also use the 7500-sample mean and standard deviation to validate spreadsheet turbulence intensities at centerline.

- i. Repeat steps f. and g. for different grid positions and repeat runs for air on/off and grid x position.
- j. Perform this procedure at exponentially changing distance increments (constant Tu increments) over the maximum streamwise range of the grid.
- k. Analyze the data, first discussing turbulence production validity (magnitude) and second discussing turbulence conditions with respect to the blade array (uniformity and trends).

Results:

The experimental results are mainly in graphical form located in Appendices. The graphical trends and significant numerical results will be discussed in this section.

The grid placement analysis in Appendix A proved to be accurate for predicting the trend of turbulence intensity vs. distance (a -0.71 power curve according to Roach) for the air off grid. Appendices G and H contain equation-labeled curves of the experimental results. This is reinforced in Appendix F where grid air on and air off are plotted across the center horizontal span of the tunnel, which due to the traverse (blade cascade) angle incorporates a change in x-distance. However, with air jets on, the decay rate is decreased slightly, with turbulence intensity equalling a function of approximately x^{-5} , due to the more energized nature of the flow. Magnitude is not of concern here. The slope of the turbulence intensity versus grid distance, or the decay rate, is. Variations that do occur in magnitude, that is, in the value of the constant multiplier, can be accepted since it is relatively simple to obtain a single location grid-specific test for C, and make predictions from there on. The range achieved in analysis of the "area of interest" with air jets off was from about 7-11%, as predicted in Appendix A. Air jets on is a unique case for the facility and could not be accurately predicted prior experimentation.

Appendix B, tunnel temperature verses time, shows the facility to have been controlling the temperature in a periodic fashion to obtain the desired mean of 19°C. Though the thermocouple was located in the turbulent portion of the flow, on the traverse arm, no correlation can be seen between temperature and position, or temperature and turbulence intensity (note that "Traverse Measurement #," as shown, can not be directly visualized as horizontal or

here to horizontal distance due to traverse geometry) across the central 12 inches of the tunnel the air on condition, due to an unexpected air jet coalescence pattern, consistently shows two peaks (turbulence) or valleys (velocity) in the central region of interest. Since this will cause the test blade to be subjected to incidents different flow conditions depending on surface position, this result is grounds for redesigning the air-supplemented turbulence grid, most likely with relocation of the air jets, smaller rod diameter, or both. In general, though, the turbulence decay rate, that is, the slope of Roach's correlation, is small enough so that the detrimental effect of combining a perpendicular grid with an angled cascade is negligible with a single, central test blade.

Finally, the macroscopic and microscopic length scale descriptors of turbulent flow were found to increase slightly with distance downstream, but this increase can be considered insignificant along the 35 inch distance covered in this experiment. Graphs showing this can be referenced in Appendix I. Macroscopic length scales of 1.5" with air jets off and 1.75" with air jets on, and microscopic length scales of about 0.3" for both conditions were produced. Another result of the length scale study was that macroscopic length scales, although labeled with a mean here, are very difficult to predict, having variations as great as $\pm 1"$ off the expected smooth line trend. The correlation factor for the data points in Appendix I is much too small to make accurate predictions of macro length scales.

Uncertainty/Error Analysis:

As discussed in the Theory section the following is the equation used to calculate turbulence intensity from voltage and velocity measurements:

$$Tu = \frac{dV}{d(\Delta e)_{Vm}} \left(\frac{e}{V} \right) 100\%$$

When applied in a spreadsheet for coordinate quality mapping of the flow field, an estimation method is used in above equation to obtain turbulence intensities at each point in the flow. Average velocity and standard deviation are calculated numerically, approximating the fourth order velocity-voltage curve with linear segments between voltage increments (over 7500 Hz hot-wire sampling frequency). The fourth order curve can, however, be more accurately analyzed for velocity and standard deviation (thus turbulence intensity) using a curve fit equation (discussed below) in computer software. Thus a more accurate method is to take all 7500 values and reduce them with an iterative statistical program. This becomes highly impractical due to

variation in flow quality across the central test section region.

This study should pave the way for future work with improved turbulence generation methods, and as a prediction tool for studying the effects of turbulence on turbine blade heat transfer, the purpose of an Aero-thermal Cascade facility.

APPENDIX A

Grid Placement Analysis

APPENDIX B

Tunnel Temperature Fluctuation Graphs

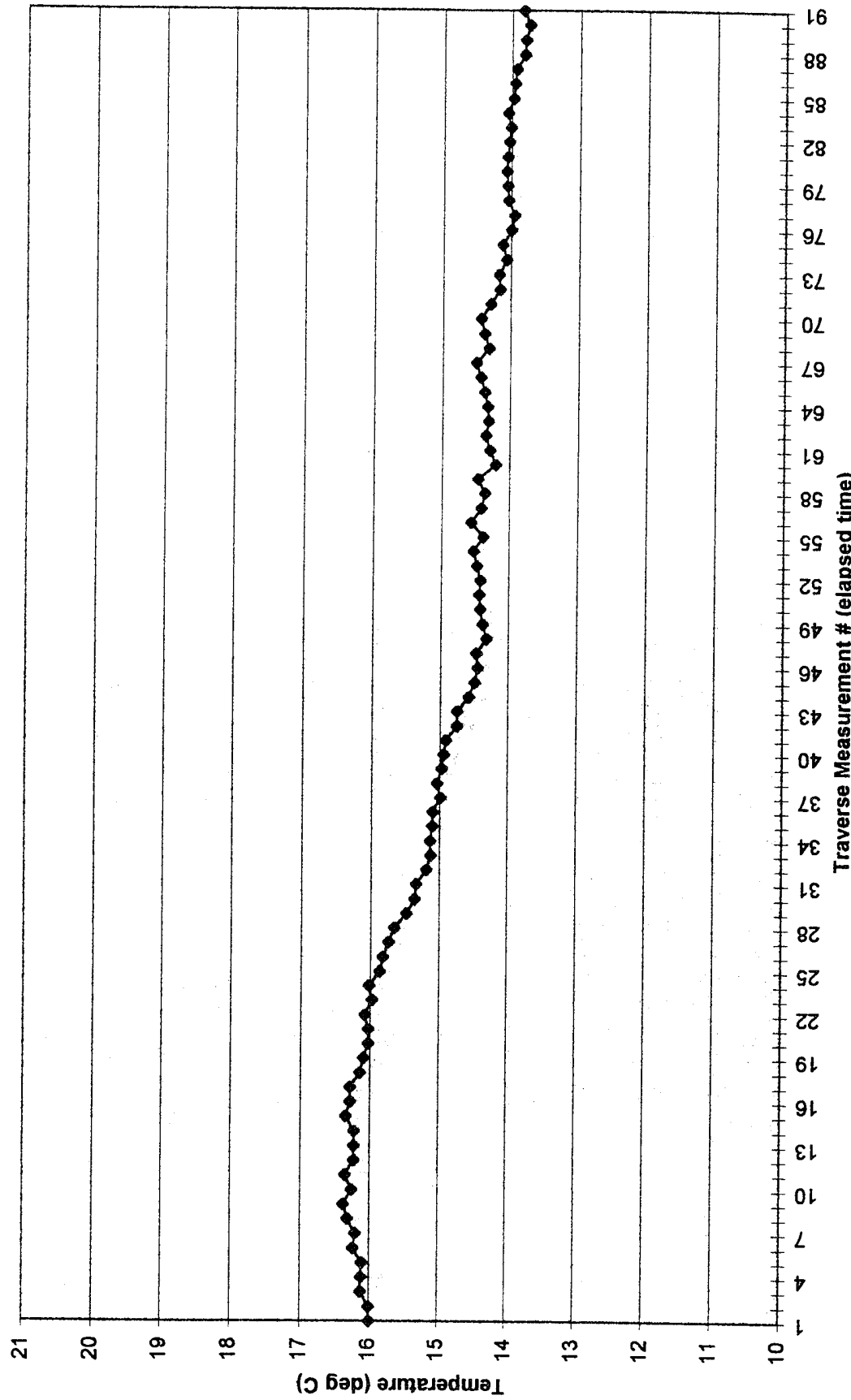
Tunnel Temperature with Air Jets OFF

Chart1

Tunnel Temperature with Air Jets ON

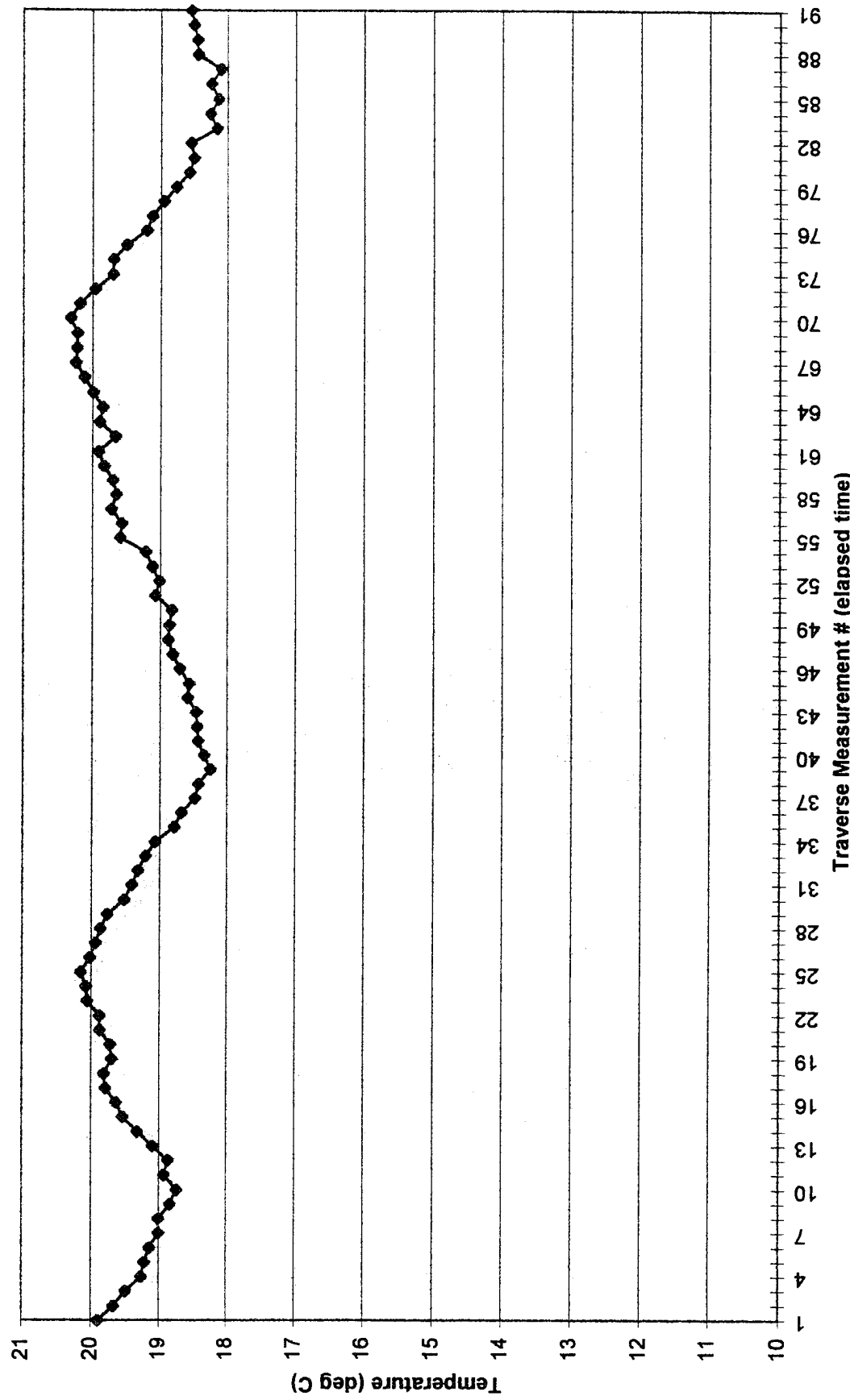


Chart1

Tunnel Temperature with Air Jets OFF

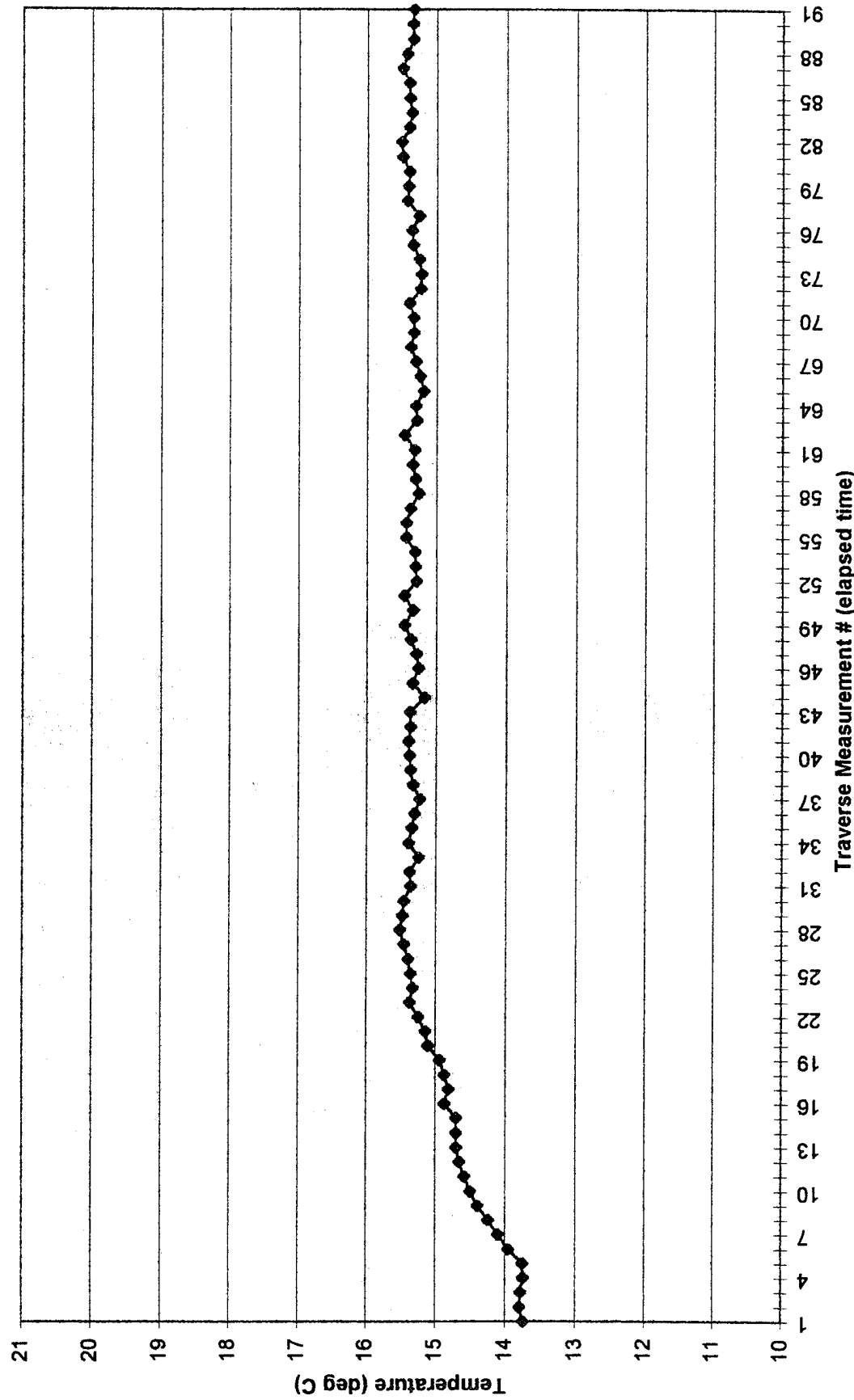


Chart1

Tunnel Temperature with Air Jets ON

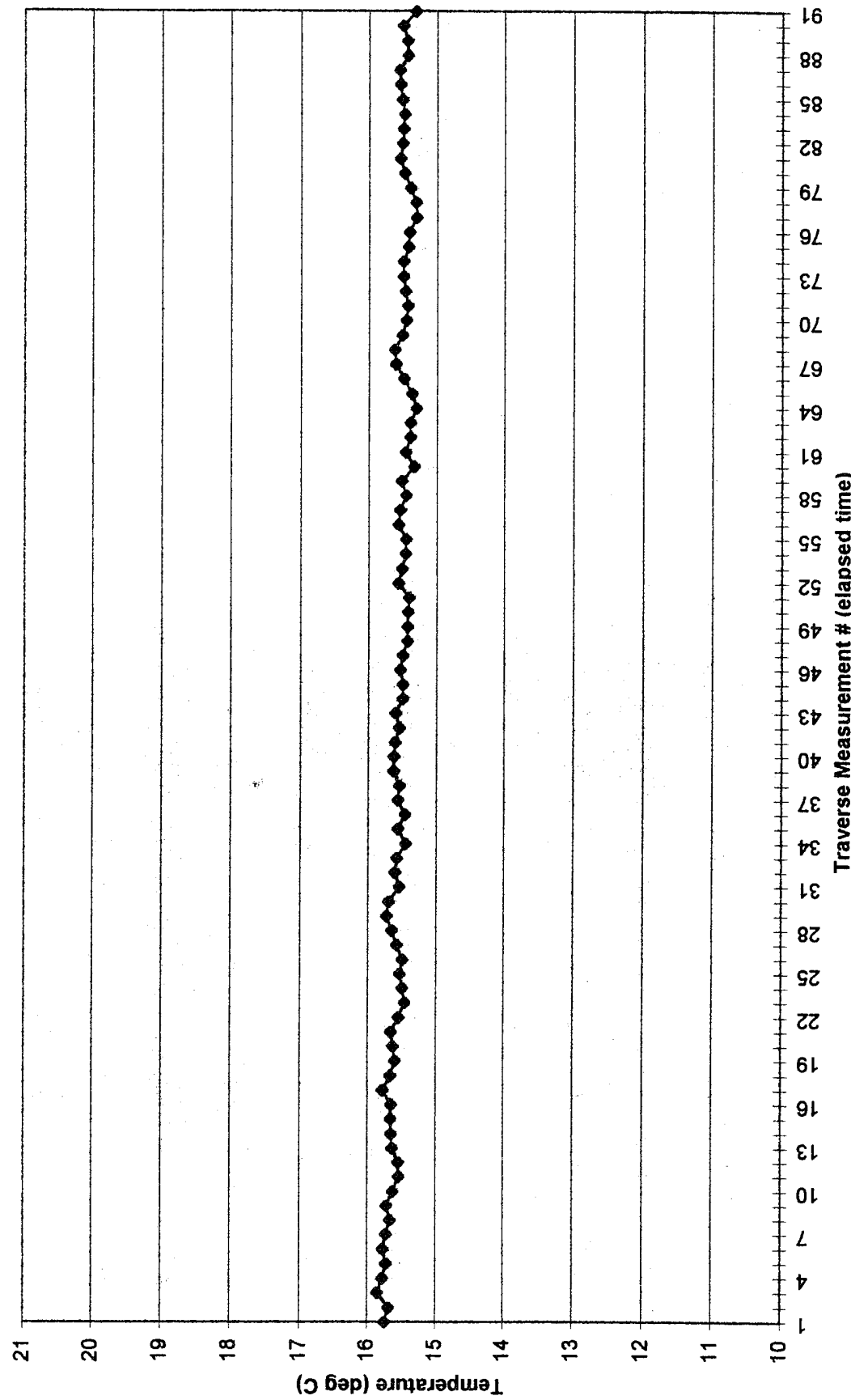


Chart1

Tunnel Temperature with Air Jets OFF

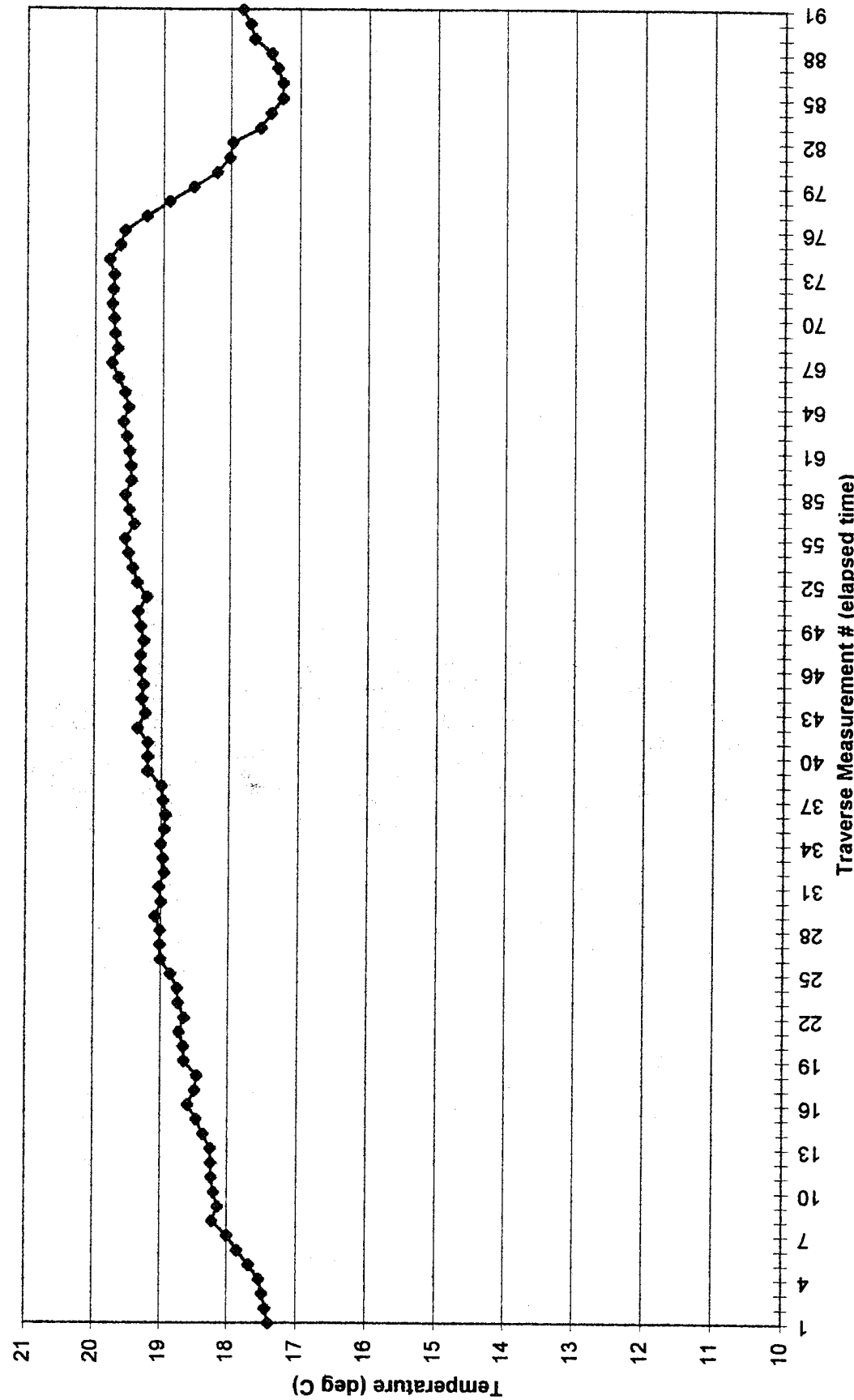


Chart1

Tunnel Temperature with Air Jets ON

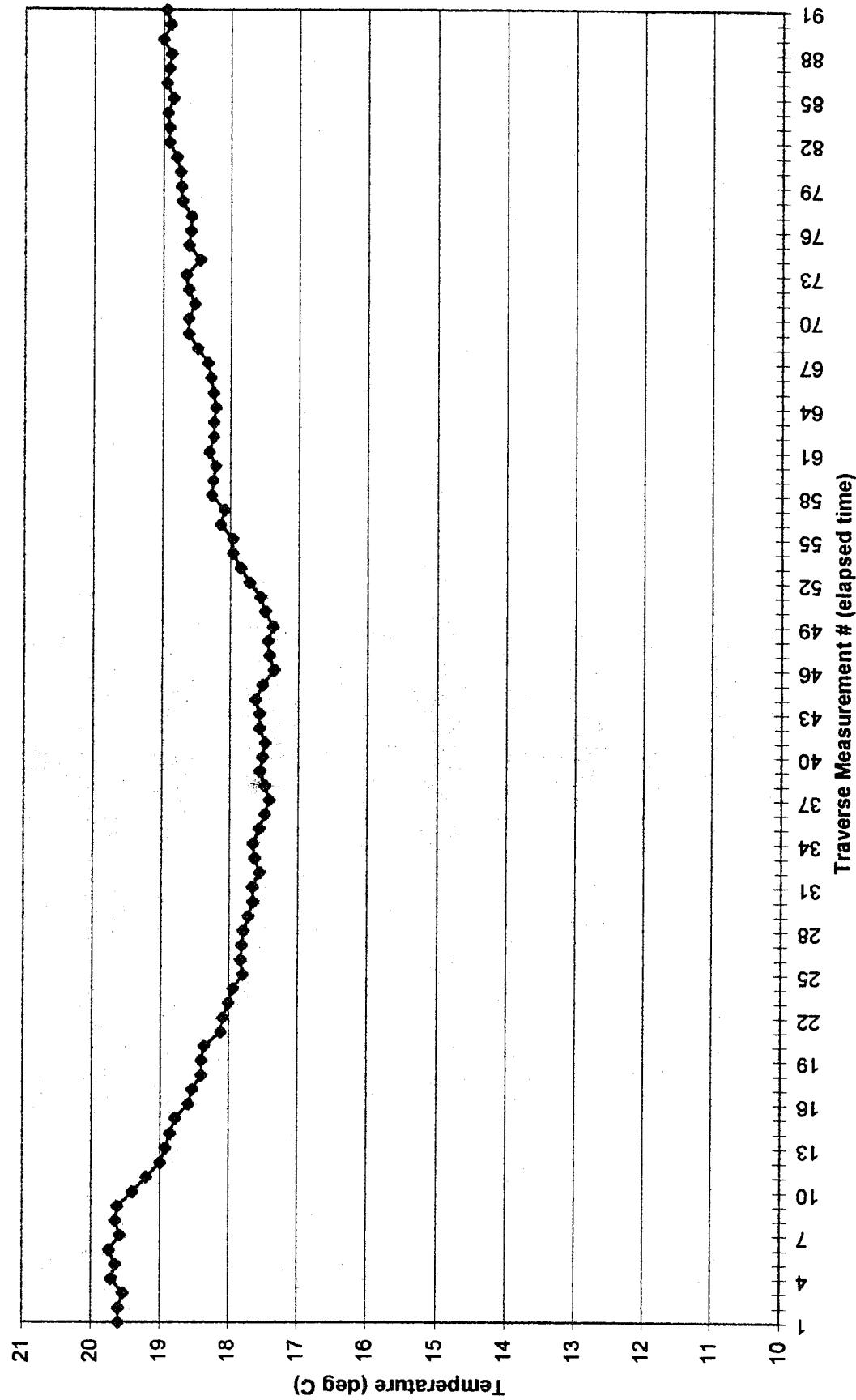
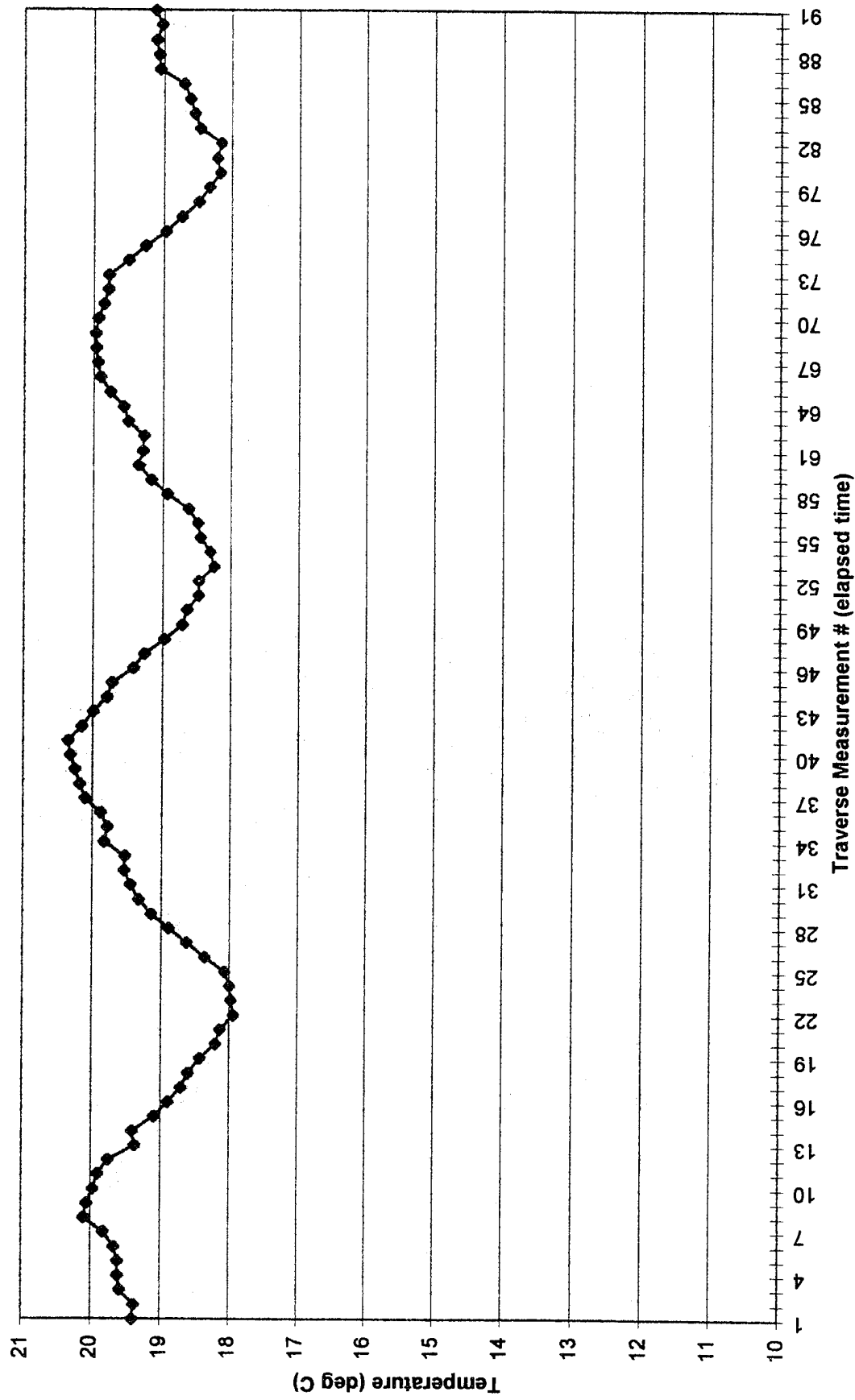


Chart1

Tunnel Temperature with Air Jets OFF



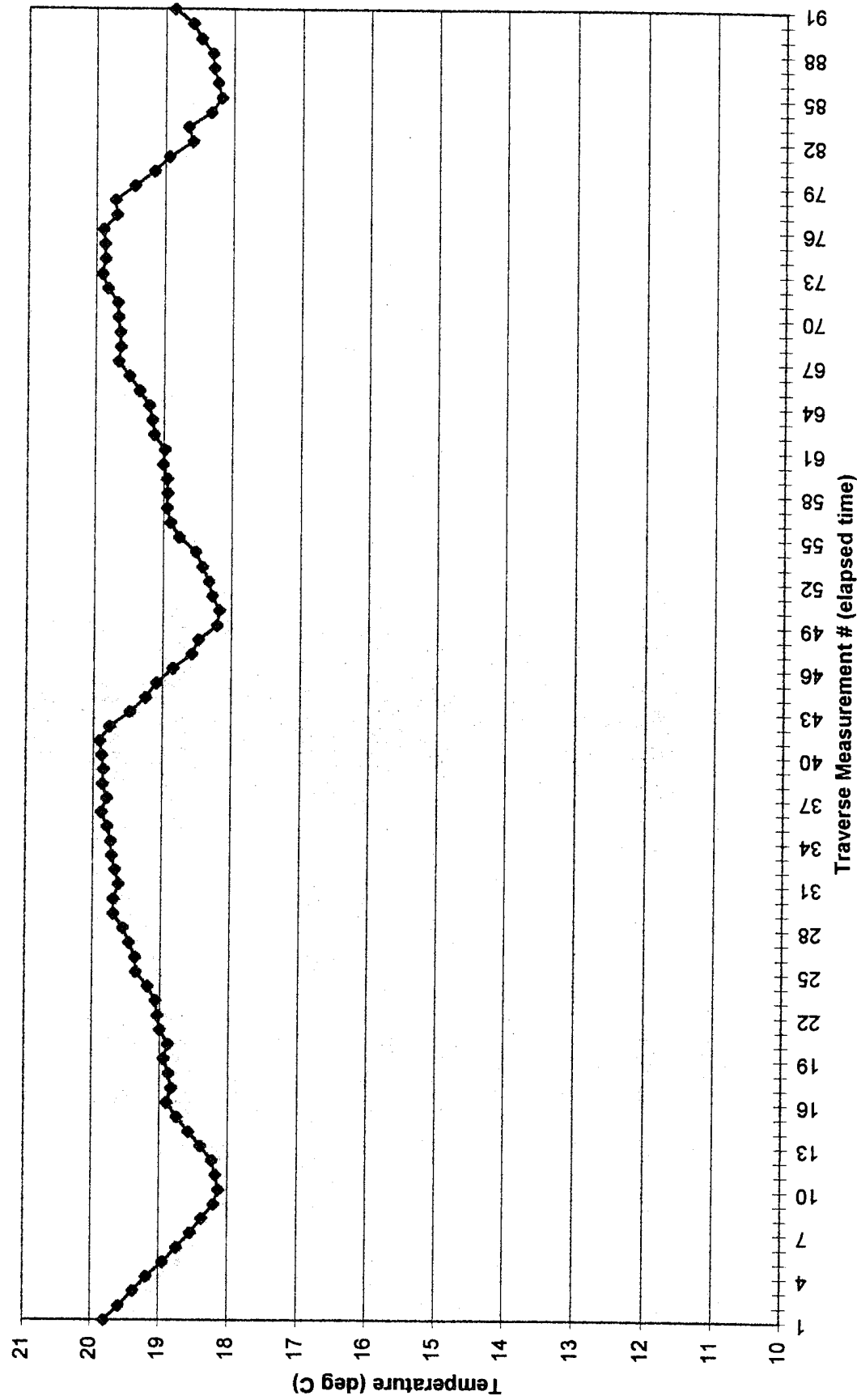
Tunnel Temperature with Air Jets OFF

Chart1

Tunnel Temperature with Air Jets ON

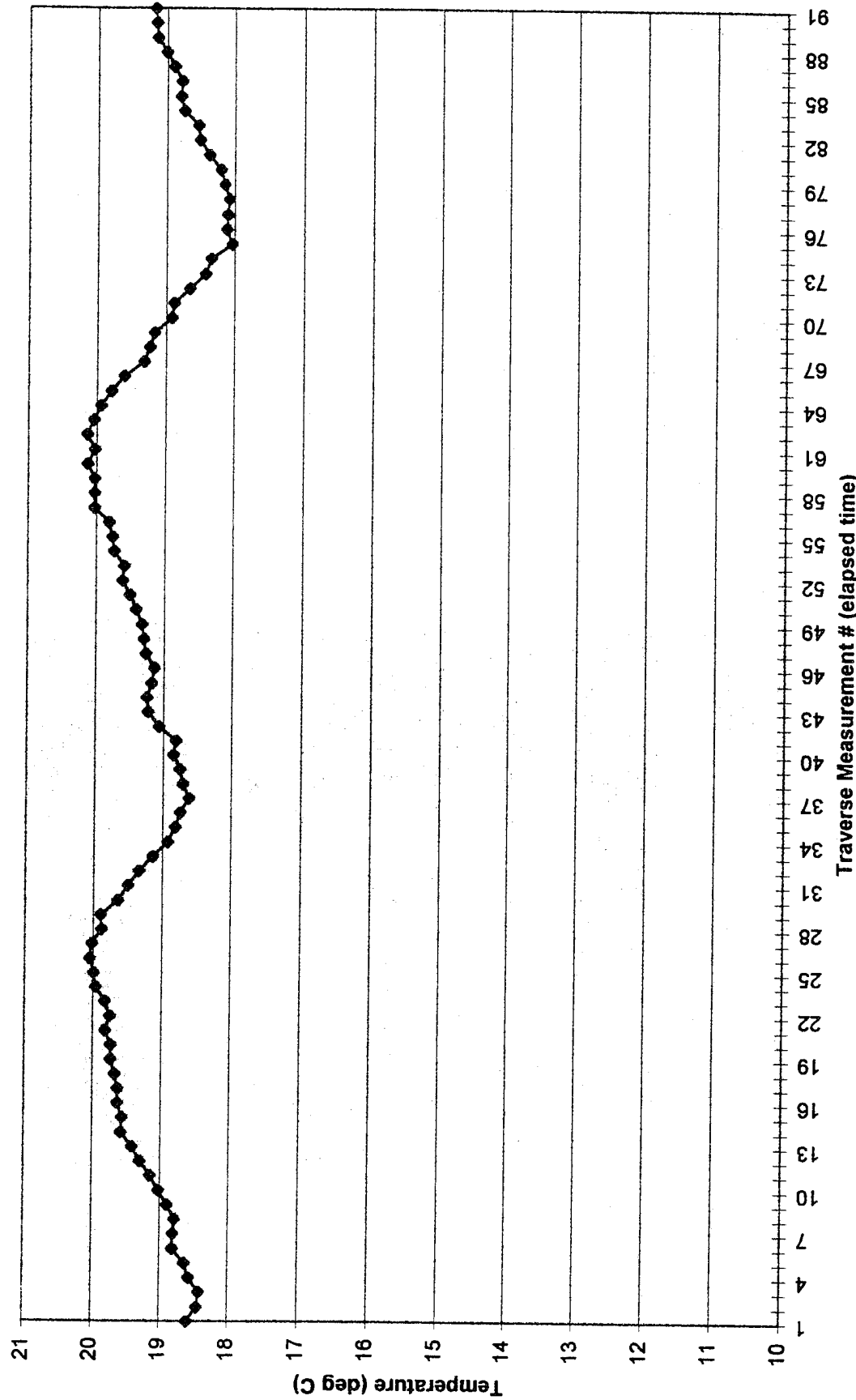
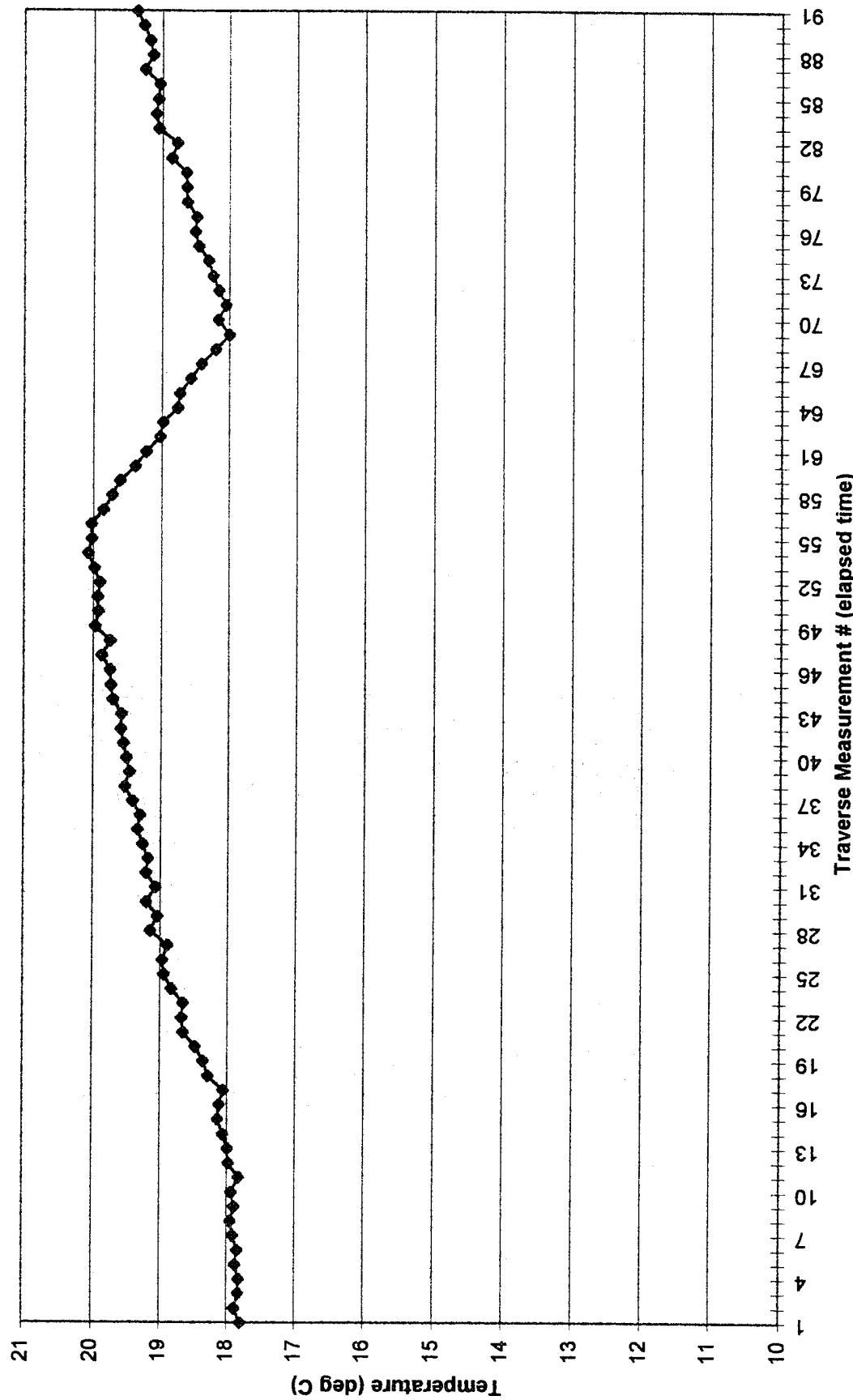
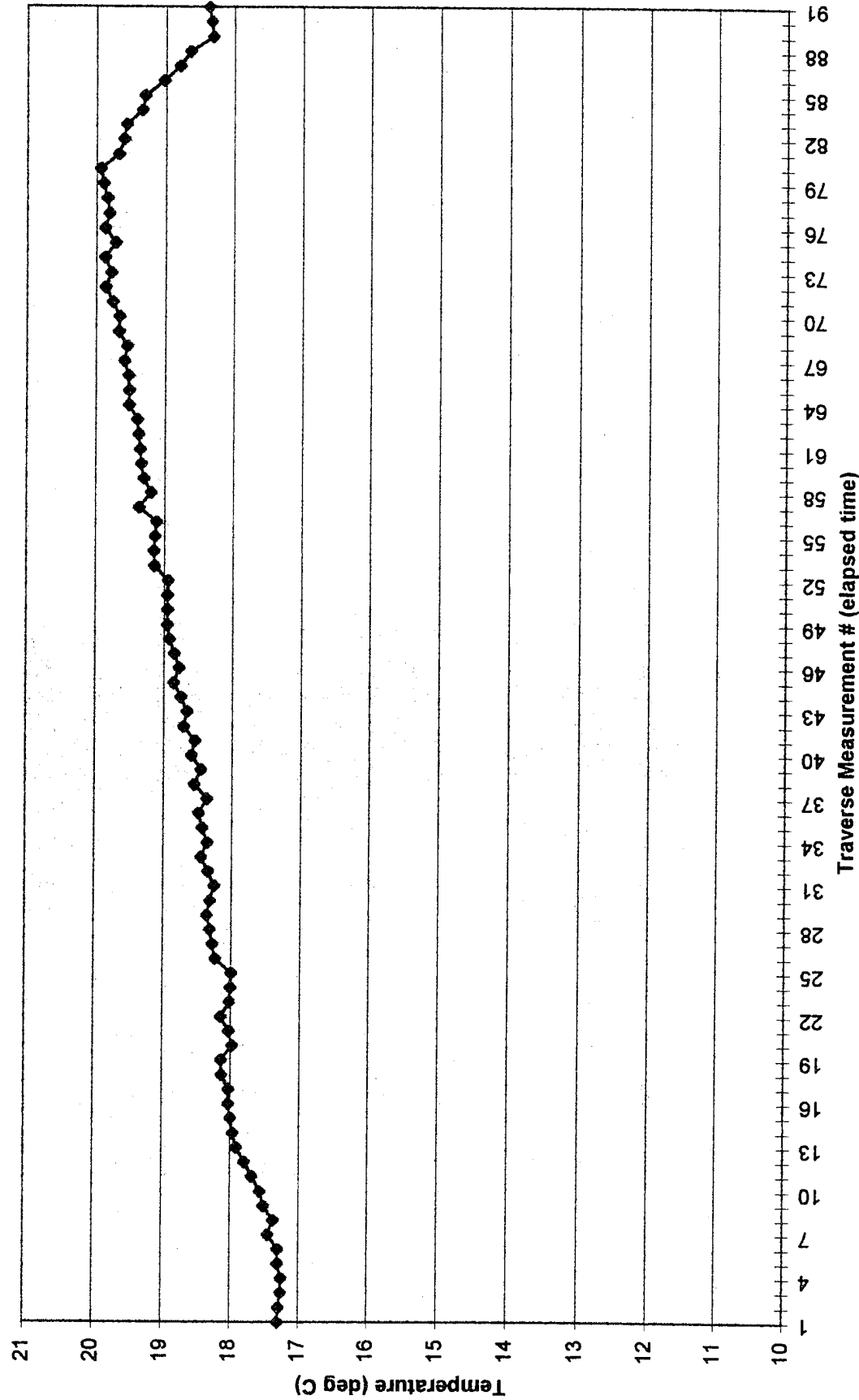


Chart1

Tunnel Temperature with Air Jets OFF



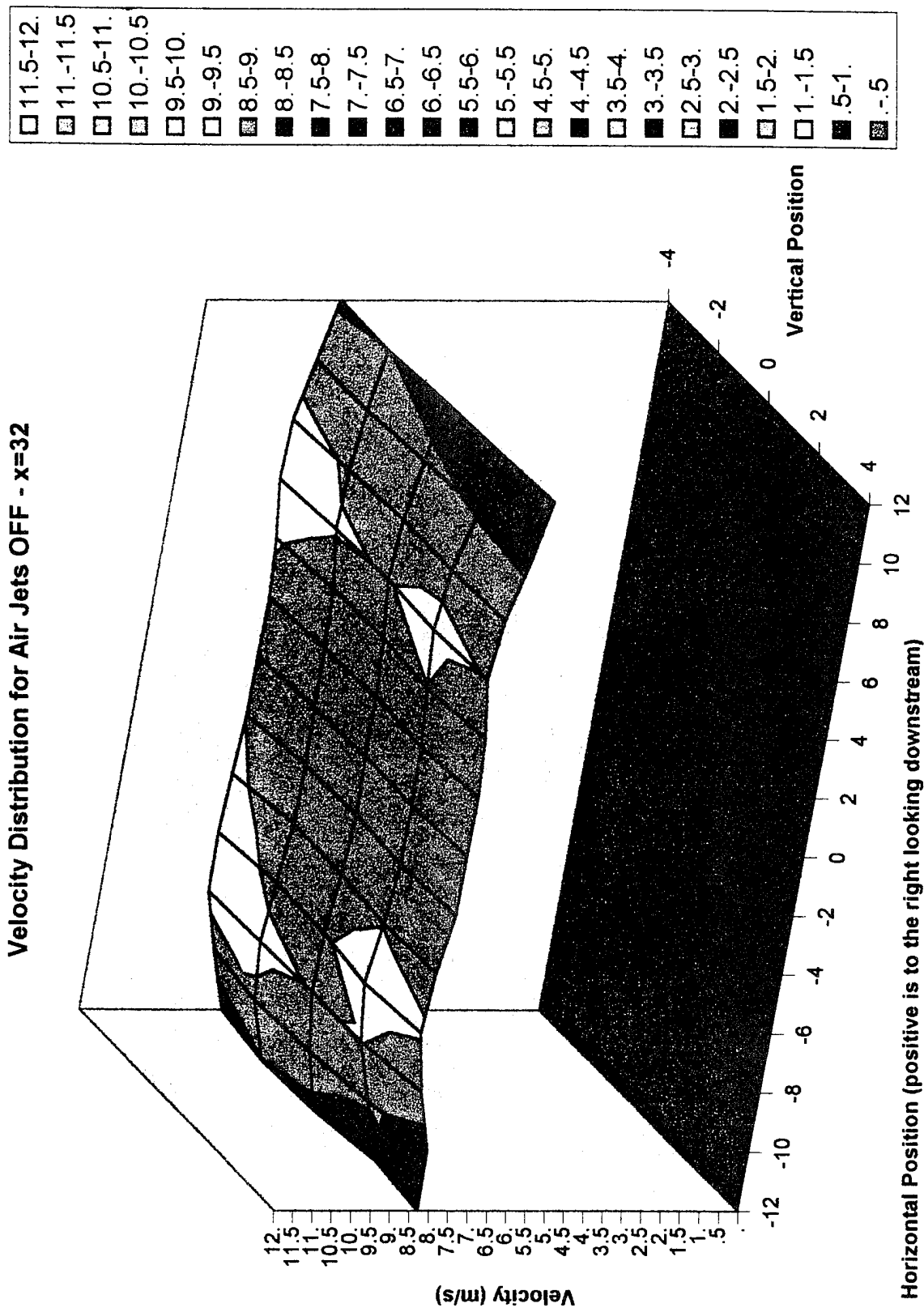
Tunnel Temperature with Air Jets ON

APPENDIX C

Velocity Distribution Plots

Chart2

Velocity Distribution for Air Jets OFF - $x=32$



Horizontal Position (positive is to the right looking downstream)

Chart2

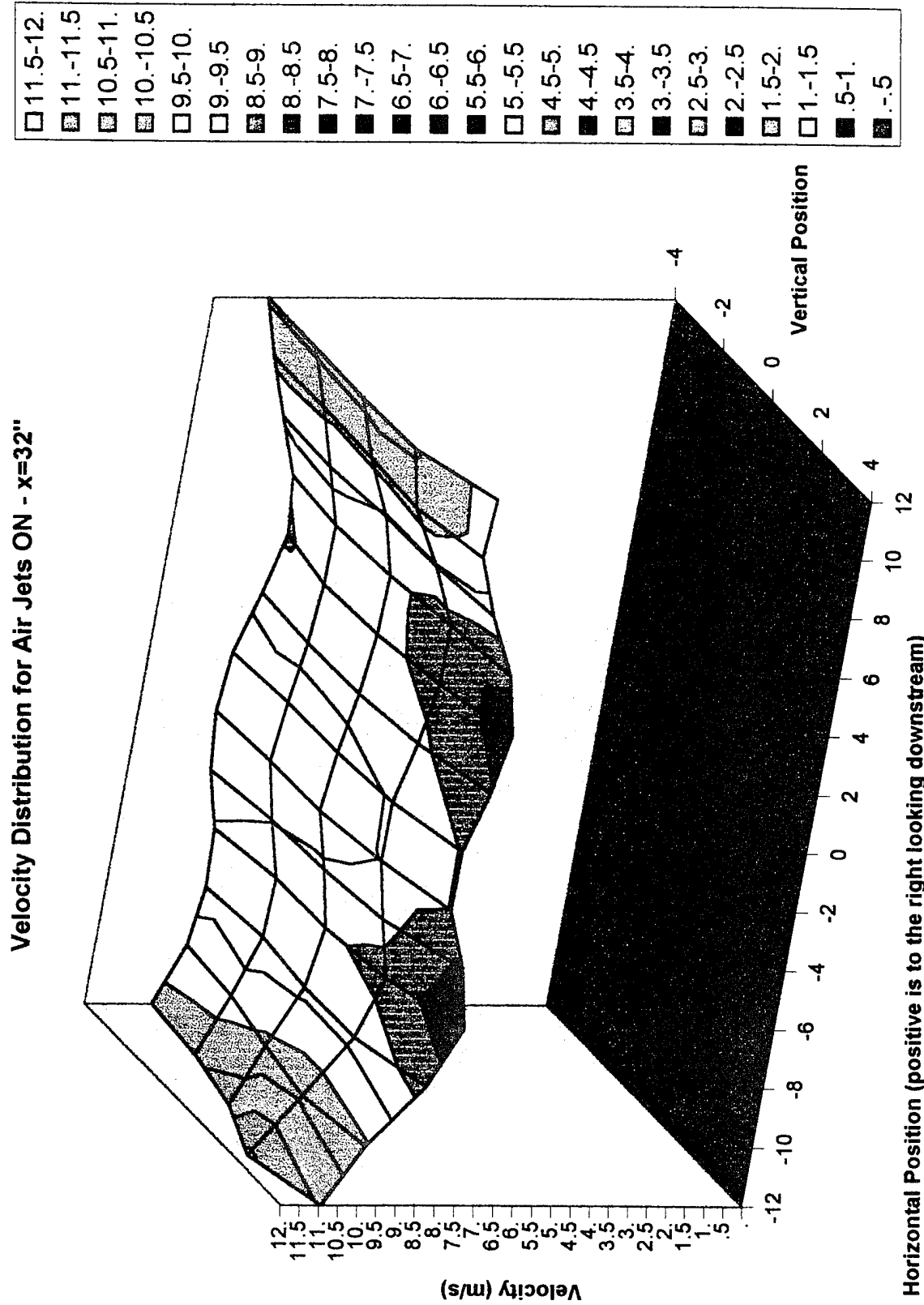


Chart2

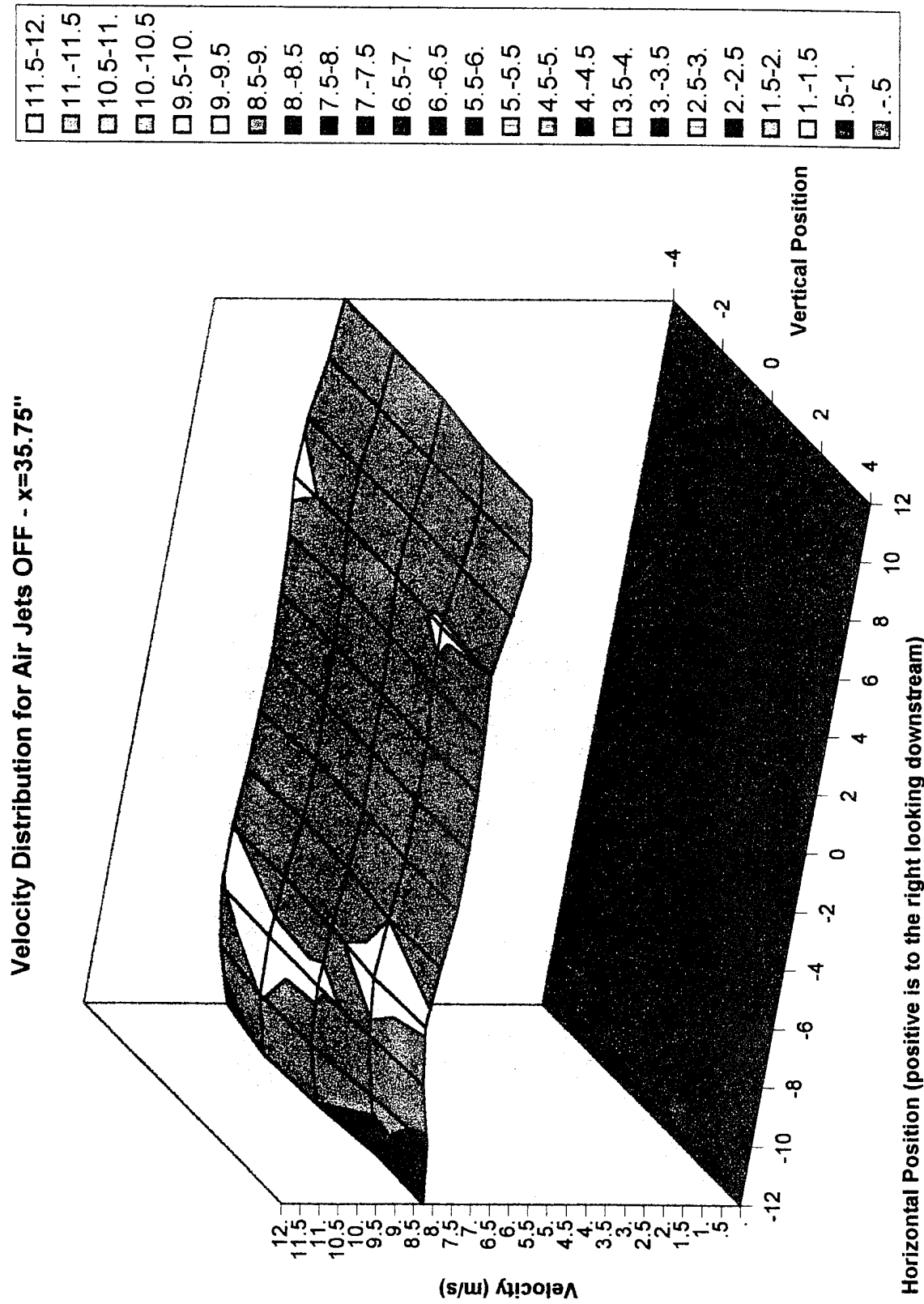


Chart2

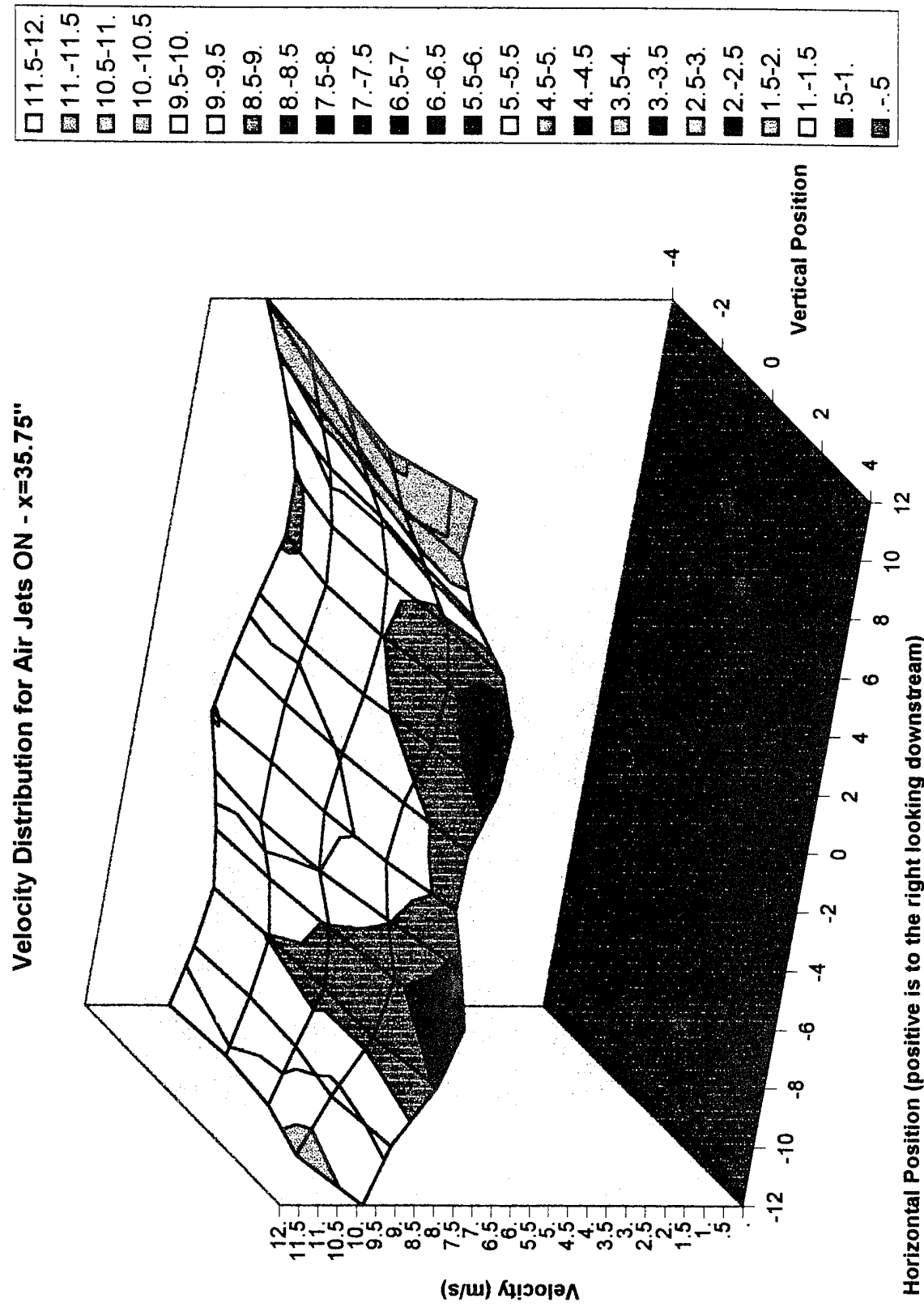


Chart2

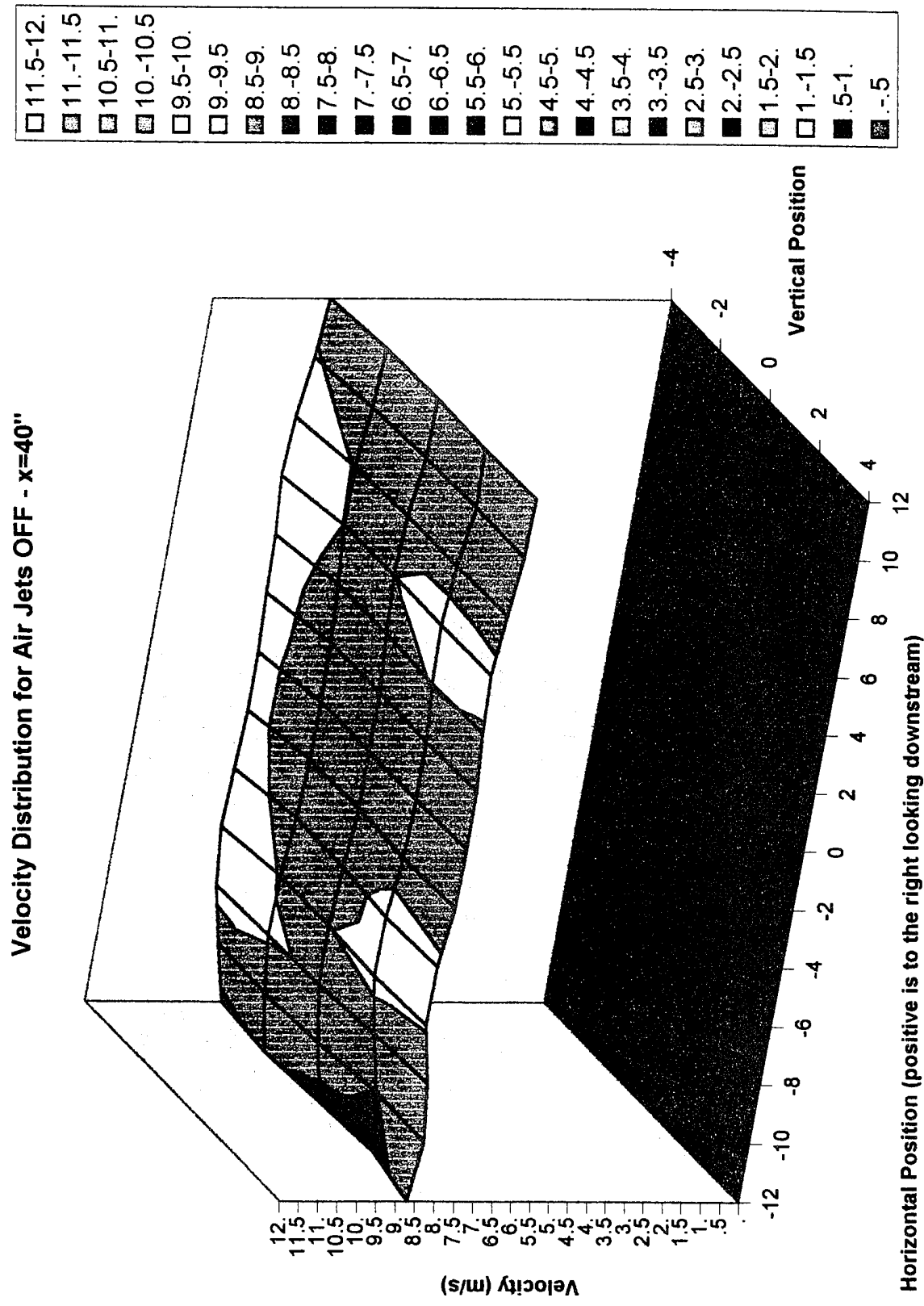


Chart2

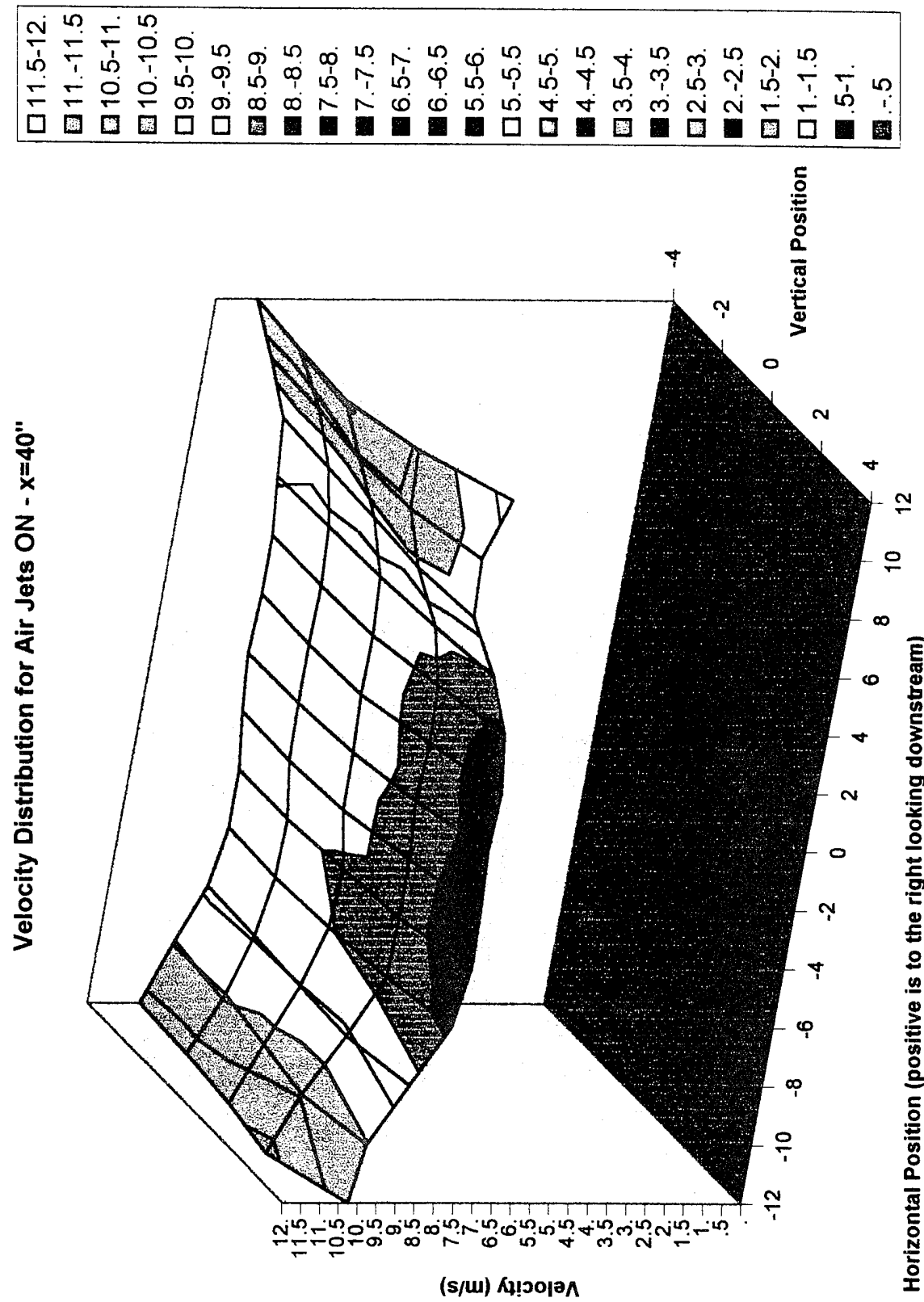


Chart2

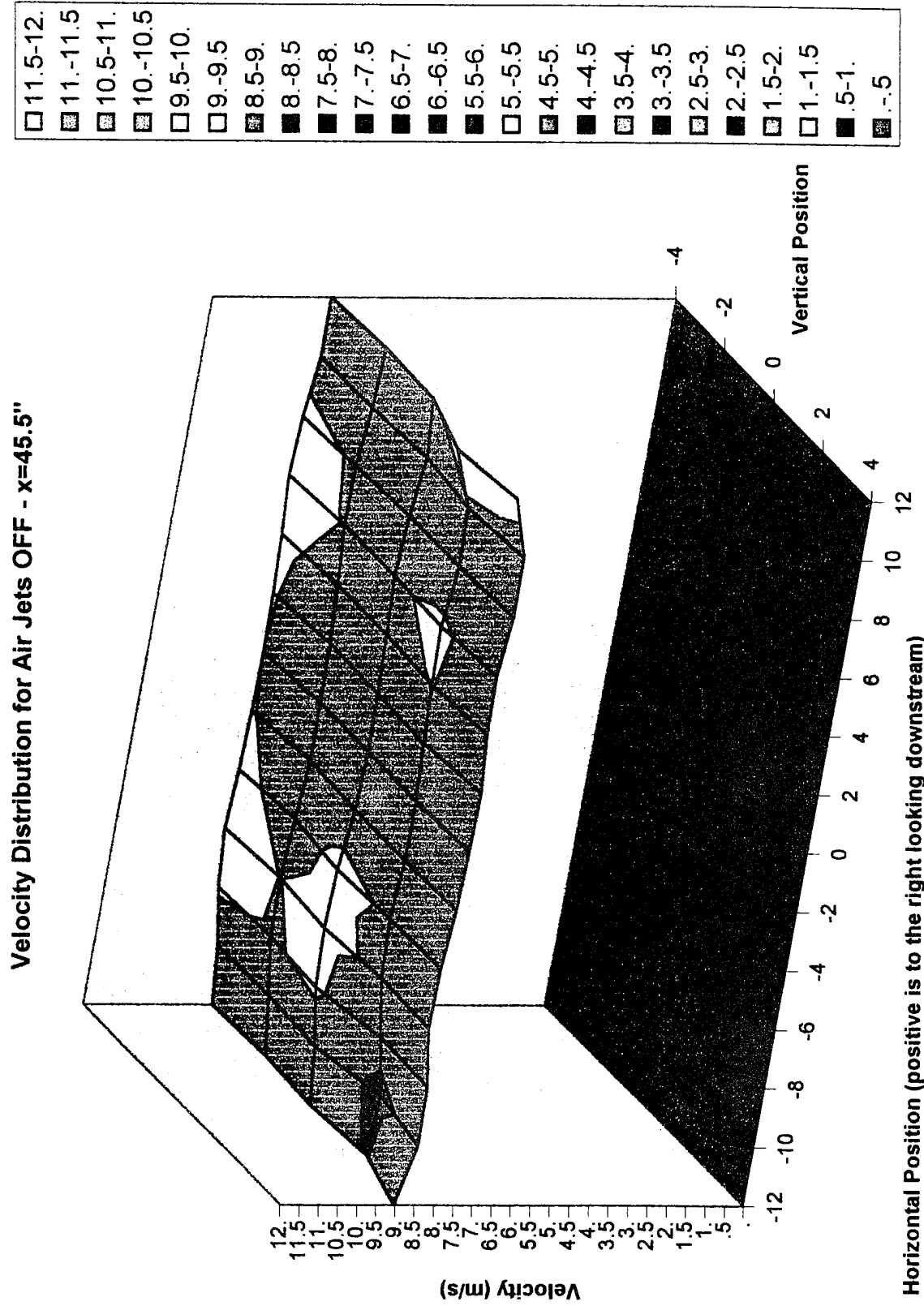


Chart2

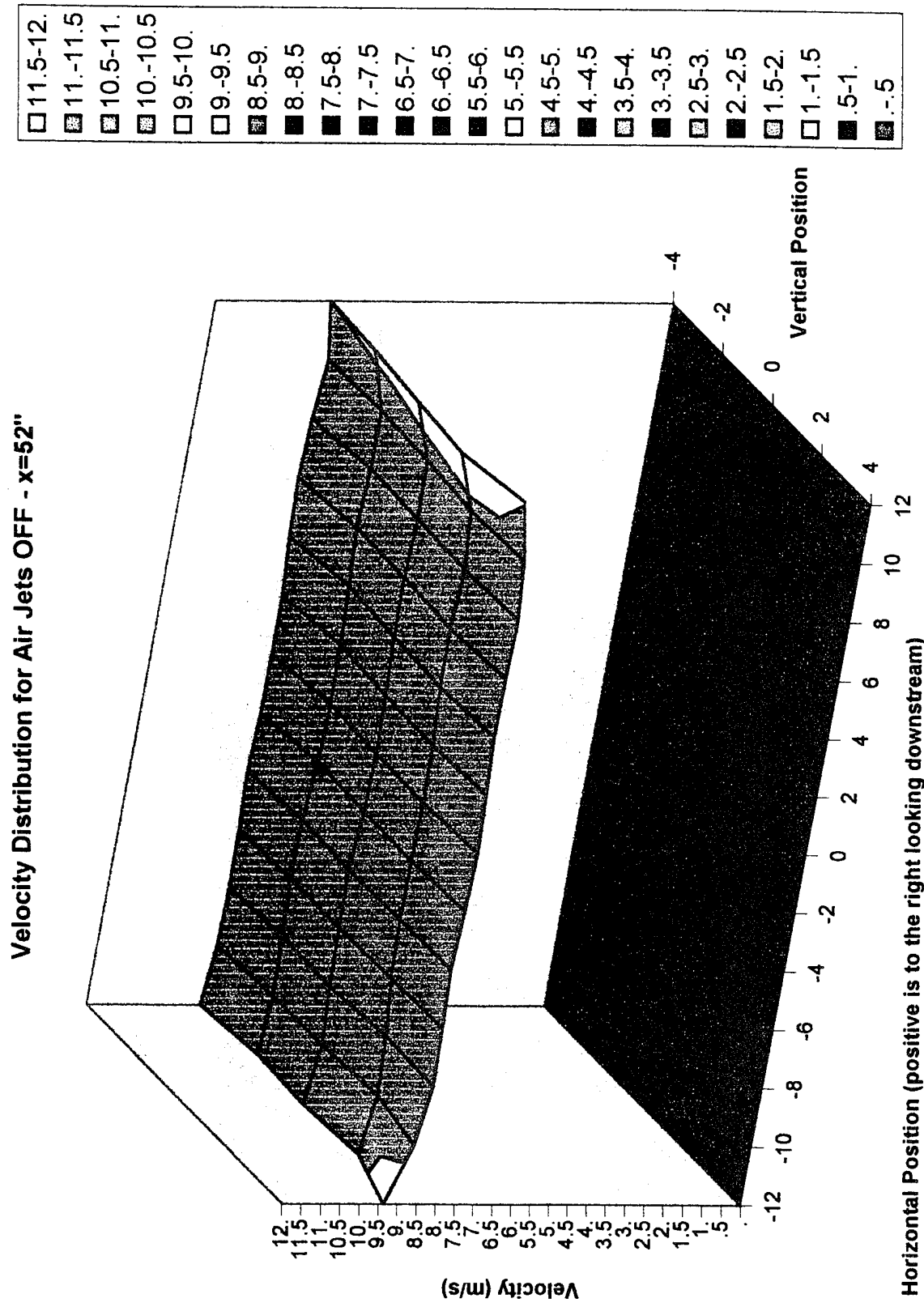
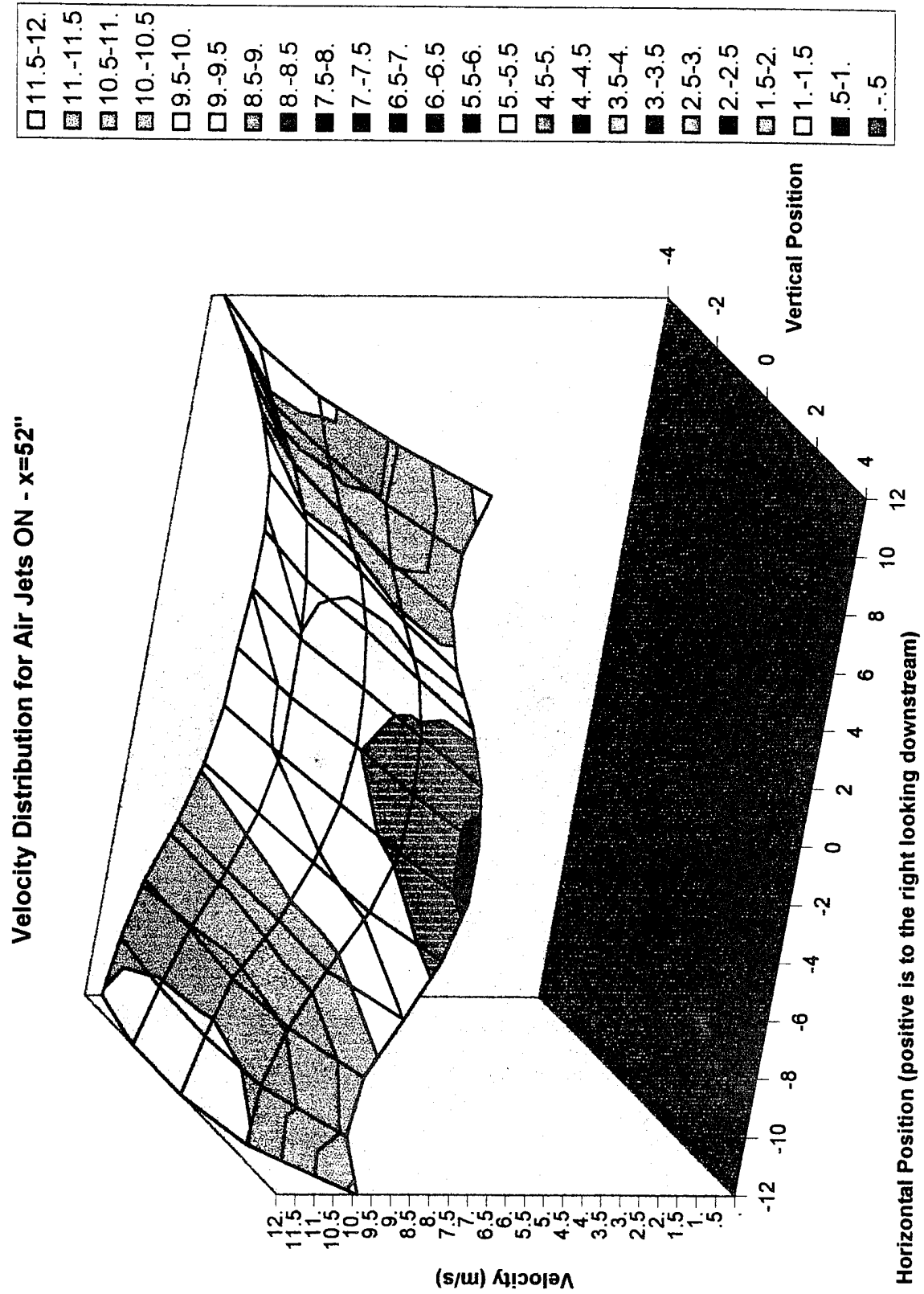


Chart2



Horizontal Position (positive is to the right looking downstream)

Chart2

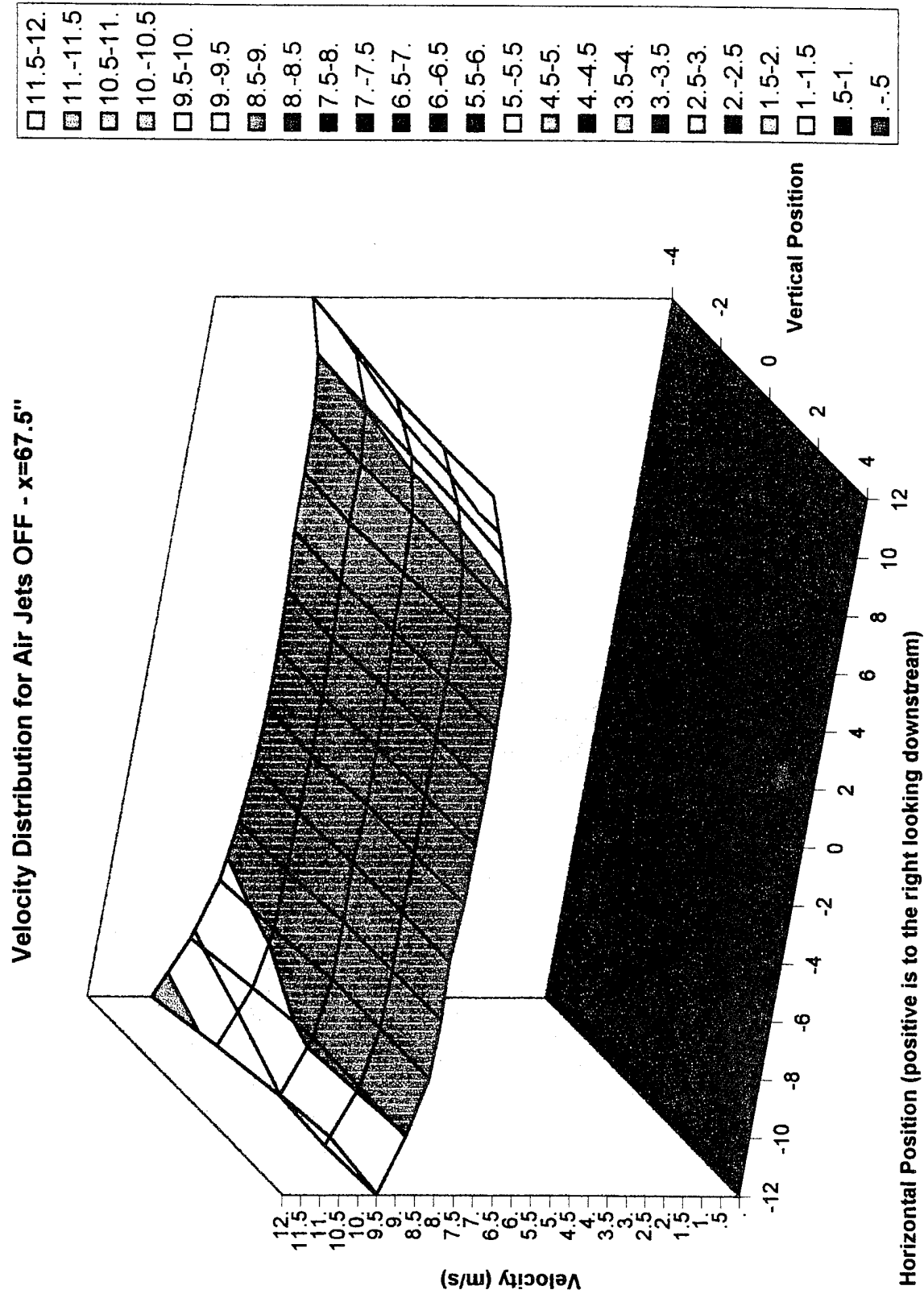
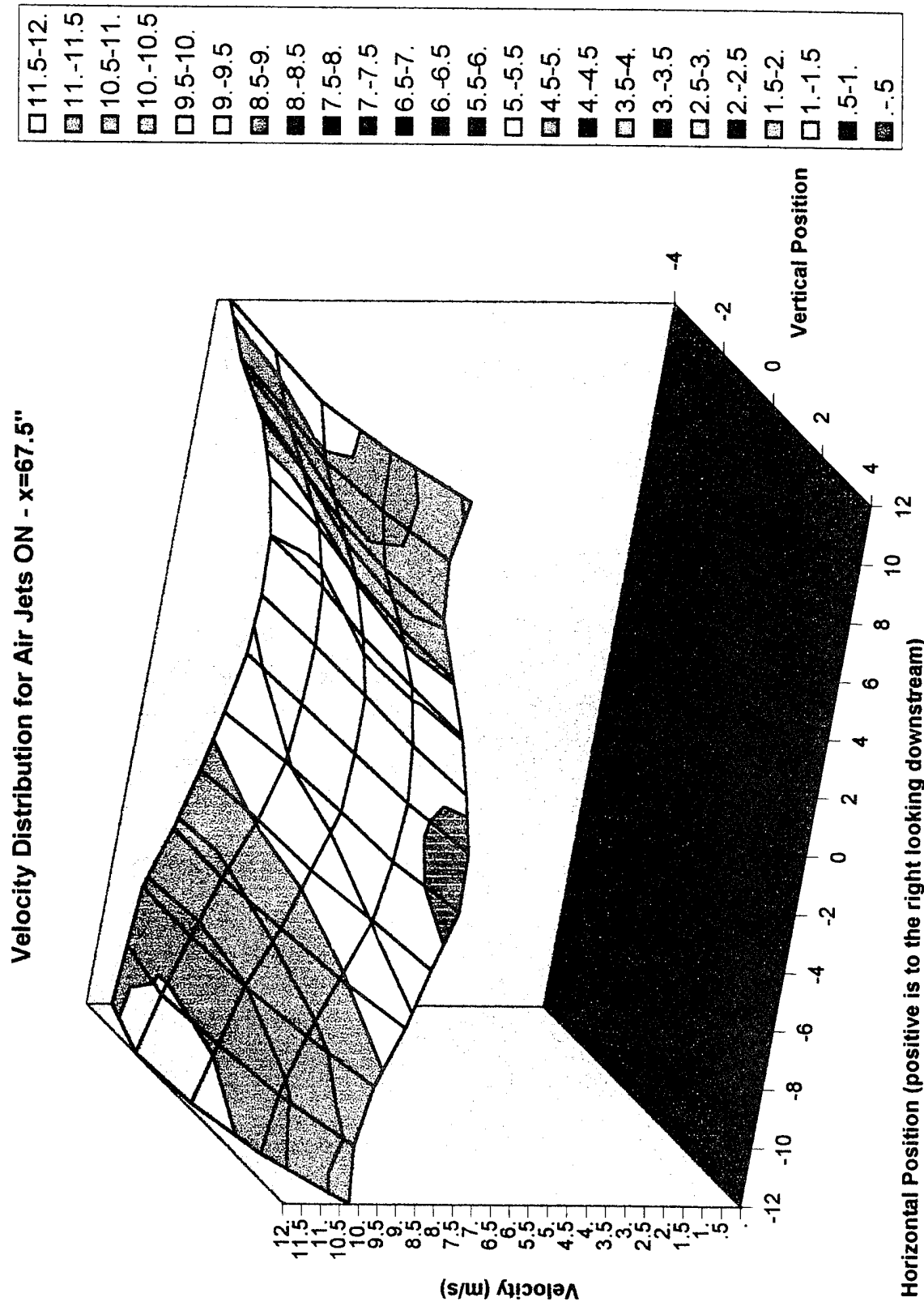


Chart2



APPENDIX D

Turbulence Intensity Traverse Plots

Chart3

Turbulence Intensity with Air Jets OFF - $x=32"$

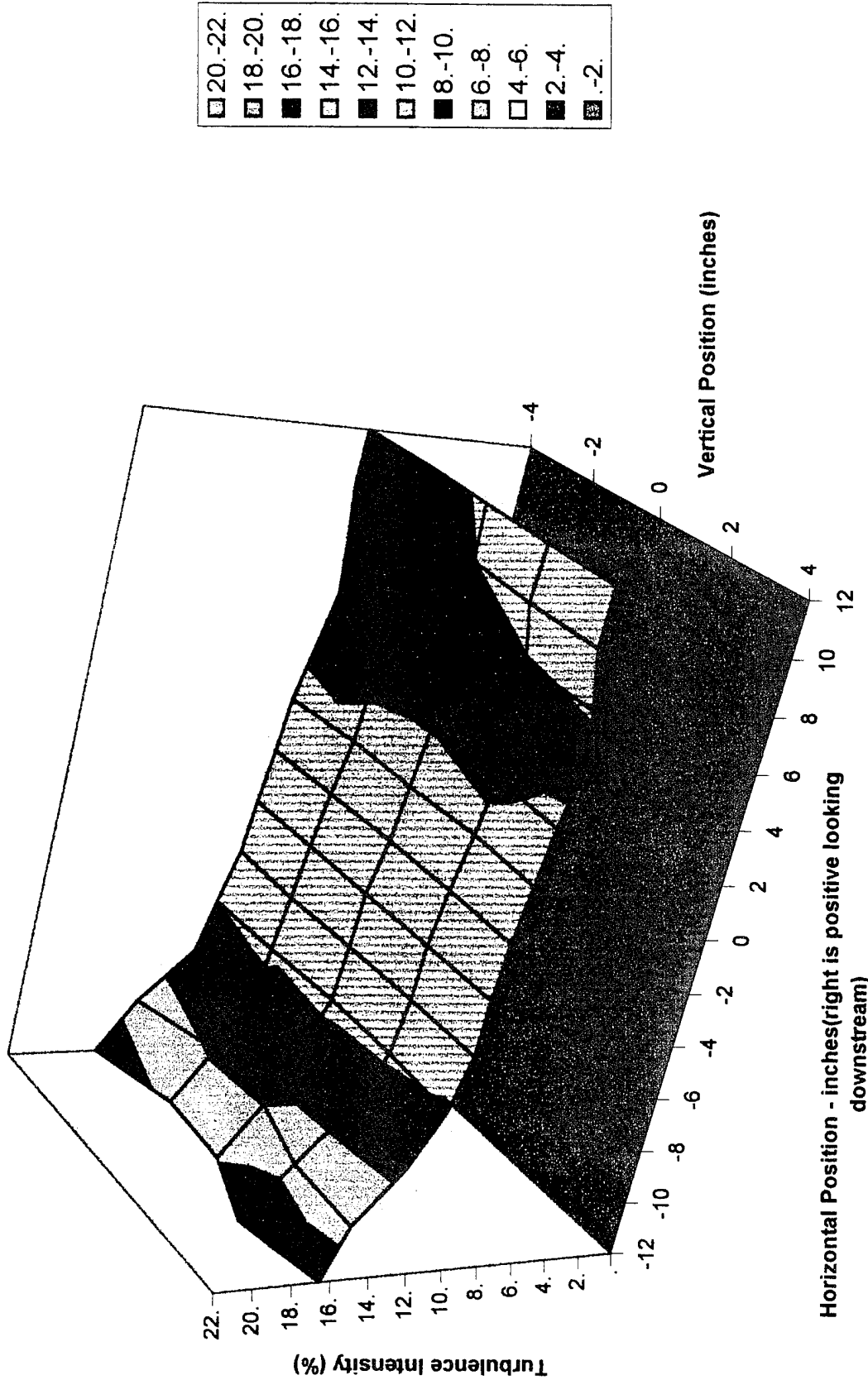


Chart3

Turbulence Intensity with Air Jets ON - x=32"

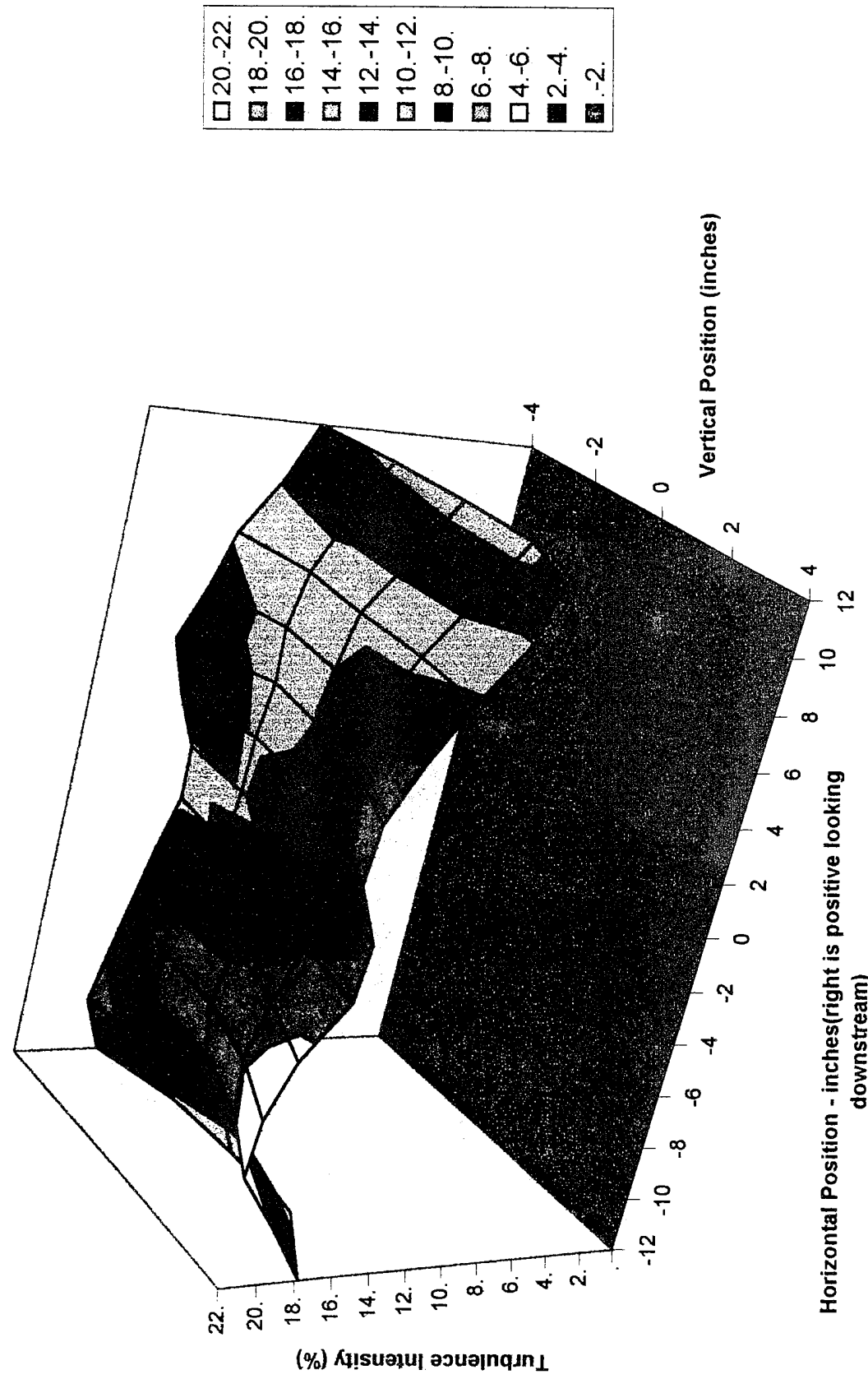


Chart3

Turbulence Intensity with Air Jets OFF - $x=35.75"$

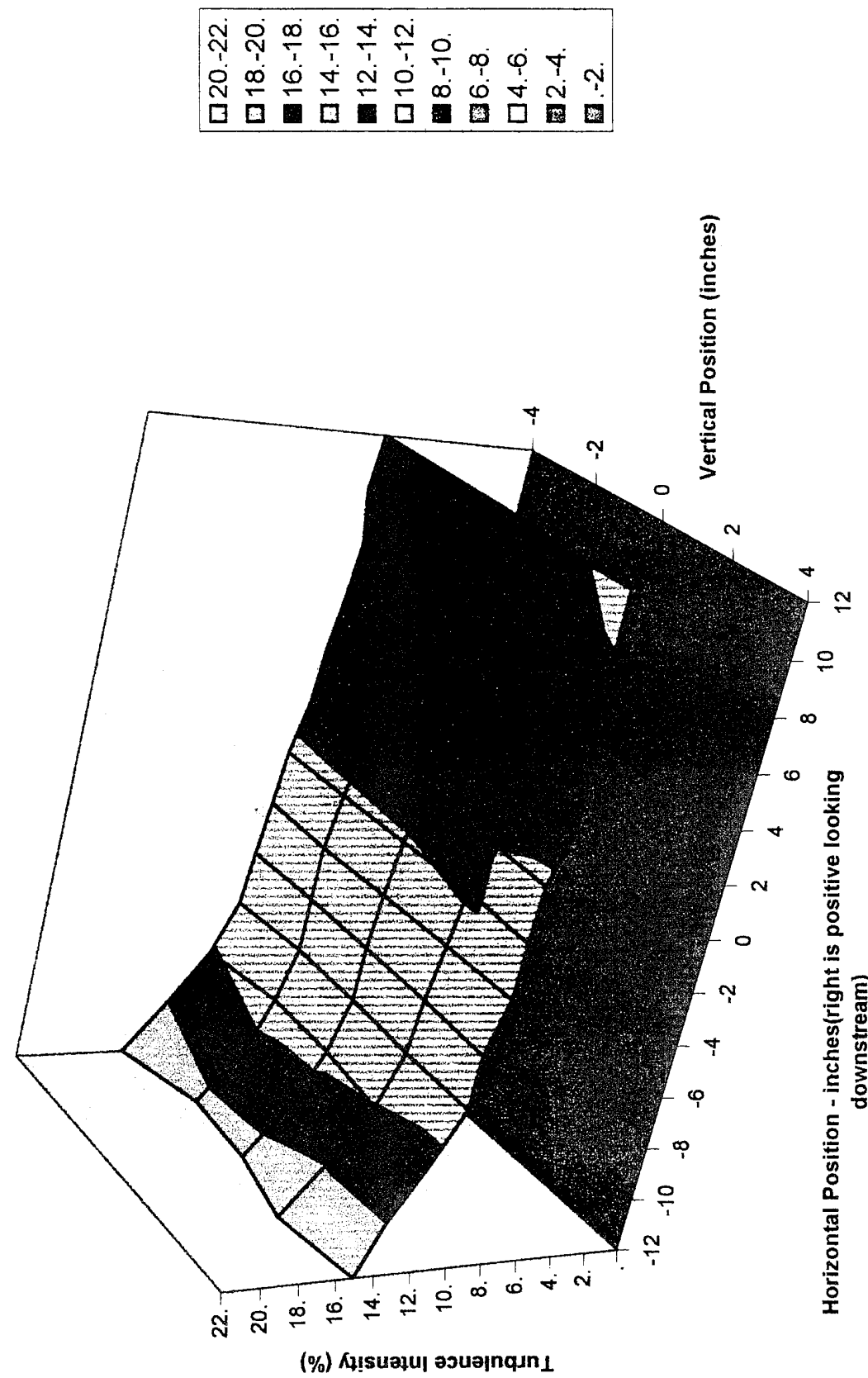
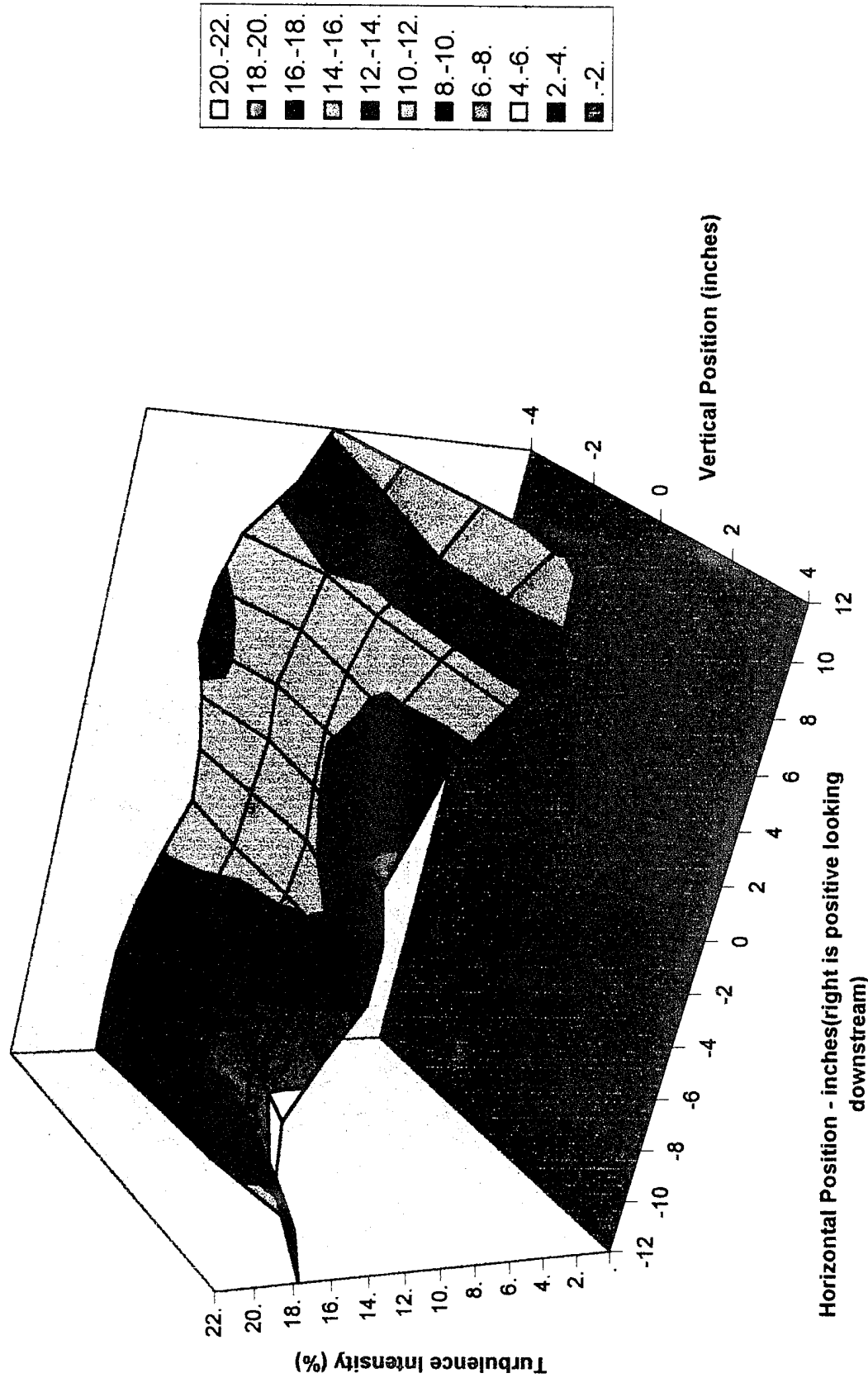


Chart3

Turbulence Intensity with Air Jets ON - $x=35.75"$



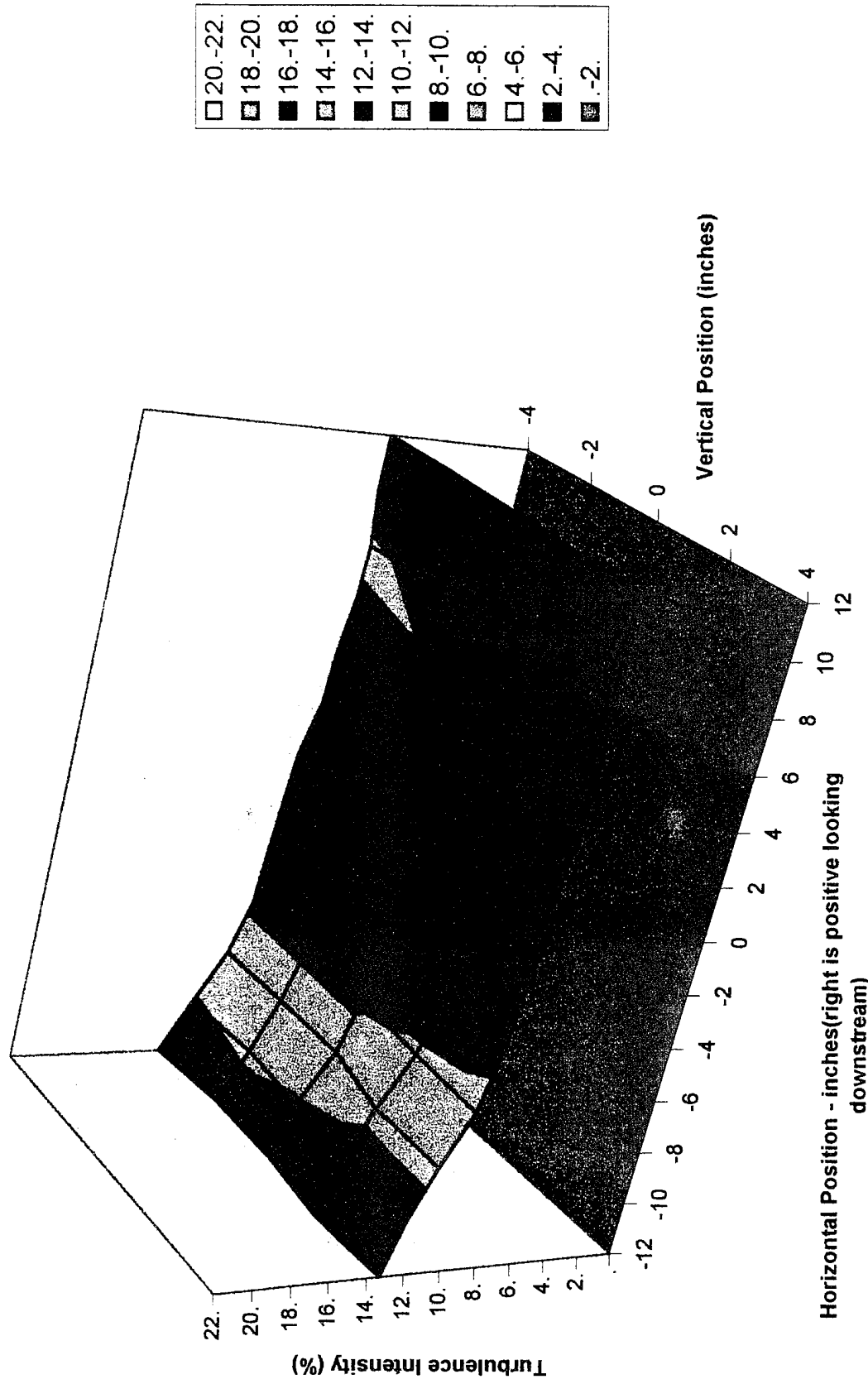
Turbulence Intensity with Air Jets OFF - x=40"

Chart3

Turbulence Intensity with Air Jets ON - $x=40''$

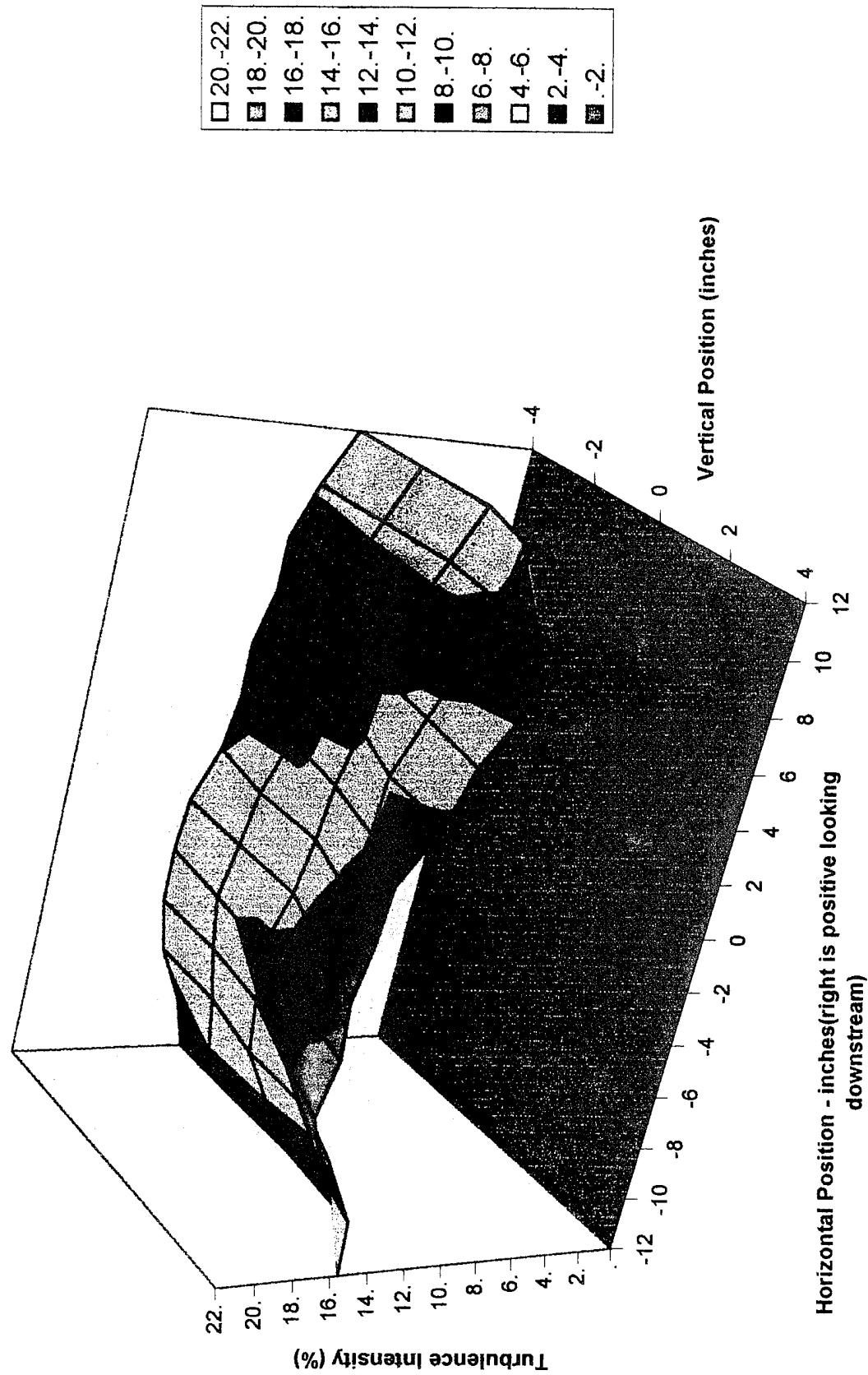


Chart3

Turbulence Intensity with Air Jets OFF - $x=45.5"$

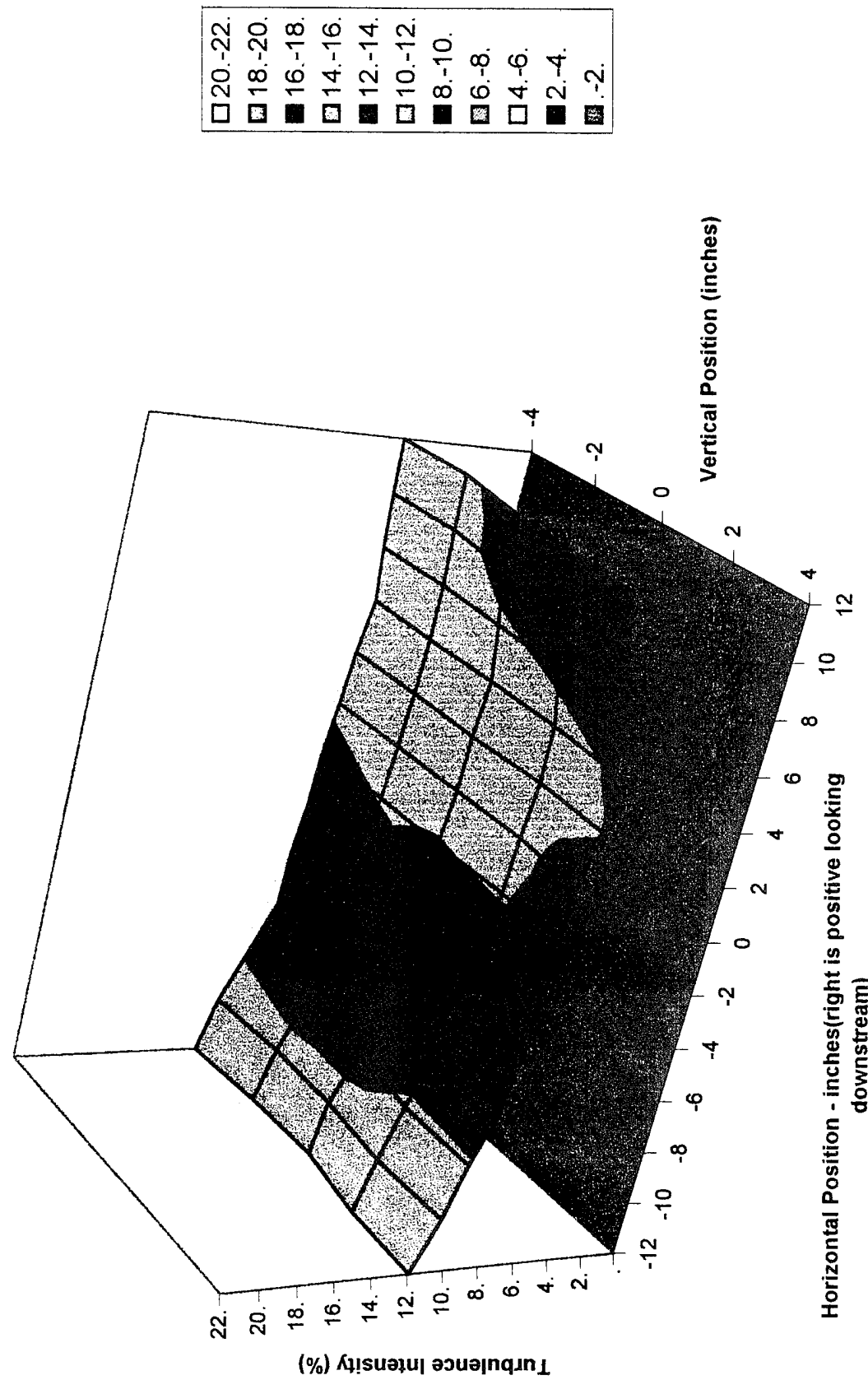


Chart3

Turbulence Intensity with Air Jets OFF - $x=52''$

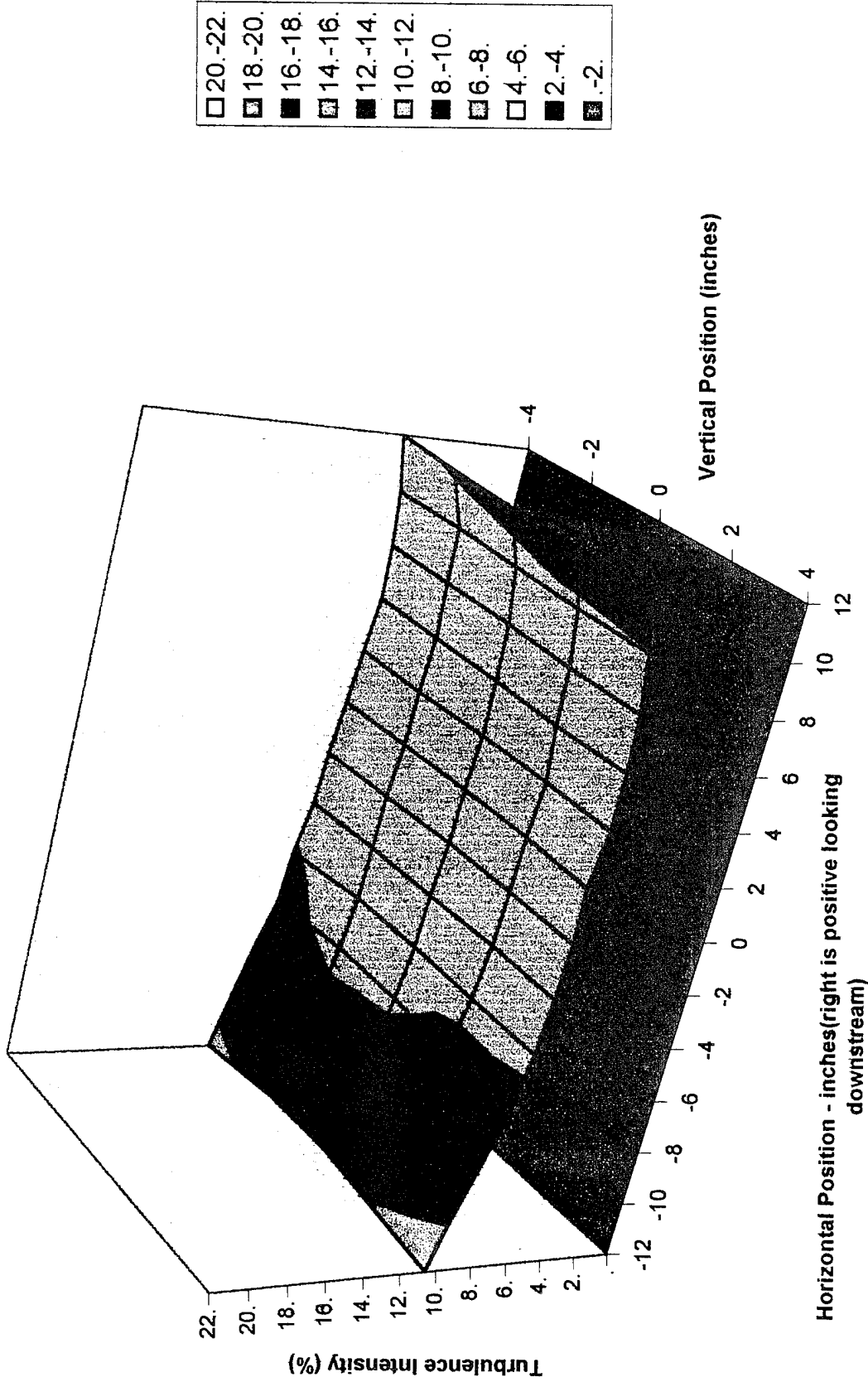


Chart3

Turbulence Intensity with Air Jets ON - $x=52"$

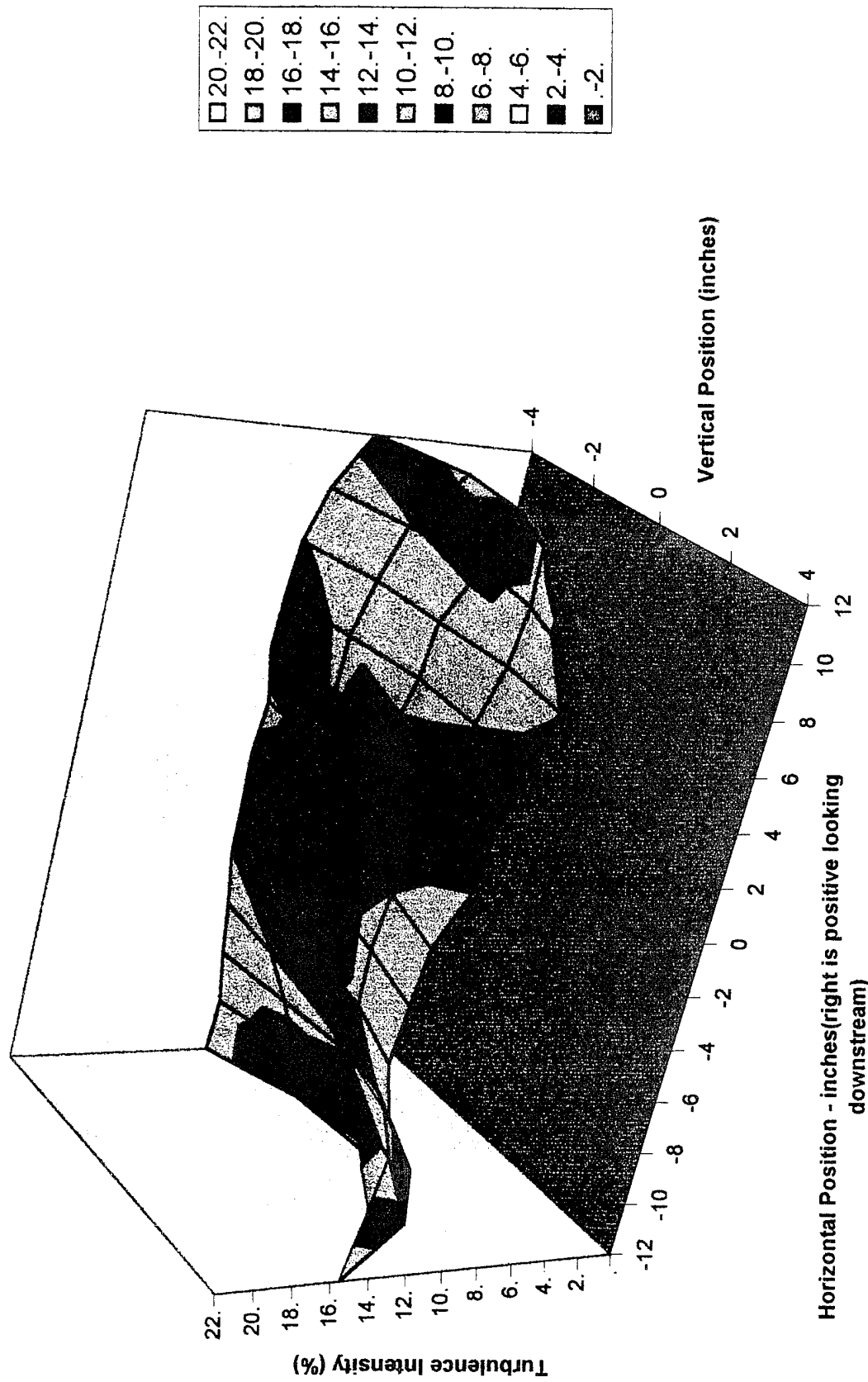


Chart3

Turbulence Intensity with Air Jets OFF - $x=67.5''$

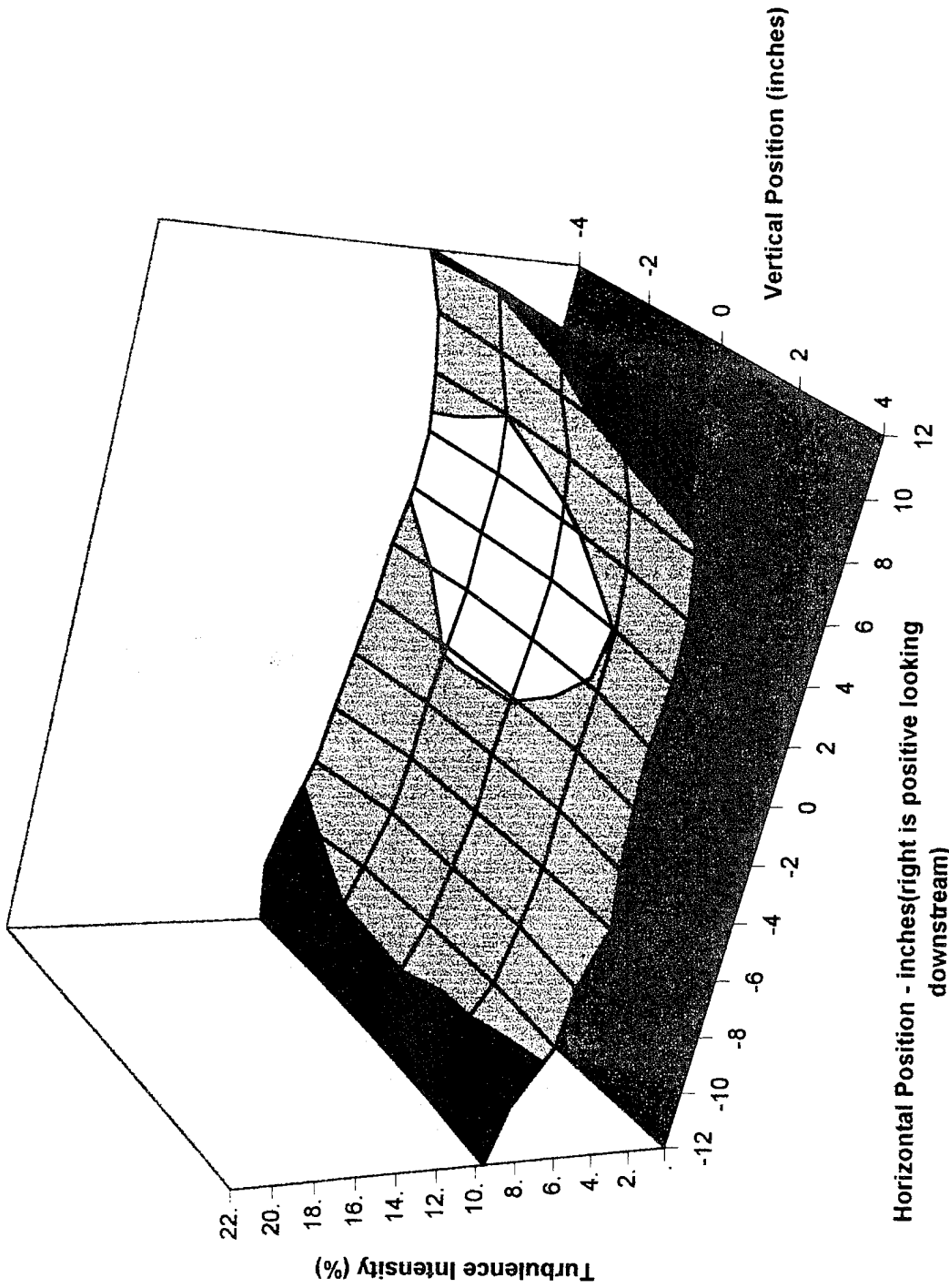
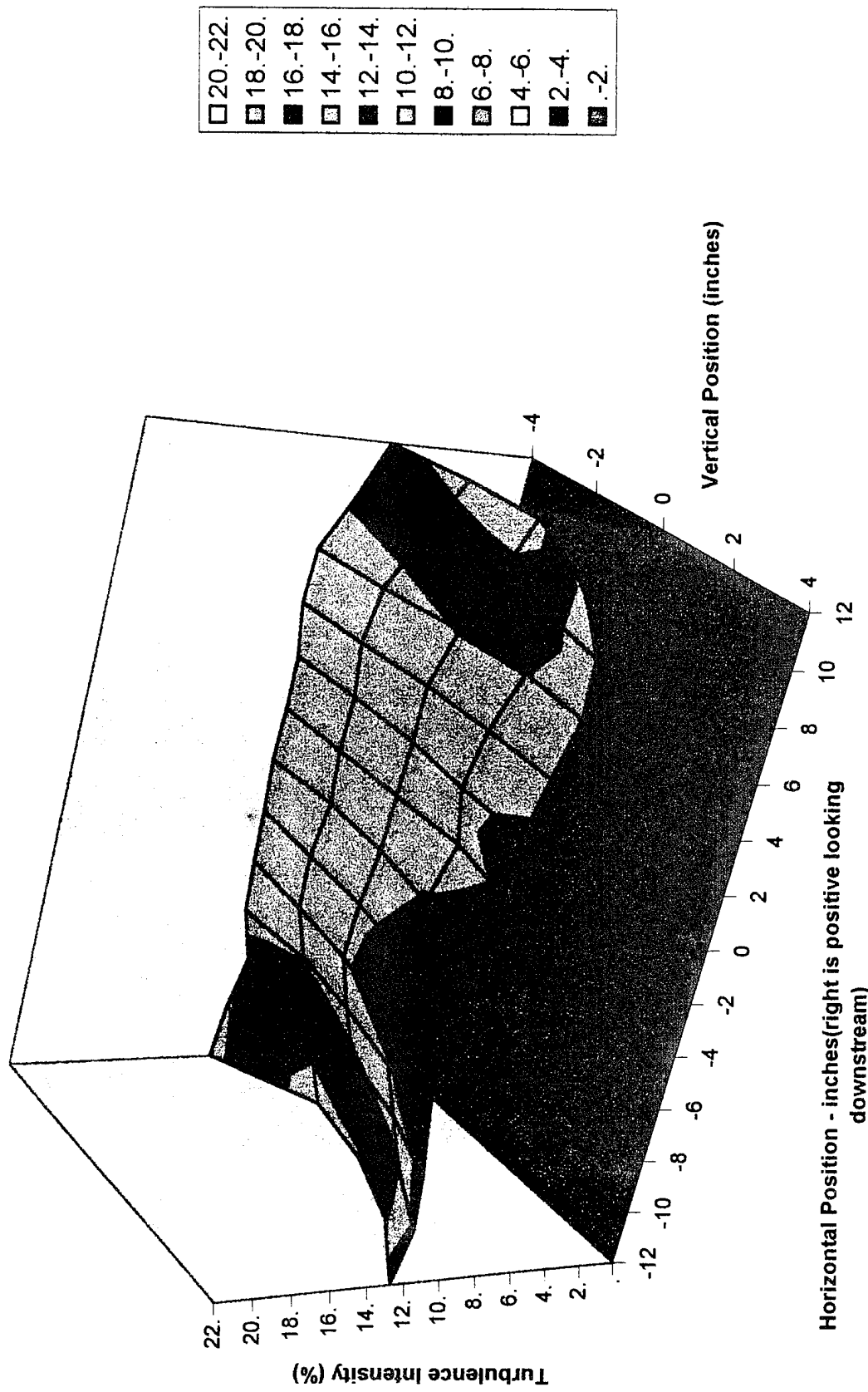


Chart3

Turbulence Intensity with Air Jets ON - $x=67.5''$



APPENDIX E

Pitot Tube vs Hot Wire Comparisons

Chart4

**Comparison of Velocities Measured by Pitot and Hot Wire
with Air Jets OFF at Tunnel Mid-span - $x=32"$**

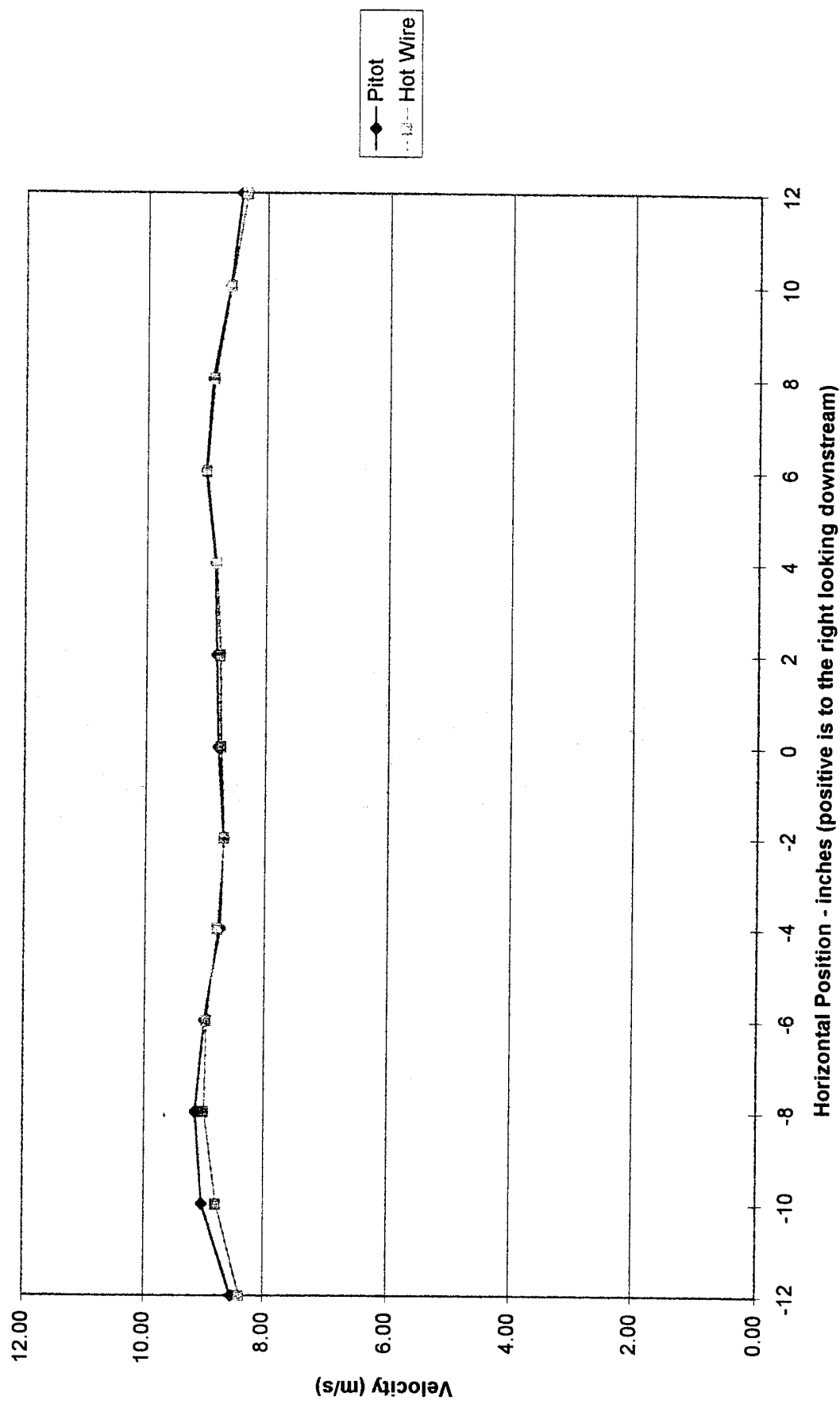


Chart4

**Comparison of Velocities Measured by Pitot and Hot Wire
with Air Jets ON at Tunnel Mid-span - $x=32"$**

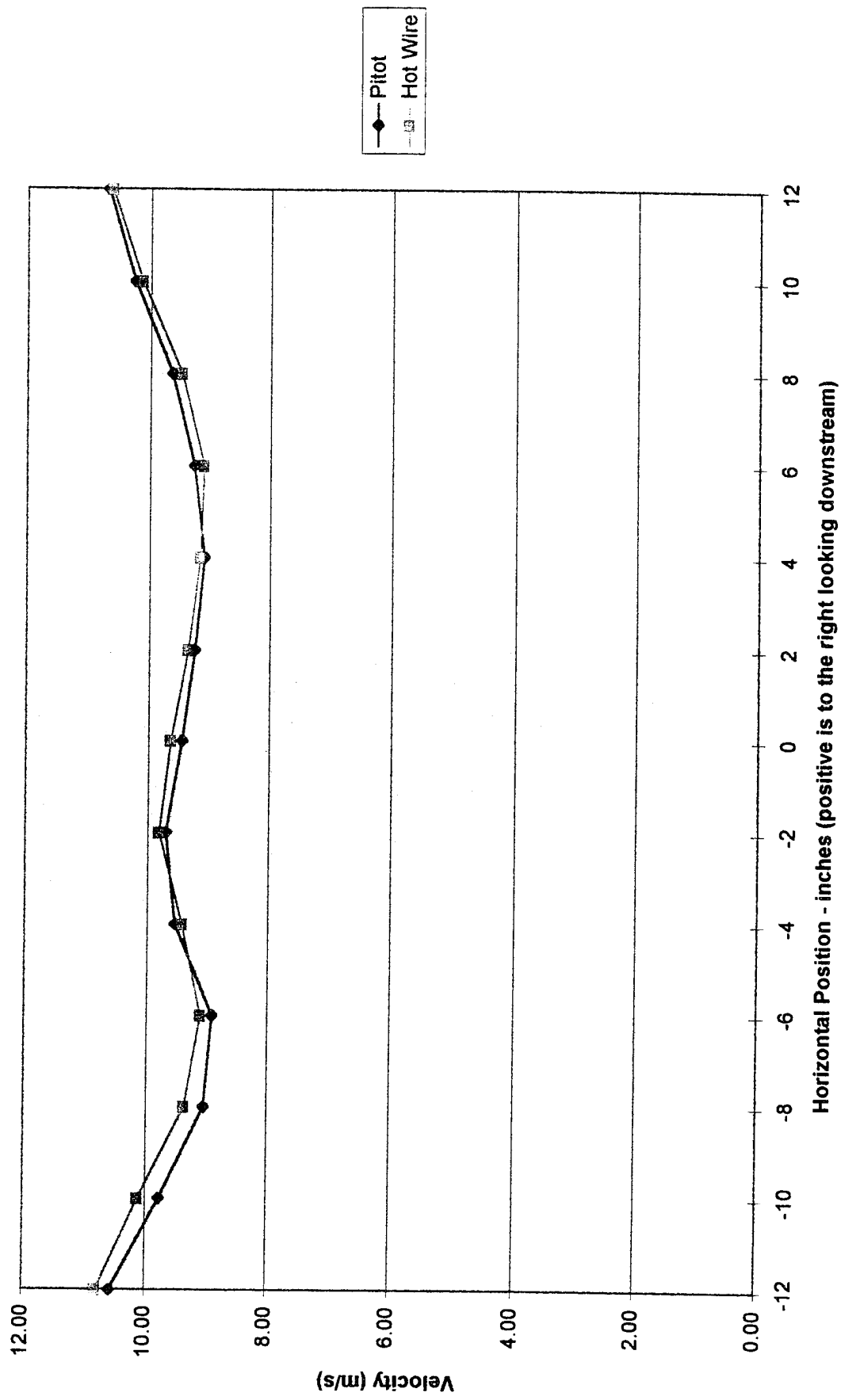
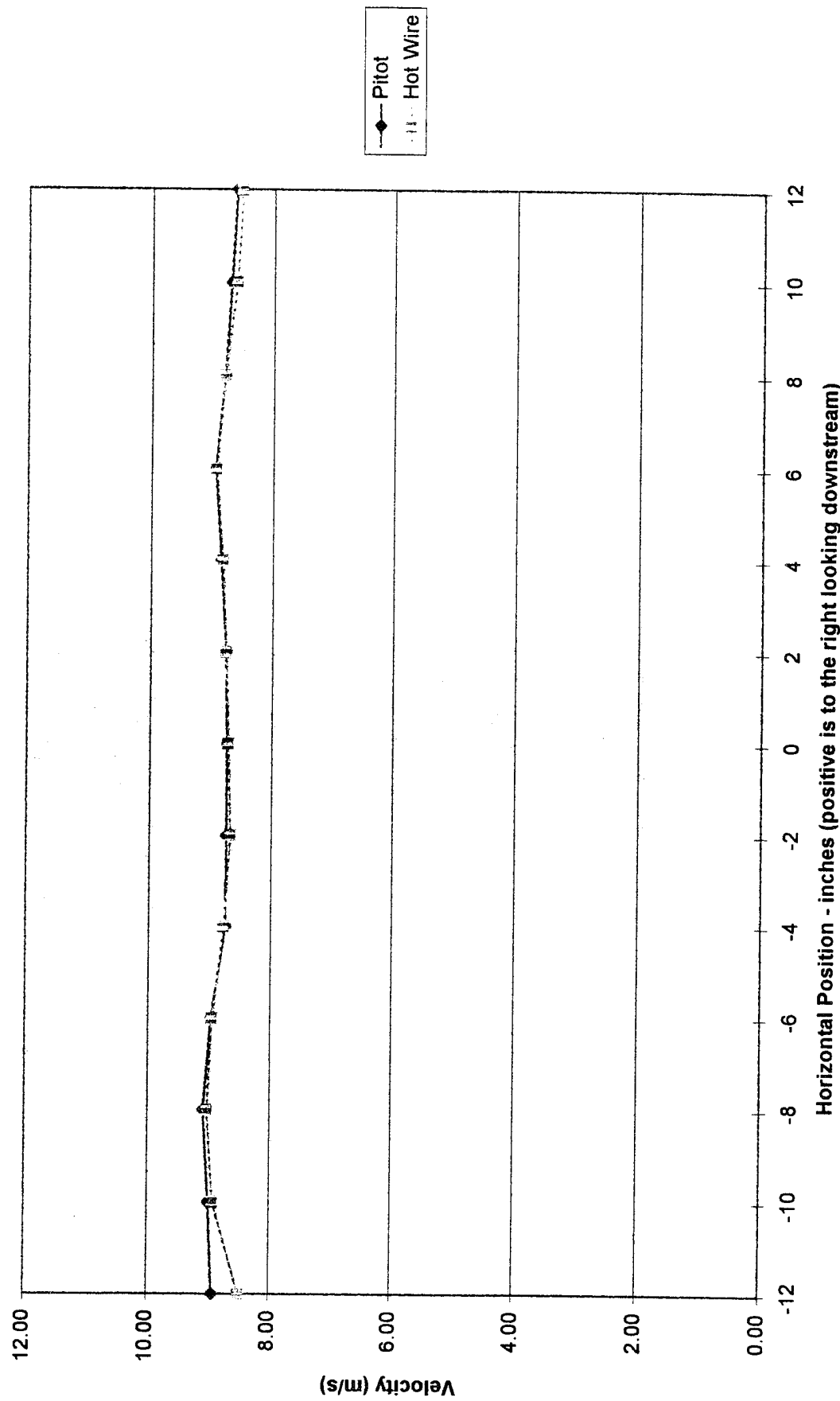


Chart4

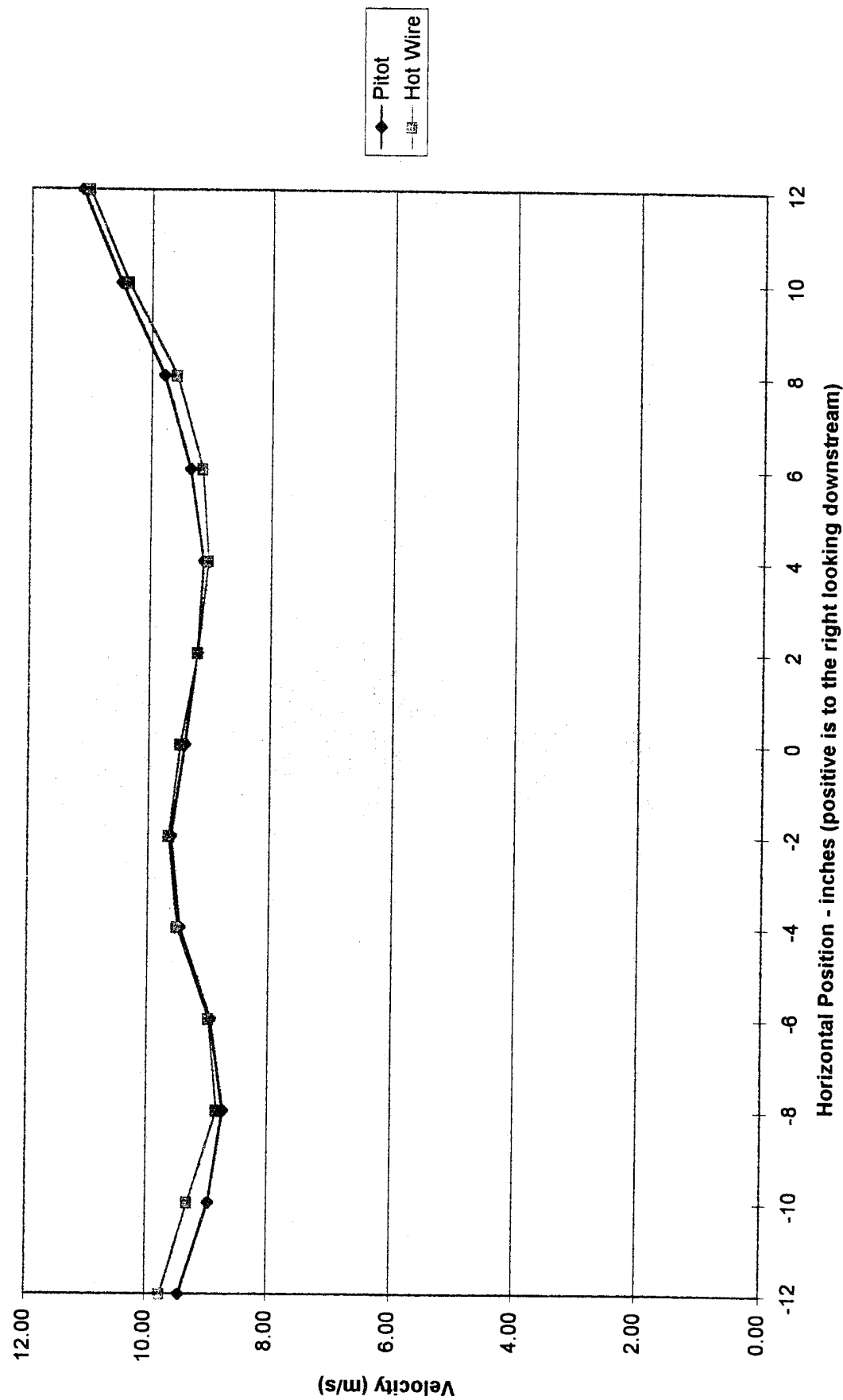
**Comparison of Velocities Measured by Pitot and Hot Wire
with Air Jets OFF at Tunnel Mid-span - $x=35.75''$**



Horizontal Position - inches (positive is to the right looking downstream)

Chart4

**Comparison of Velocities Measured by Pitot and Hot Wire
with Air Jets ON at Tunnel Mid-span - $x=35.75''$**



Horizontal Position - inches (positive is to the right looking downstream)

Chart4

**Comparison of Velocities Measured by Pitot and Hot Wire
with Air Jets OFF at Tunnel Mid-span - $x=40''$**

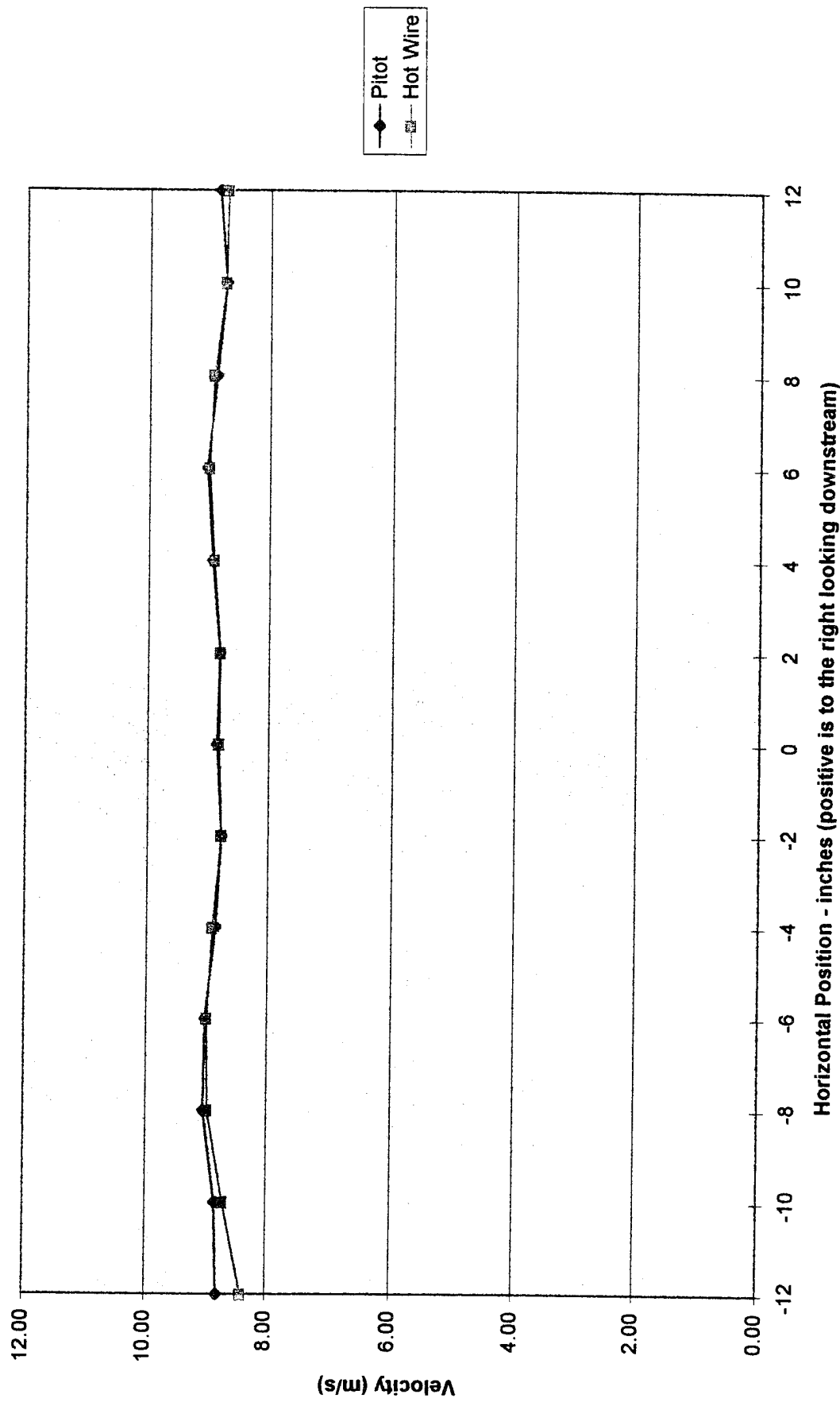
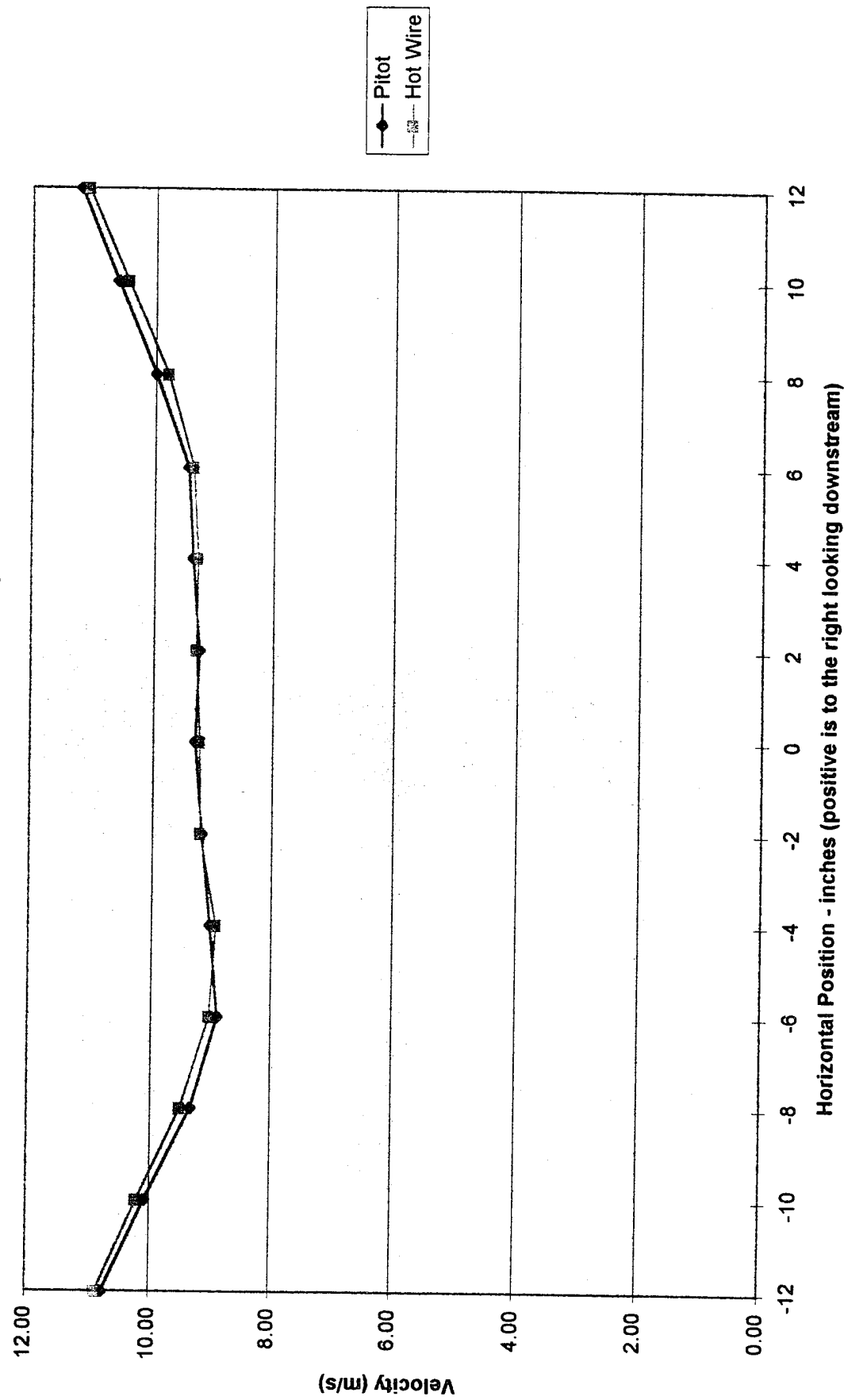


Chart4

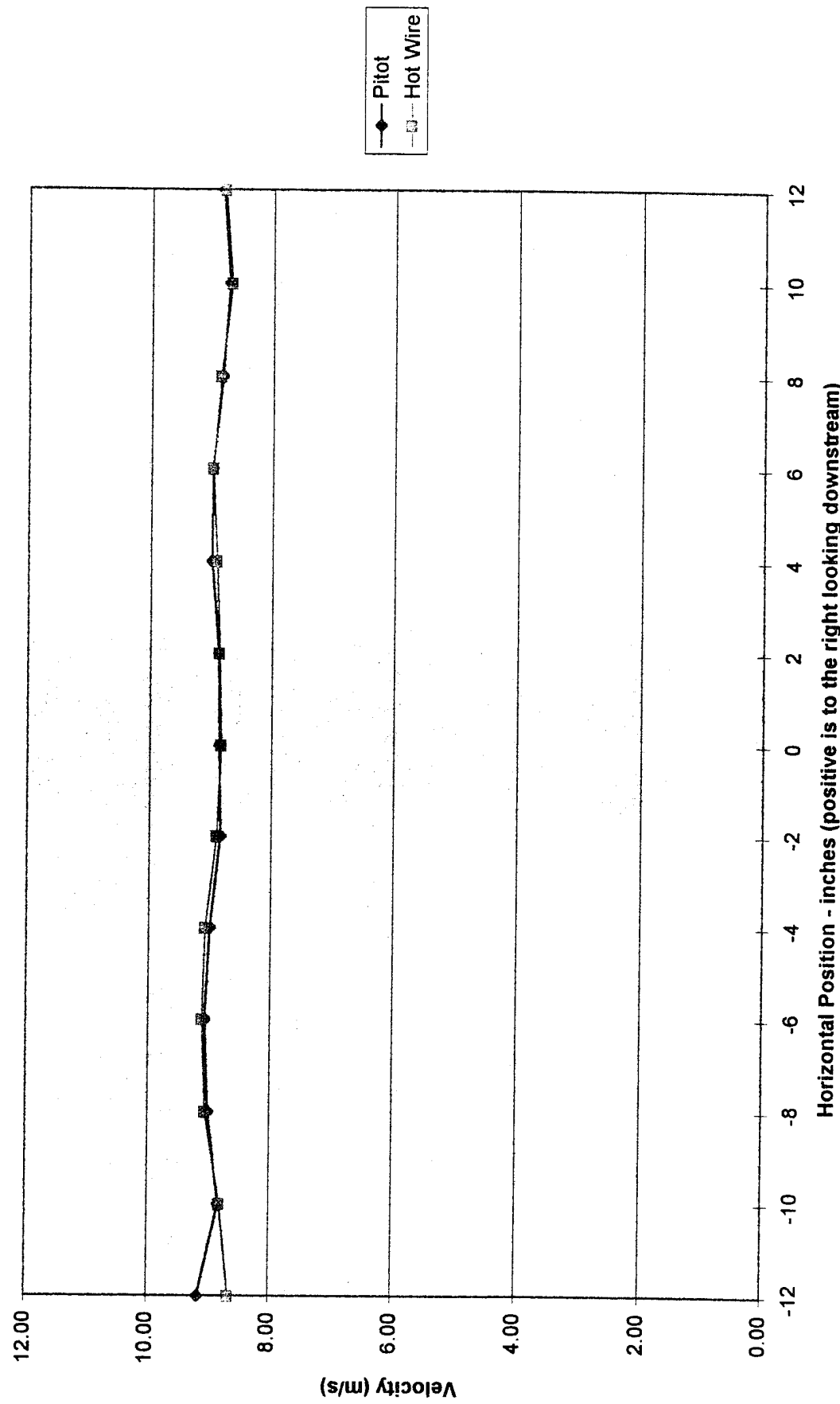
**Comparison of Velocities Measured by Pitot and Hot Wire
with Air Jets ON at Tunnel Mid-span - $x=40"$**



Horizontal Position - inches (positive is to the right looking downstream)

Chart4

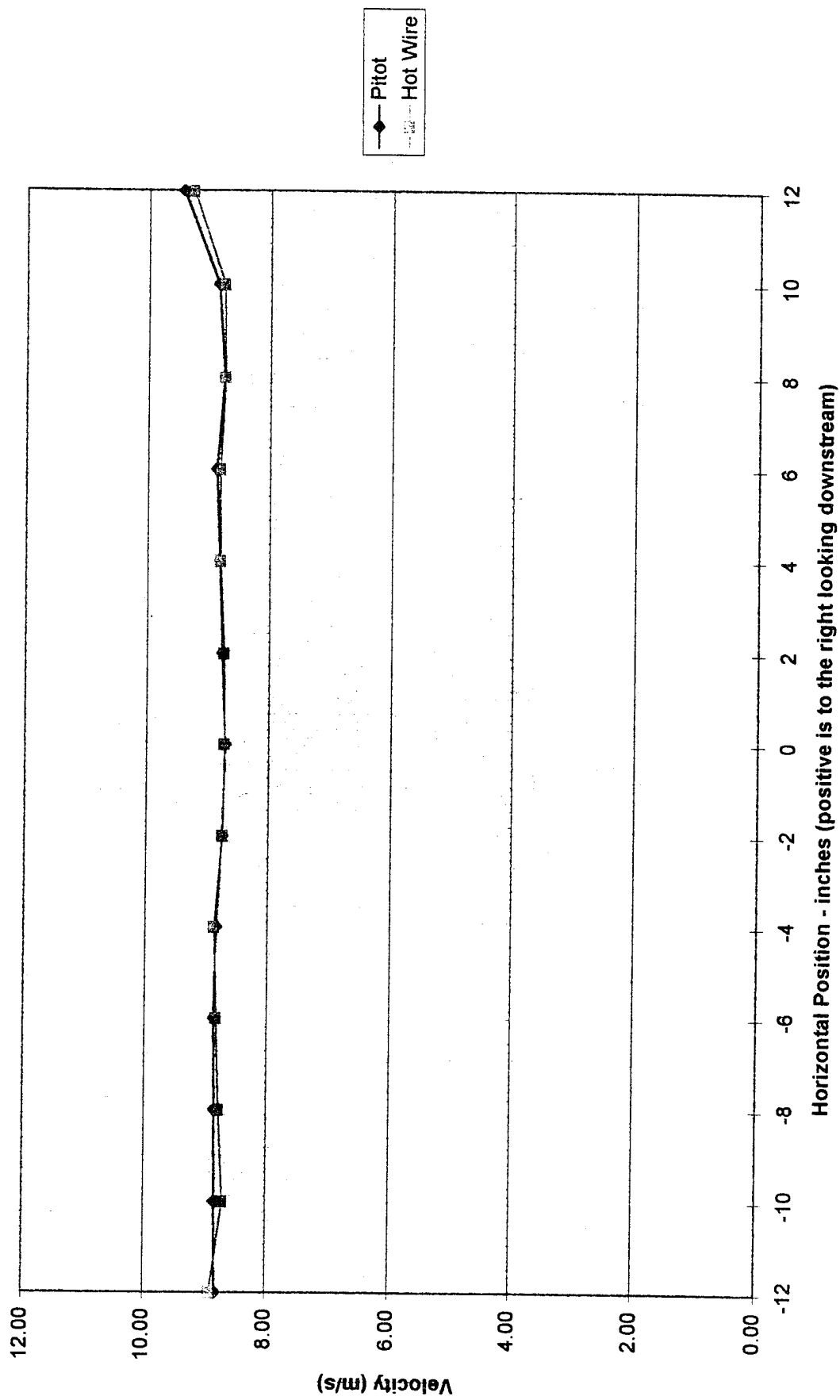
**Comparison of Velocities Measured by Pitot and Hot Wire
with Air Jets OFF at Tunnel Mid-span - $x=45.5''$**



Horizontal Position - inches (positive is to the right looking downstream)

Chart4

**Comparison of Velocities Measured by Pitot and Hot Wire
with Air Jets OFF at Tunnel Mid-span - $x=52''$**



Horizontal Position - inches (positive is to the right looking downstream)

Chart4

**Comparison of Velocities Measured by Pitot and Hot Wire
with Air Jets ON at Tunnel Mid-span - x=52"**

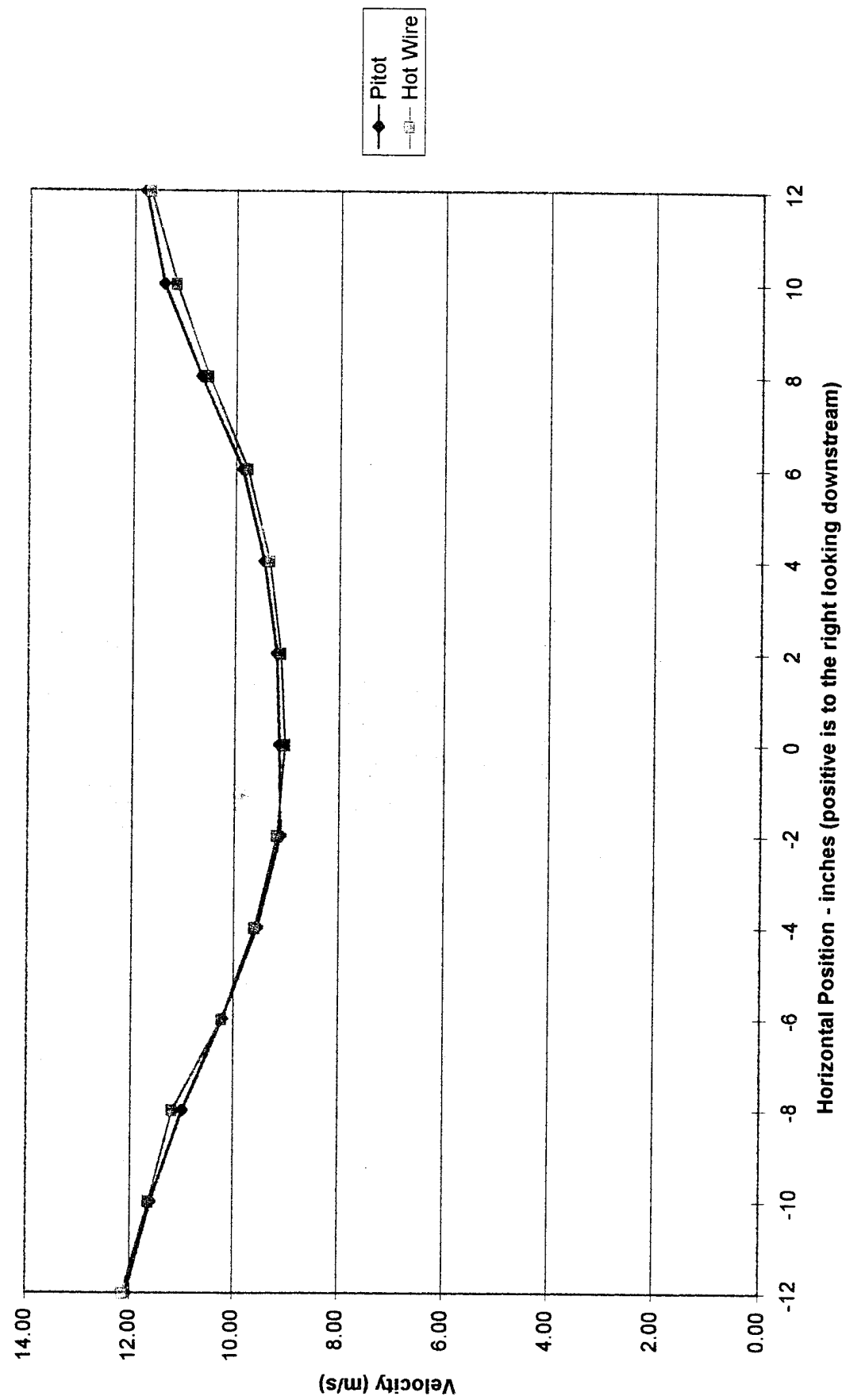


Chart4

**Comparison of Velocities Measured by Pitot and Hot Wire
with Air Jets OFF at Tunnel Mid-span - $x=67.5"$**

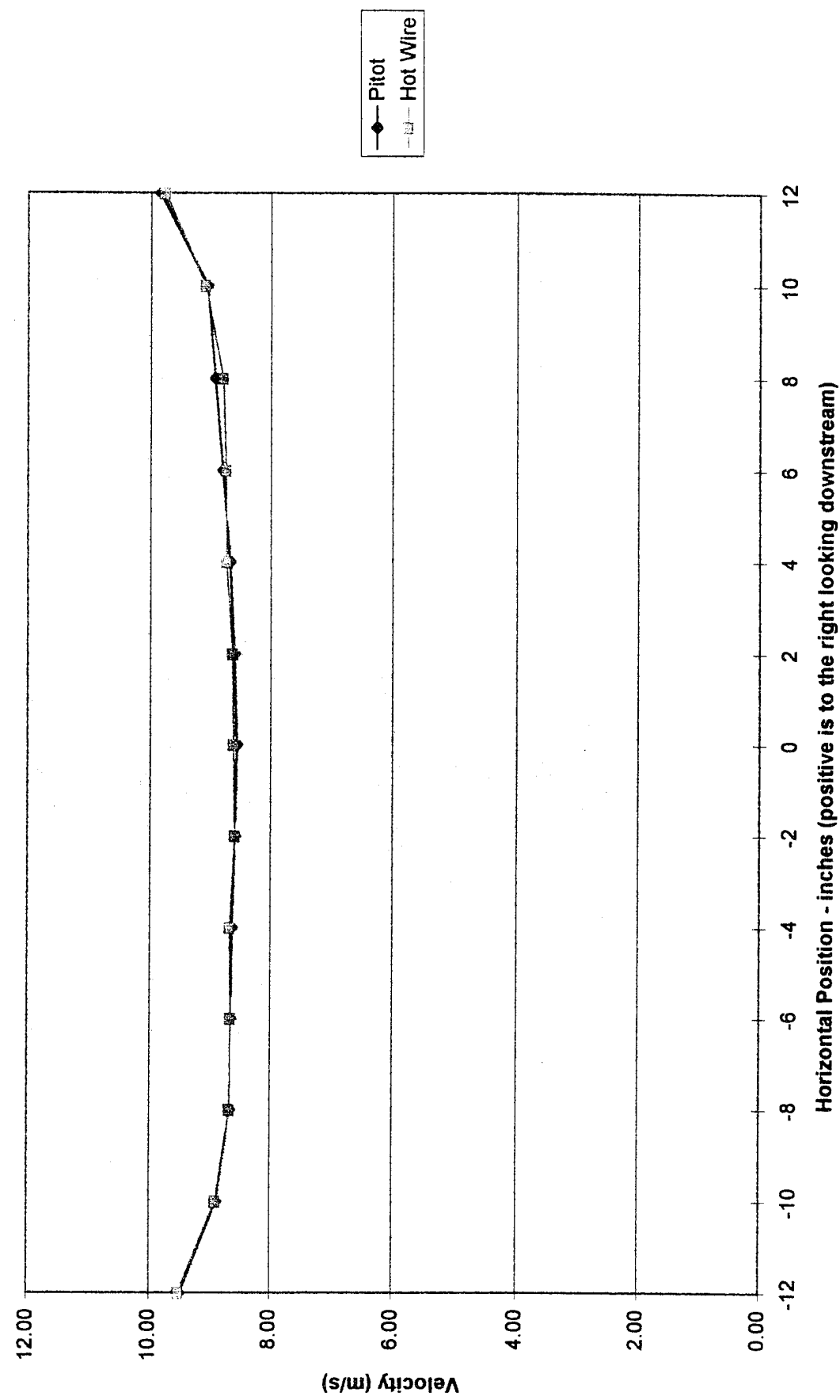
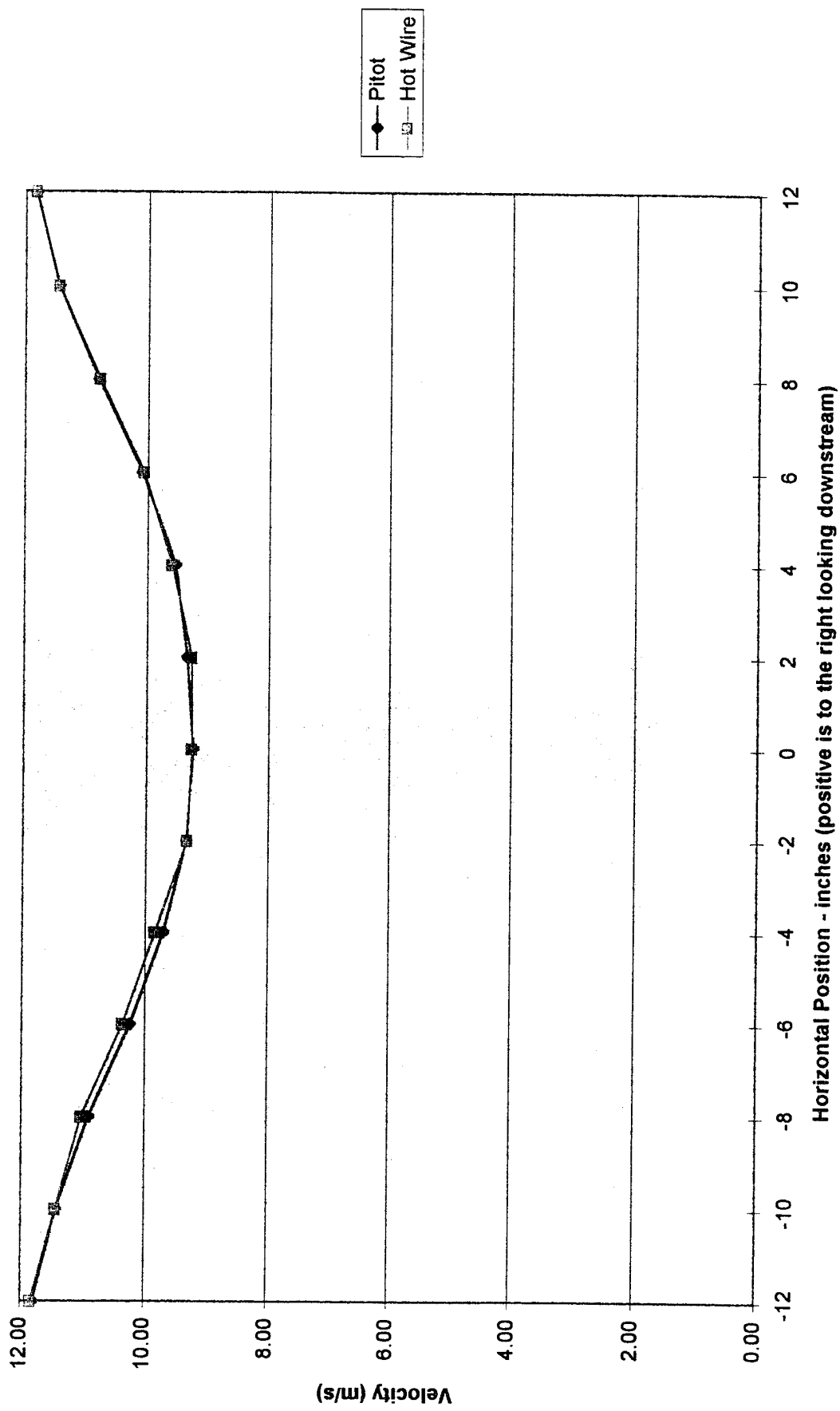


Chart4

**Comparison of Velocities Measured by Pitot and Hot Wire
with Air Jets ON at Tunnel Mid-span - $x=67.5"$ - Sep 1**



Horizontal Position - inches (positive is to the right looking downstream)

APPENDIX F

Air Jet Induced Turbulence Effects

Chart5

Effect of Air Jets on Turbulence Intensity - $x=32"$

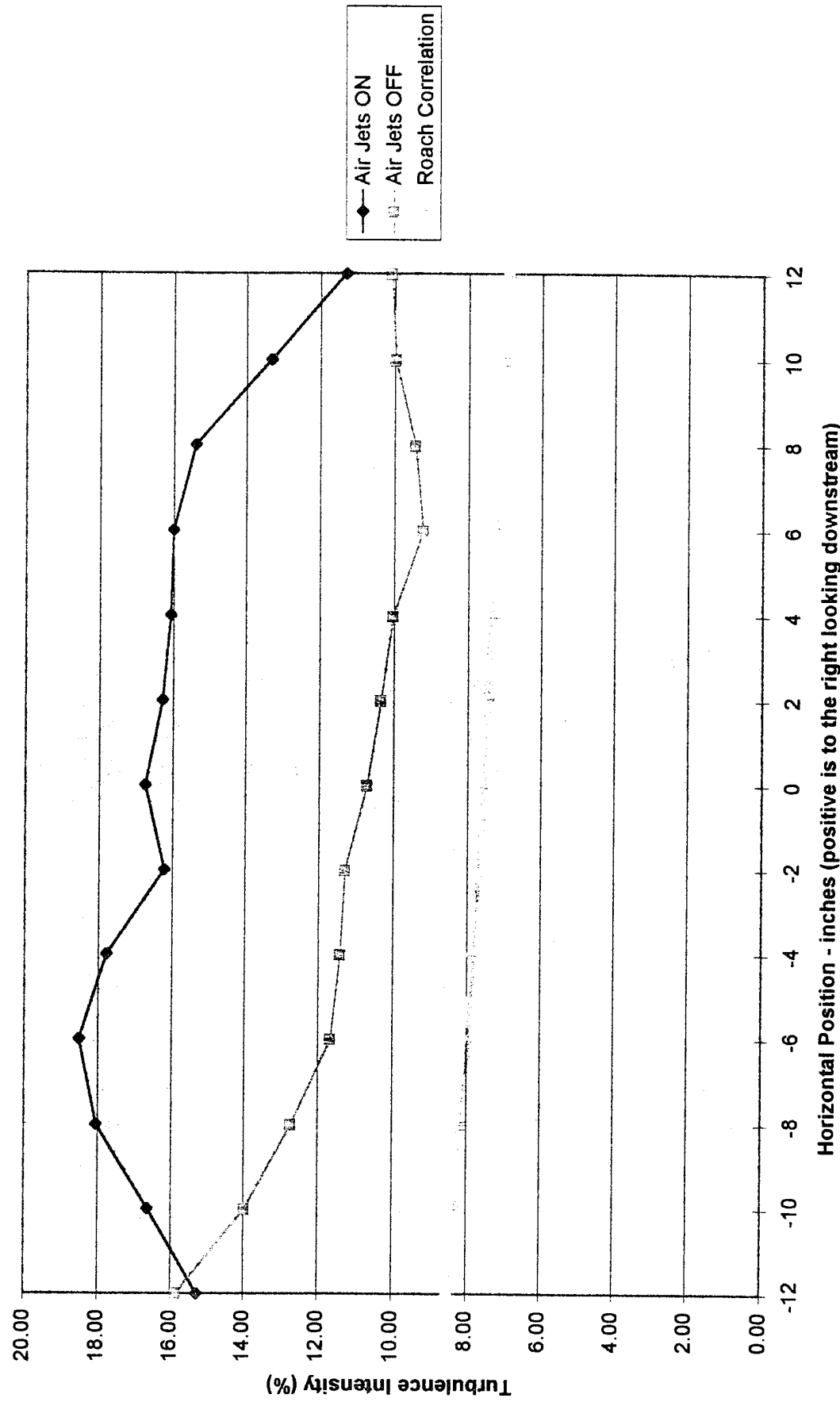


Chart5

Effect of Air Jets on Turbulence Intensity - $x=32"$

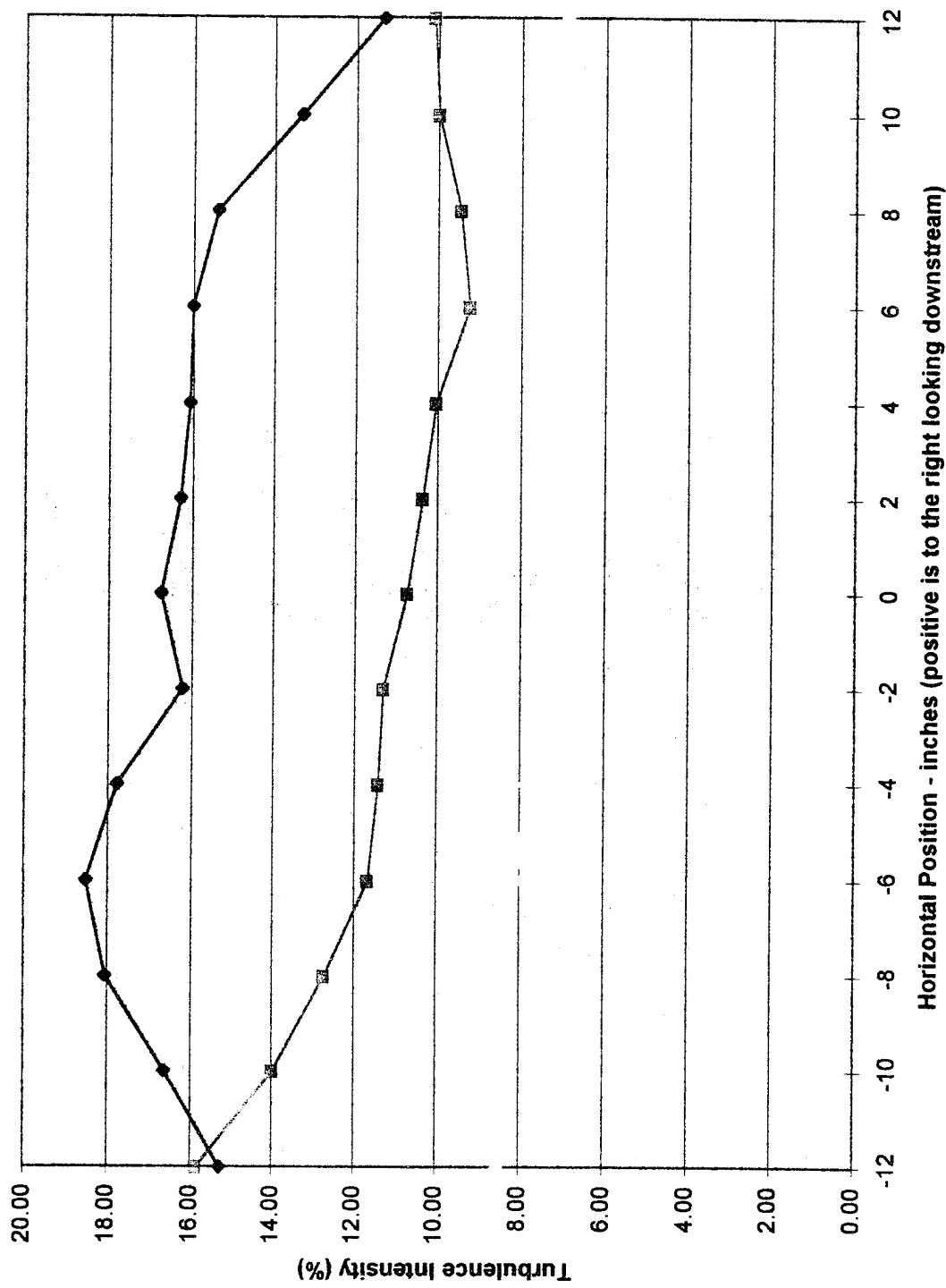


Chart5

Effect of Air Jets on Turbulence Intensity - $x=35.75''$

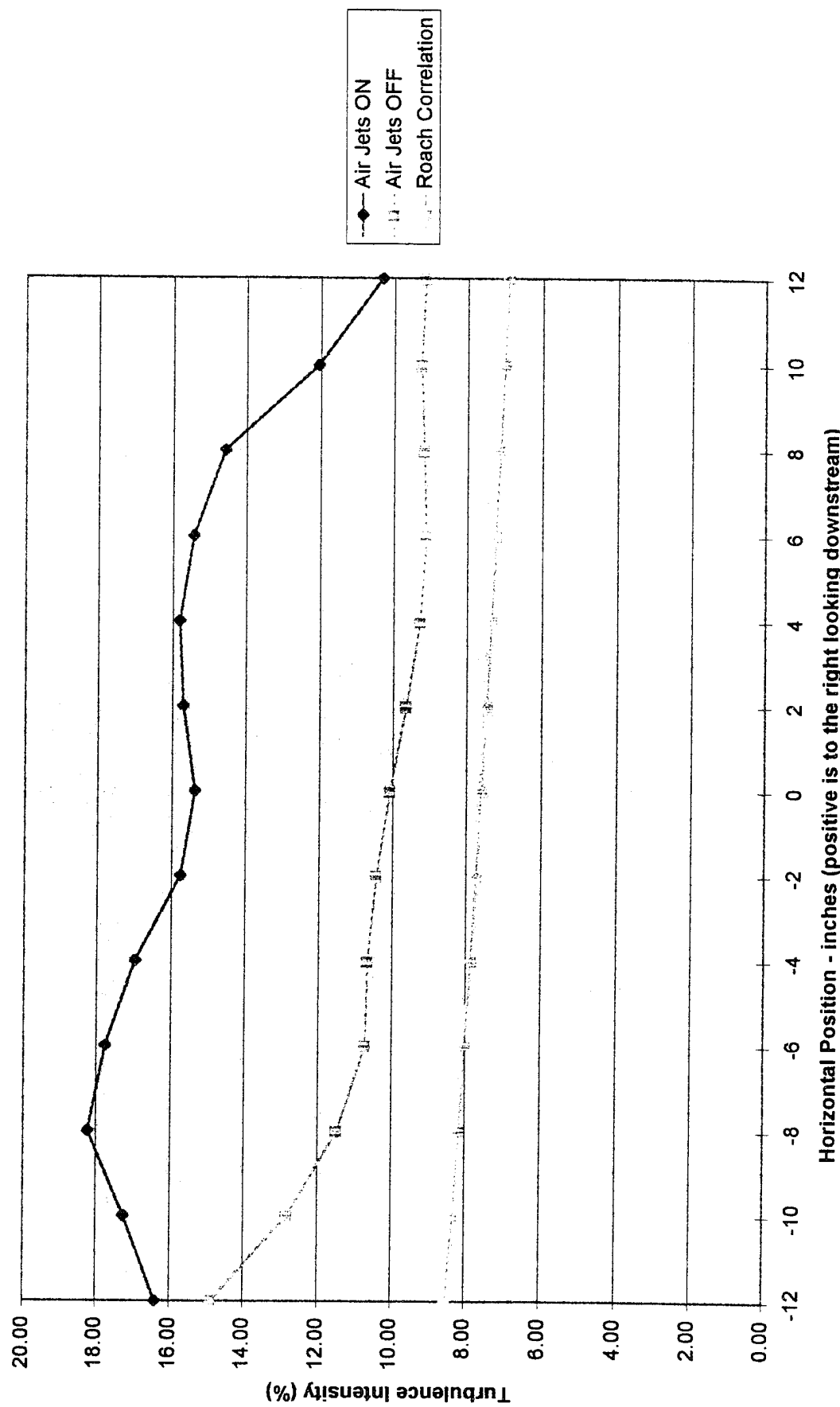


Chart5

Effect of Air Jets on Turbulence Intensity - $x=35.75"$

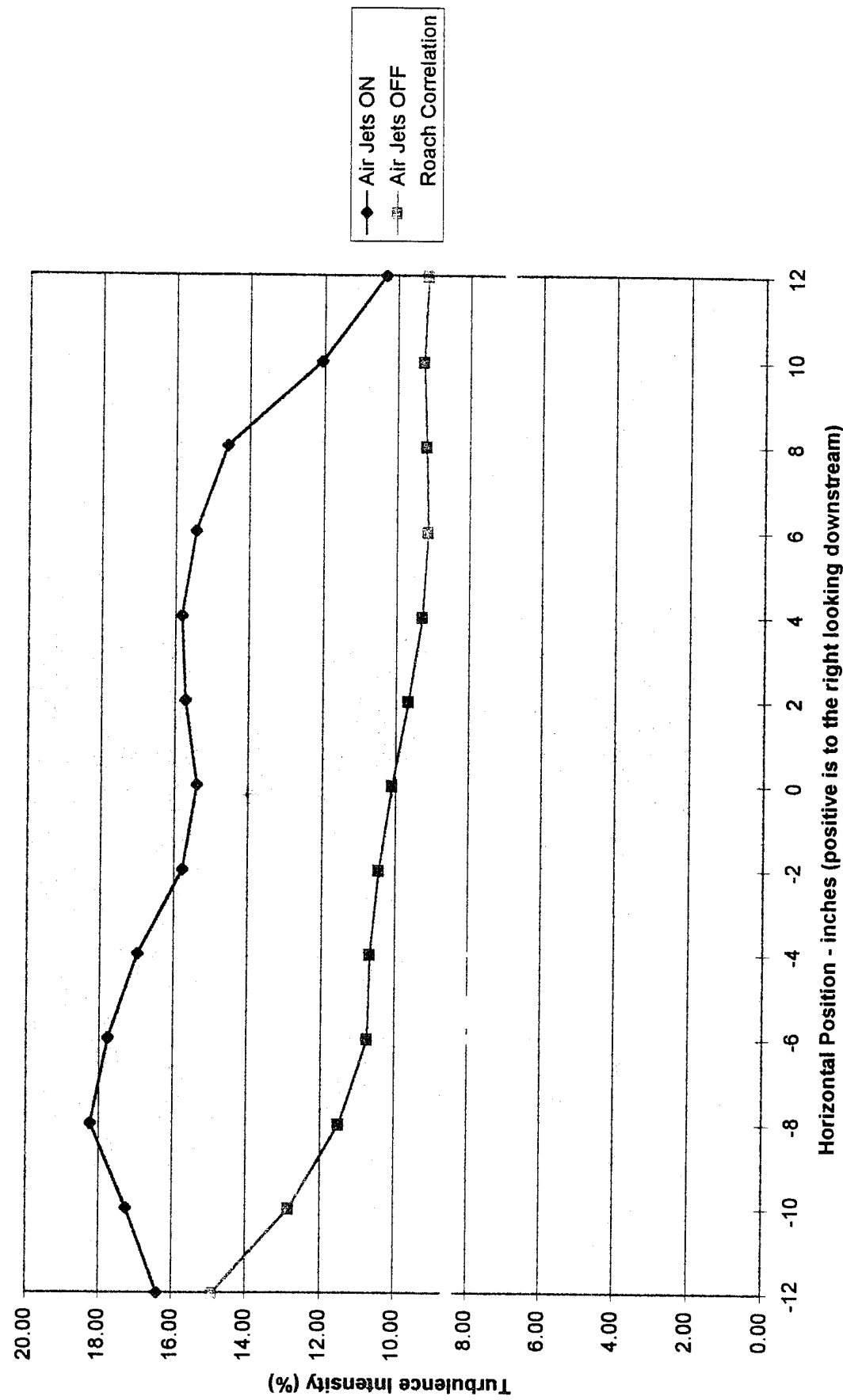
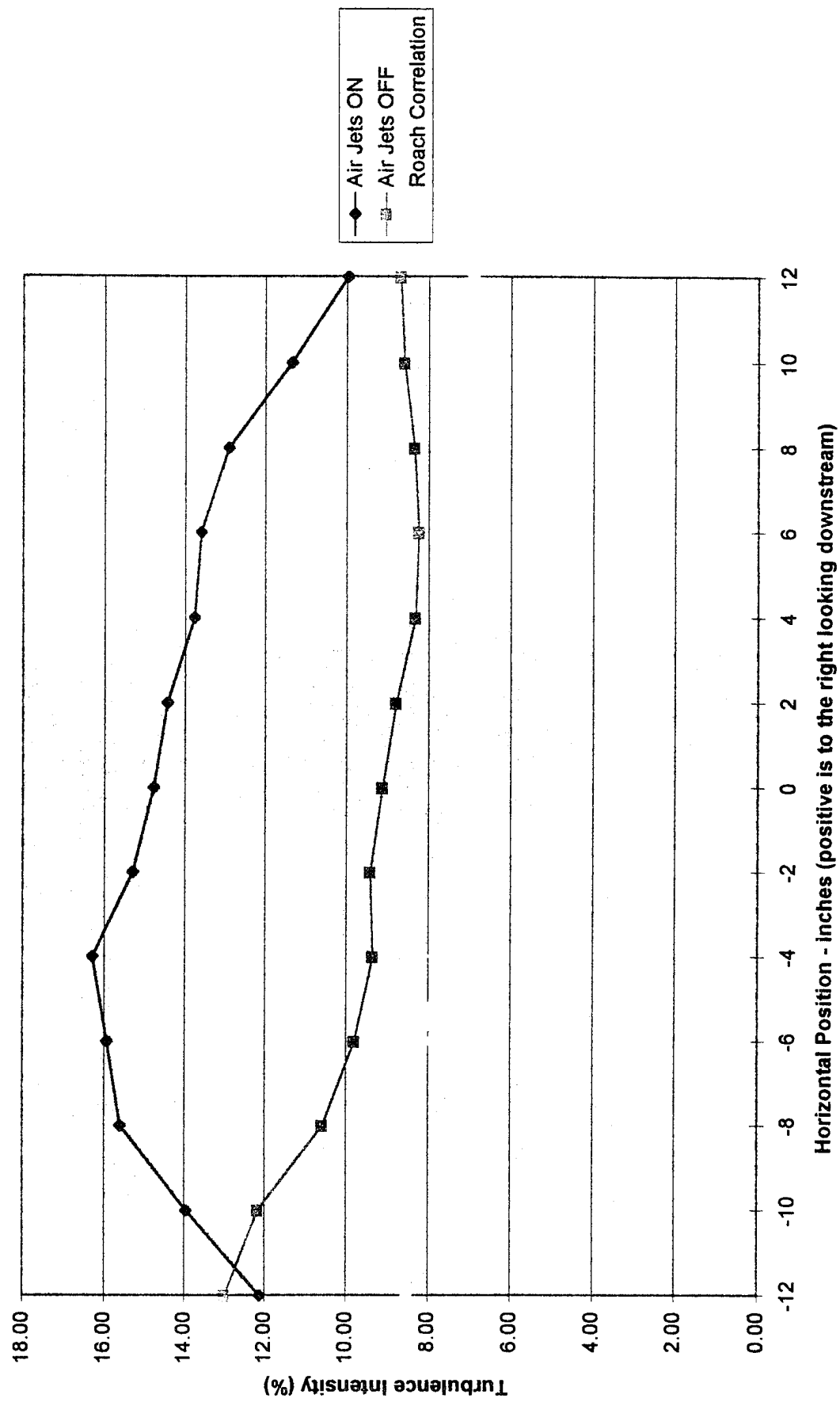


Chart5

Effect of Air Jets on Turbulence Intensity - $x=40"$



—◆— Air Jets ON
—□— Air Jets OFF
Roach Correlation

Chart5

Effect of Air Jets on Turbulence Intensity - $x=40''$

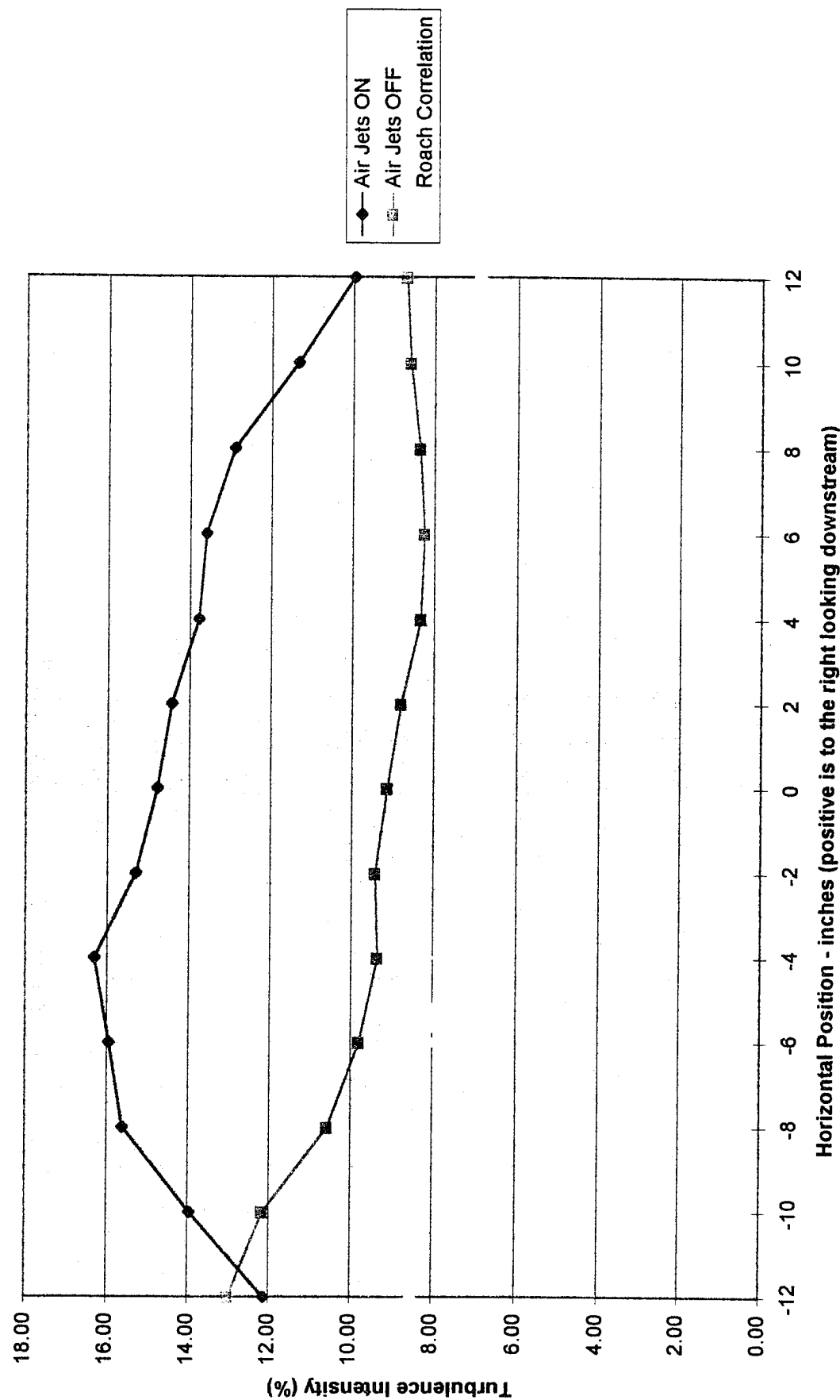
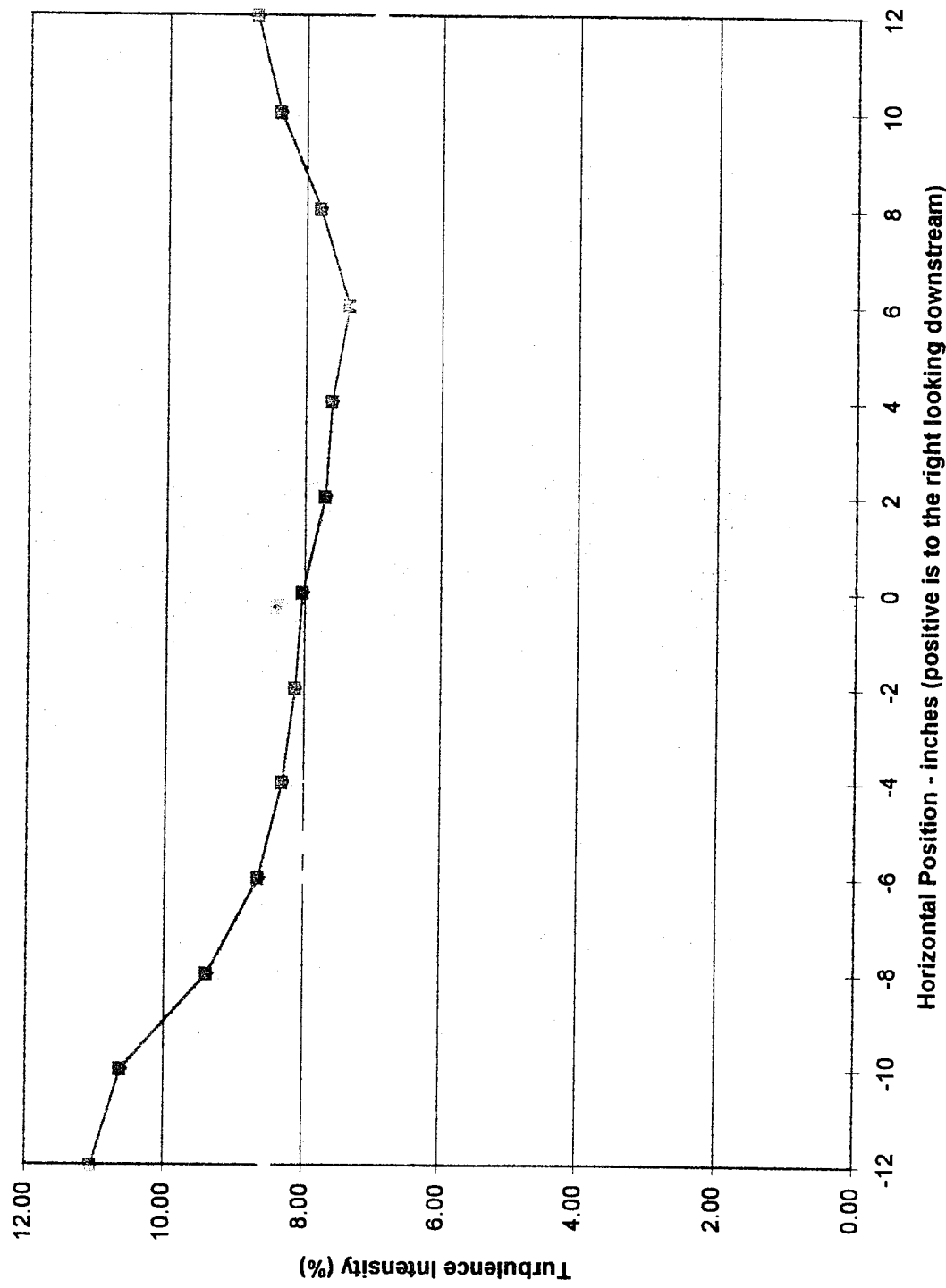


Chart5

Effect of Air Jets on Turbulence Intensity - x=45.5"



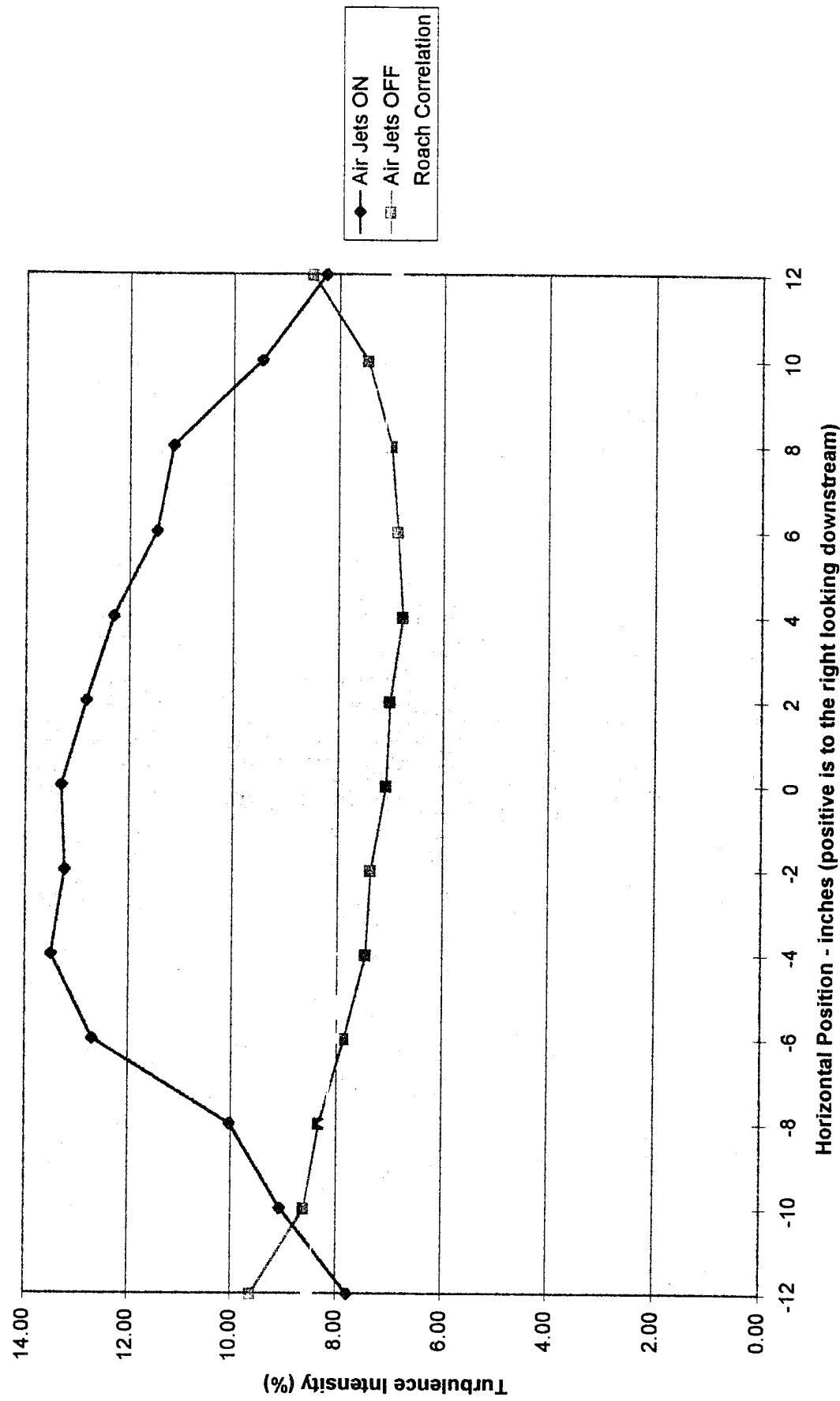
Effect of Air Jets on Turbulence Intensity - x=52"

Chart5

Effect of Air Jets on Turbulence Intensity - x=52"

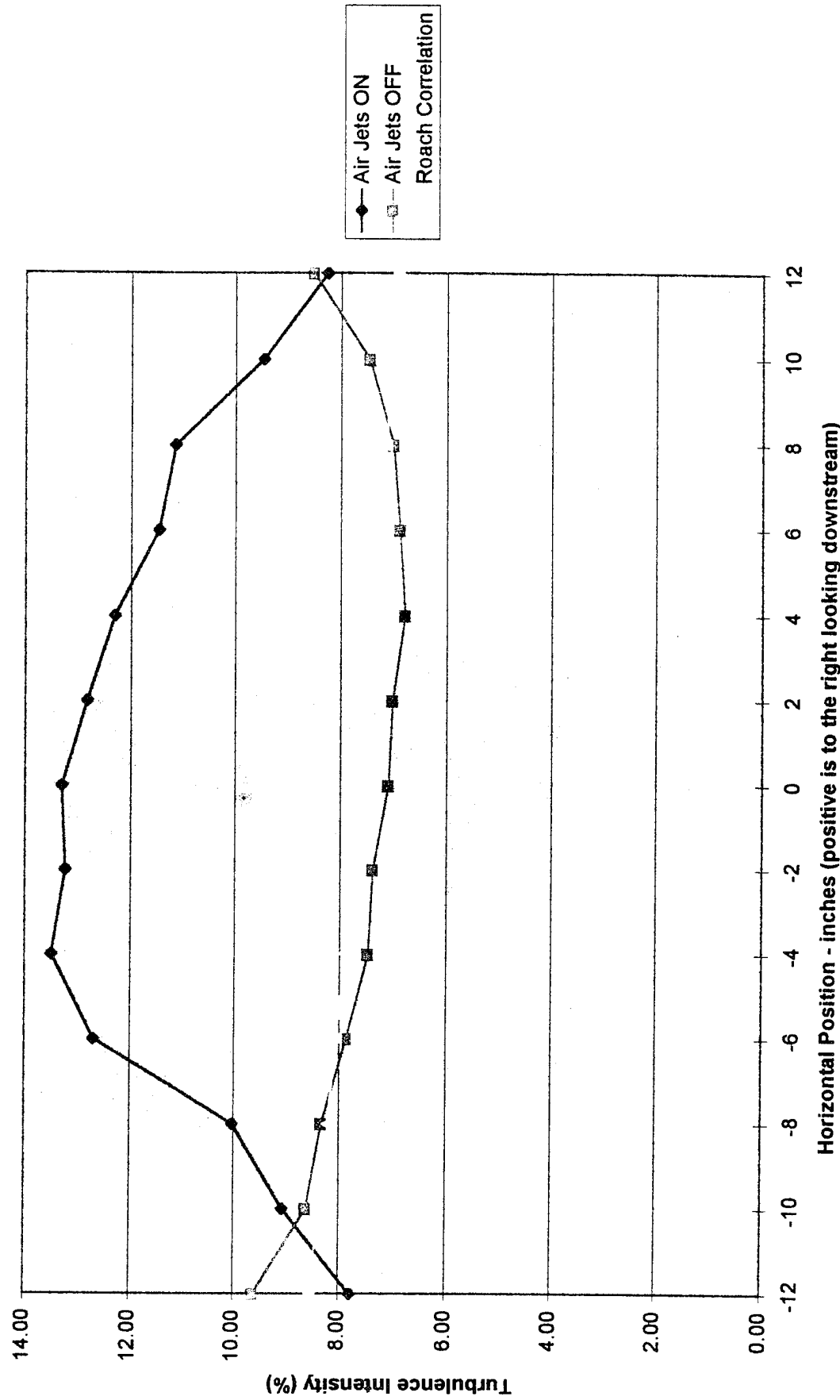


Chart5

Effect of Air Jets on Turbulence Intensity - $x=67.5"$

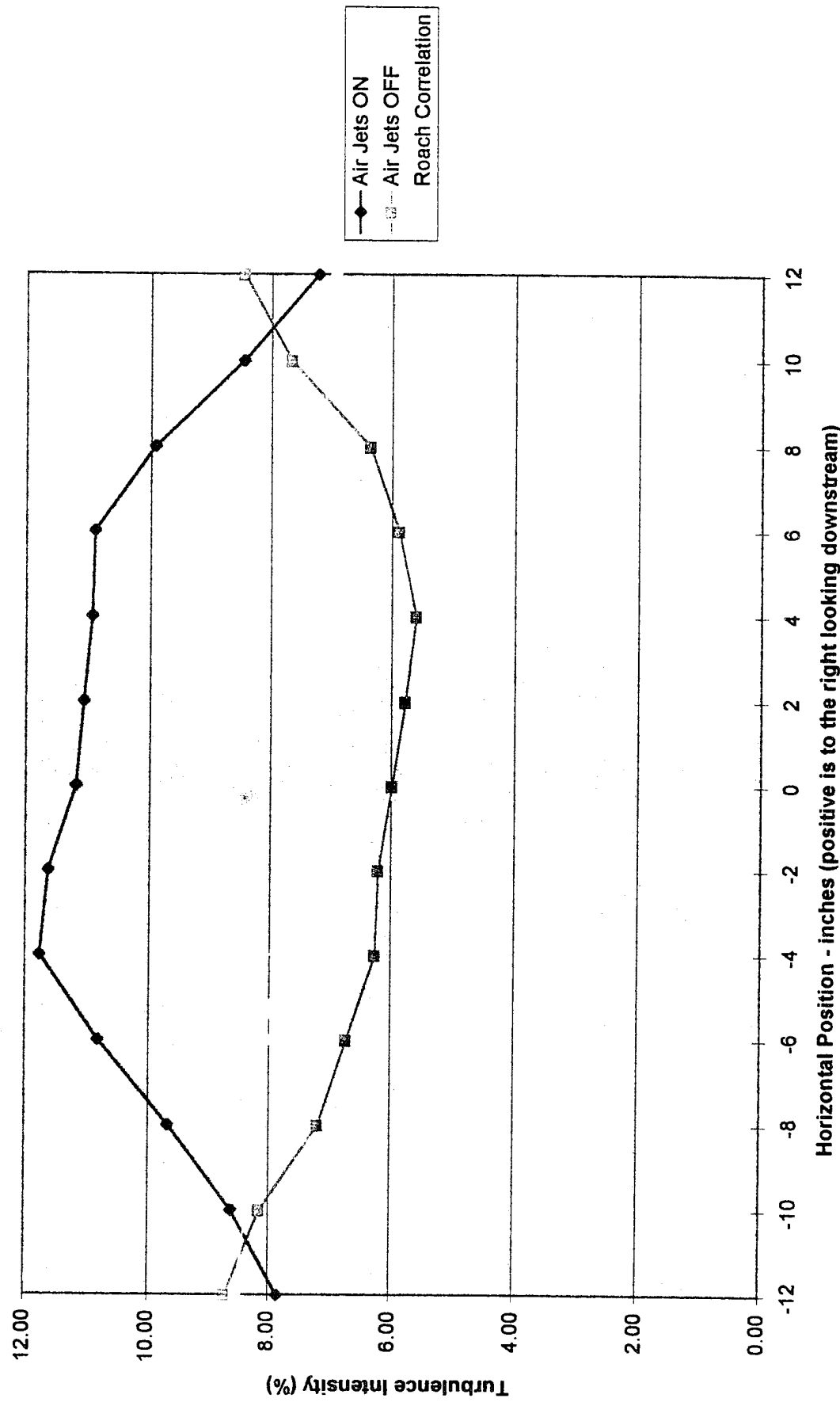
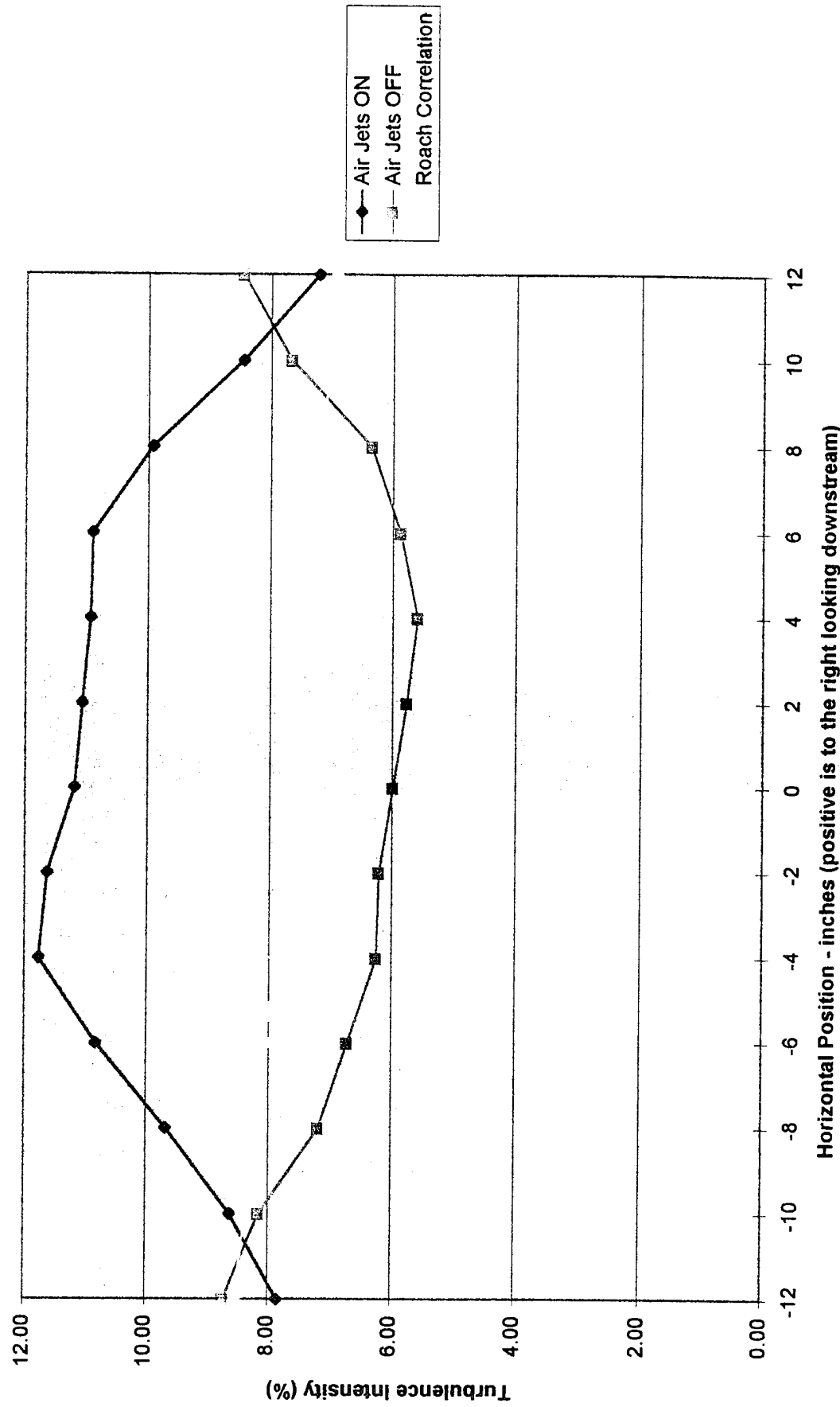


Chart5

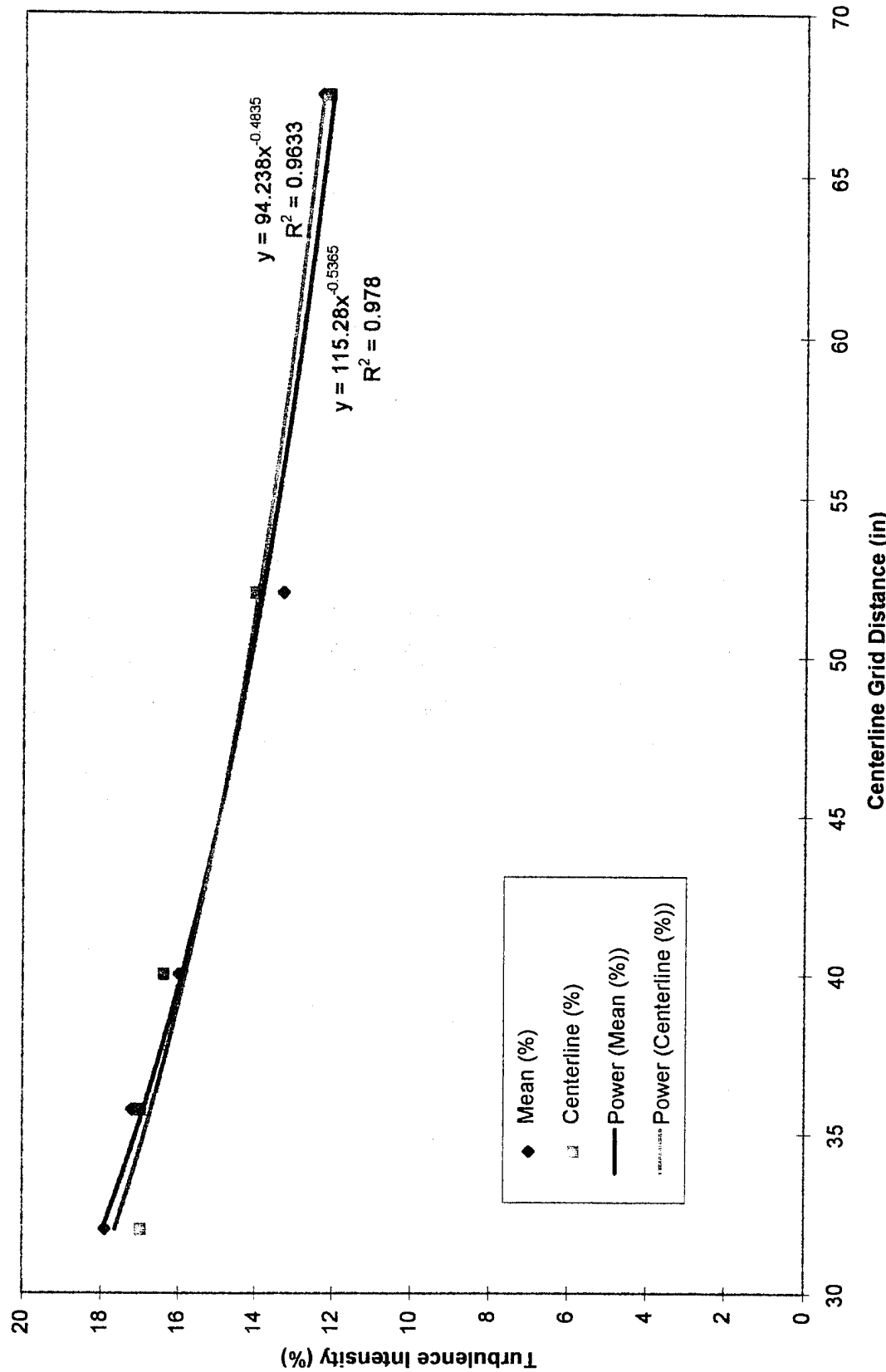
Effect of Air Jets on Turbulence Intensity - $x=67.5''$



APPENDIX G:

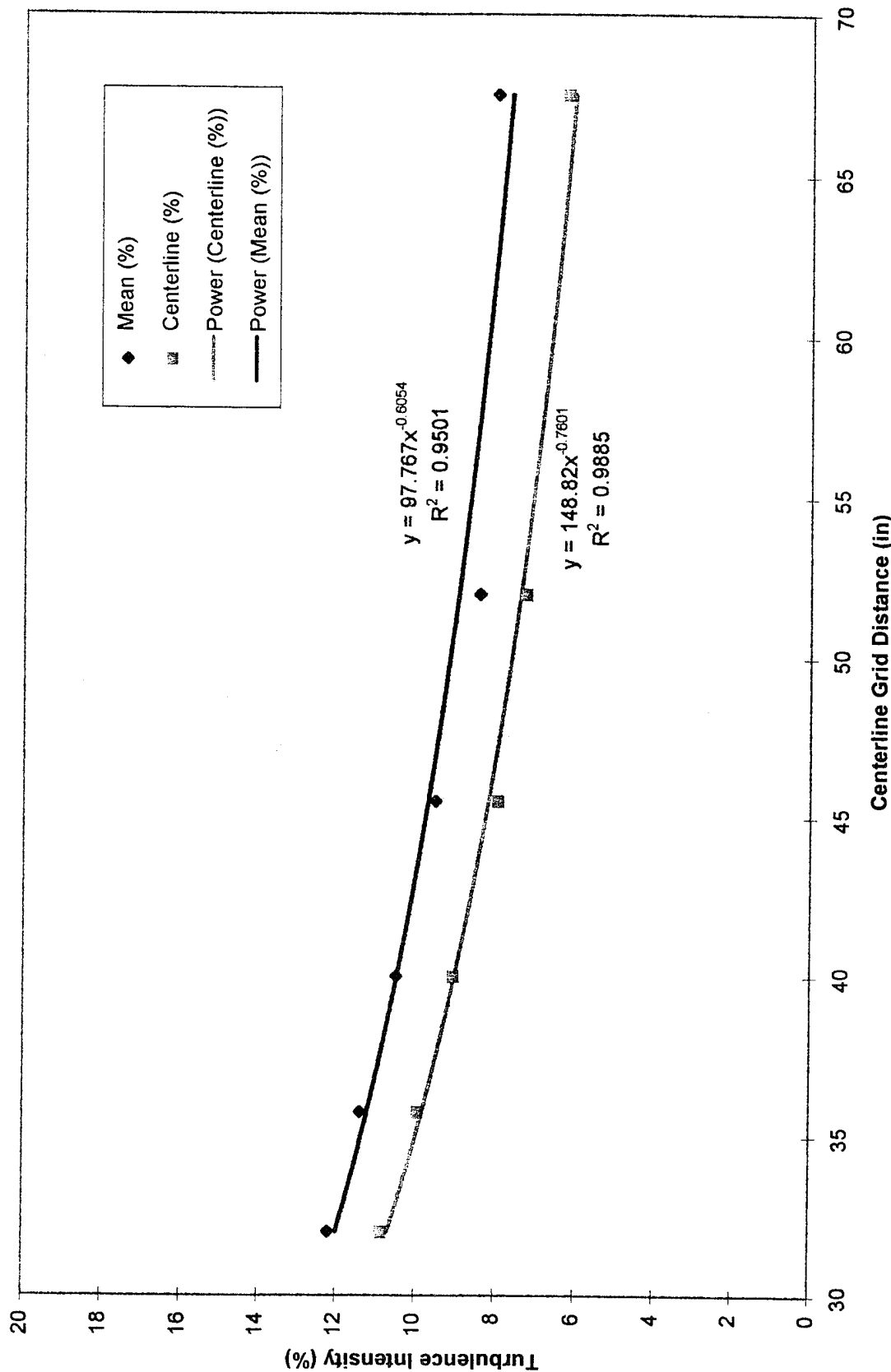
Turbulence Intensity Variation with Grid Distance
(Decay Rates)

Full Field Turbulence Intensities-Air Jets ON



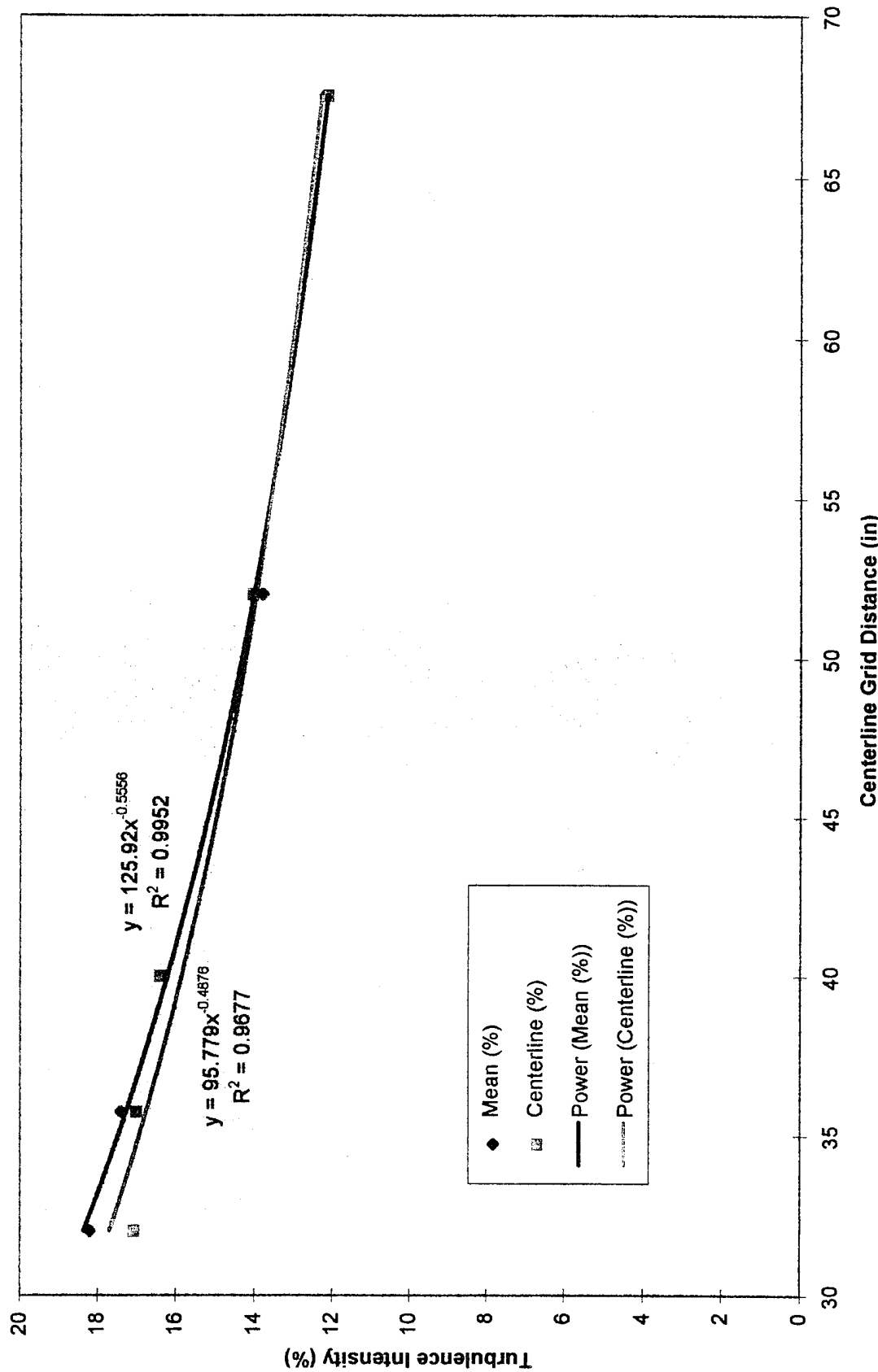
full off

Full Field Turbulence Intensities-Air Jets OFF



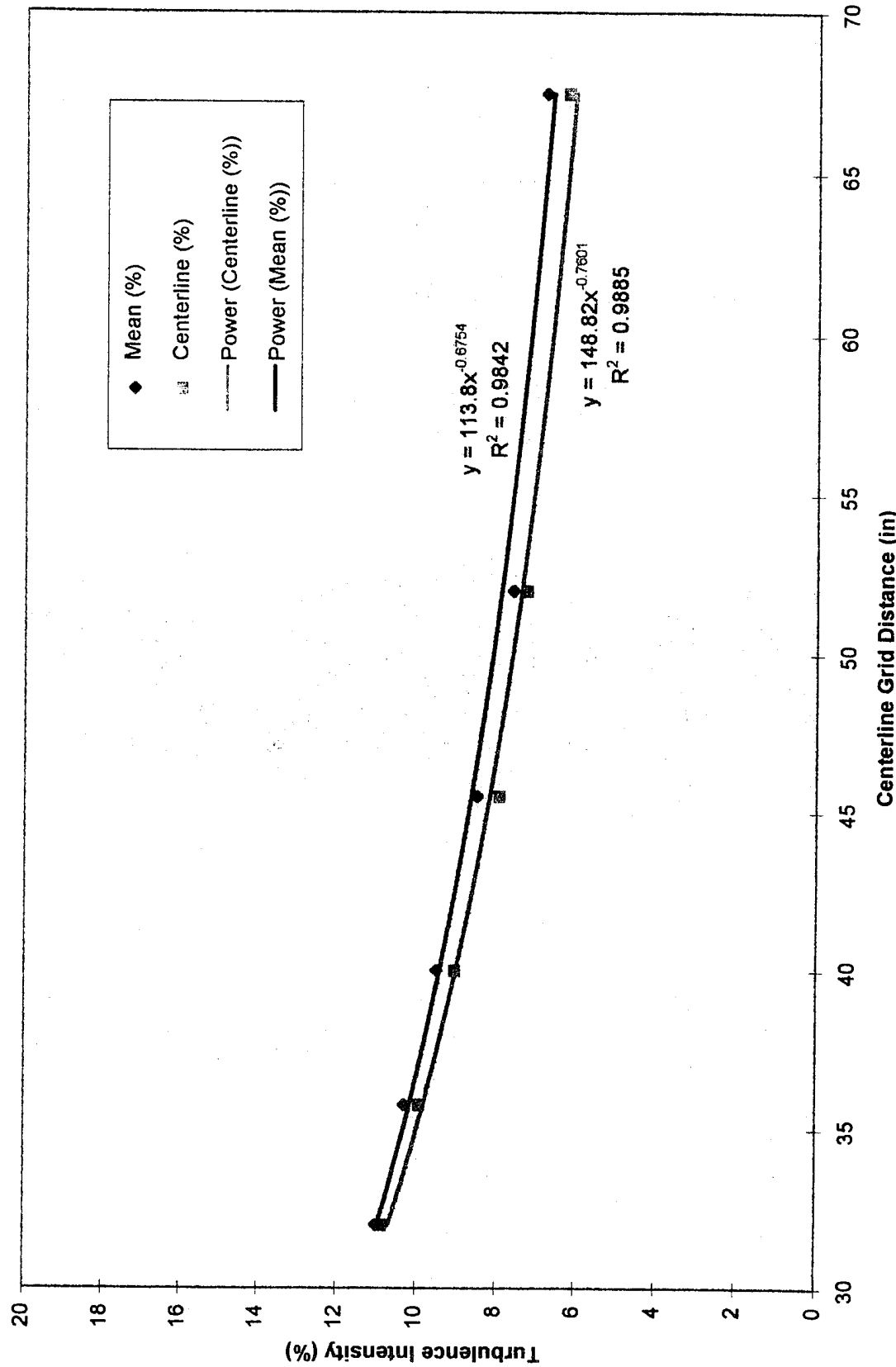
centron

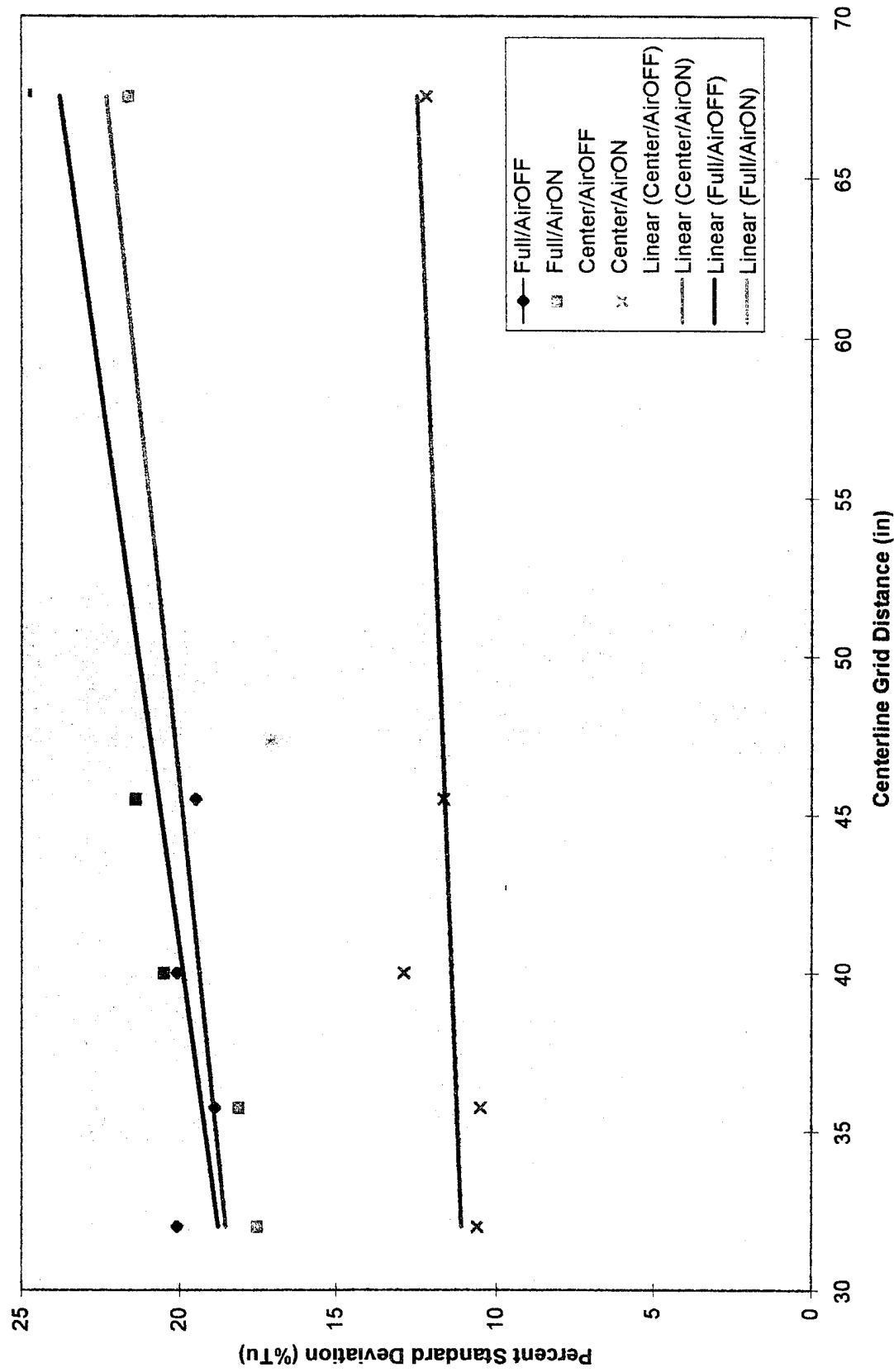
Center Area Turbulence Intensities-Air Jets ON



centroff

Center Area Turbulence Intensities-Air Jets OFF



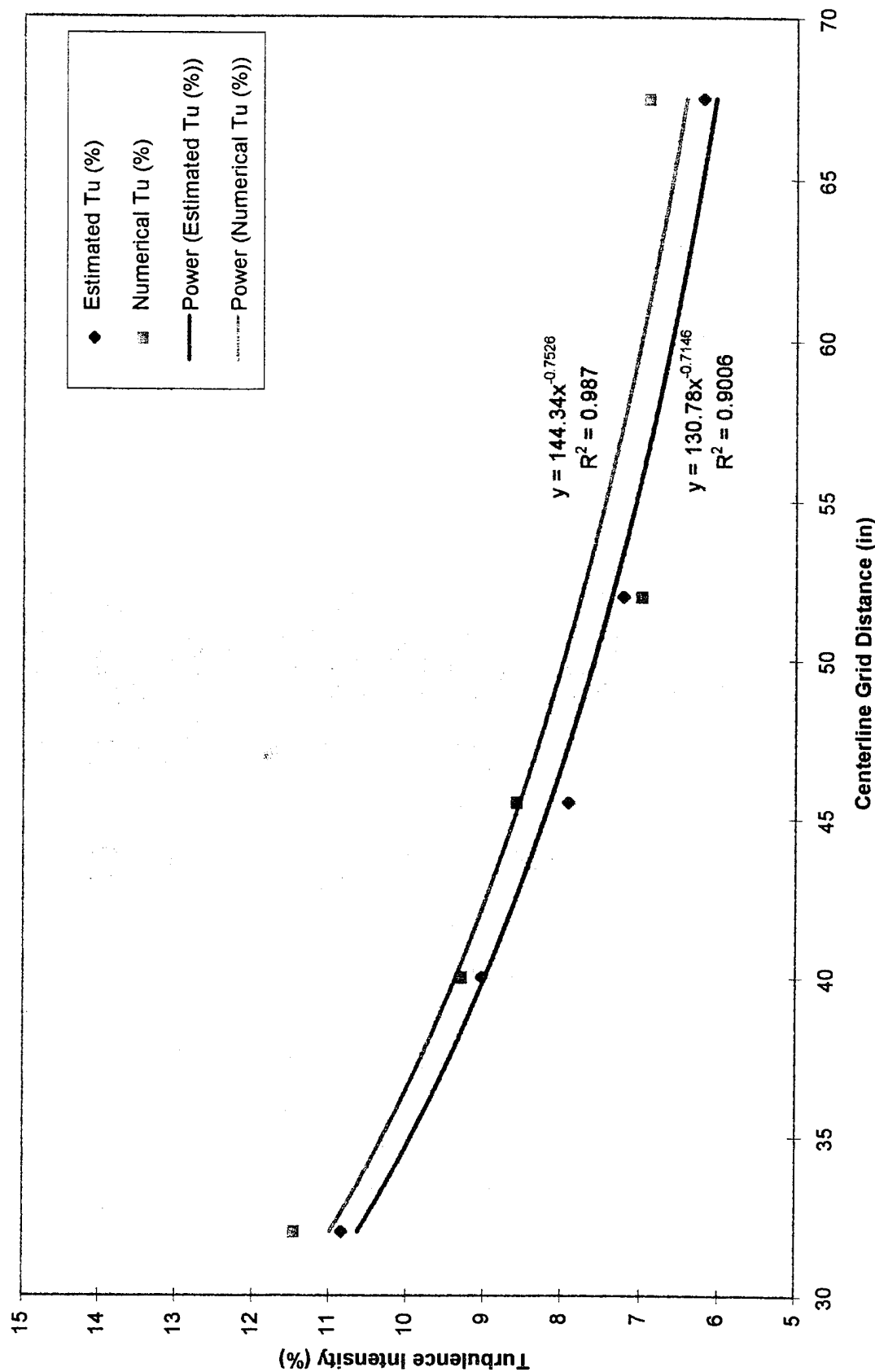
Standard Deviation in Turbulence Intensity vs Grid Distance

APPENDIX H:

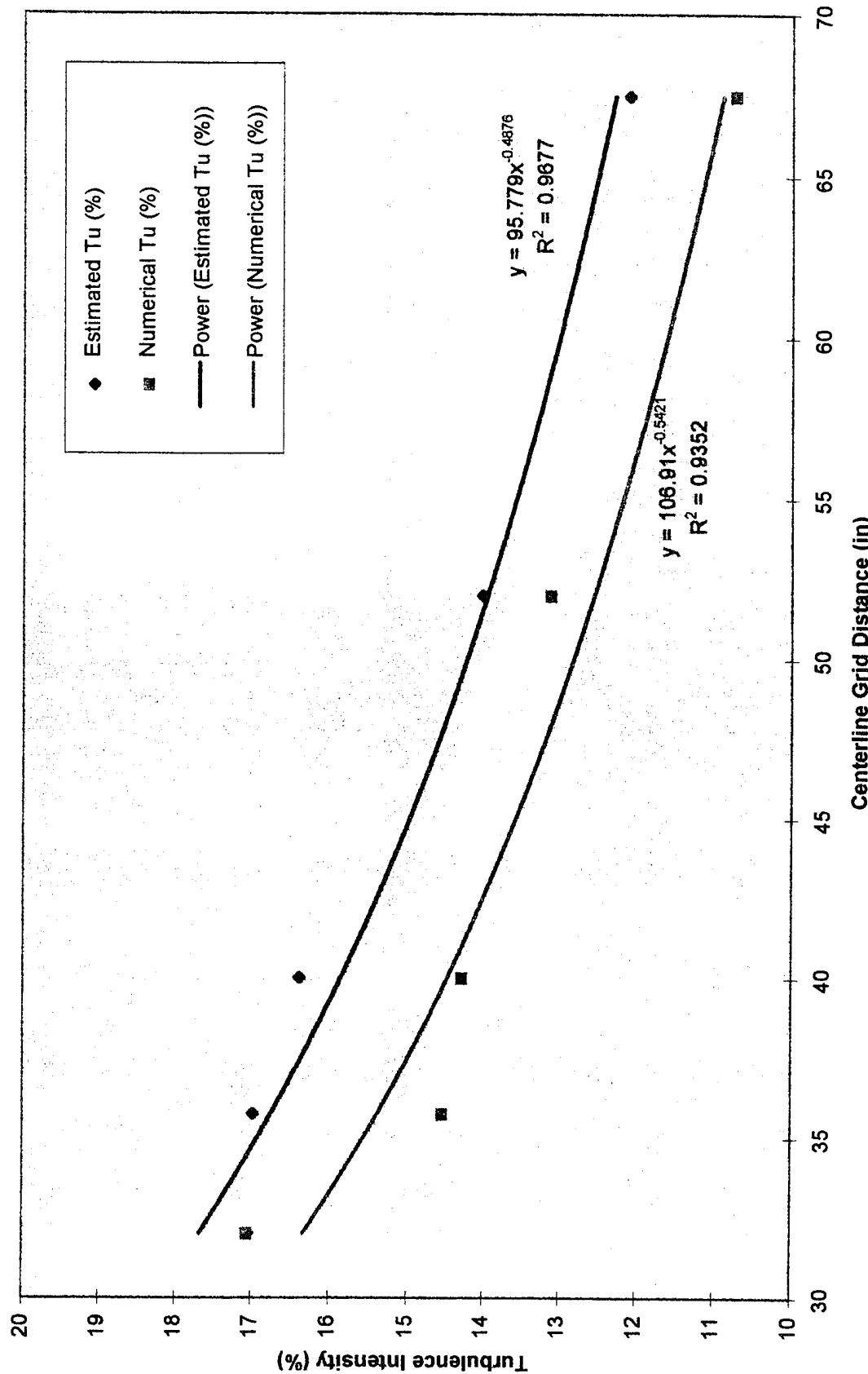
Turbulence Intensity Calculation Method Comparison

airoff

Turbulence Intensity Calculation Method Comparison - Air OFF

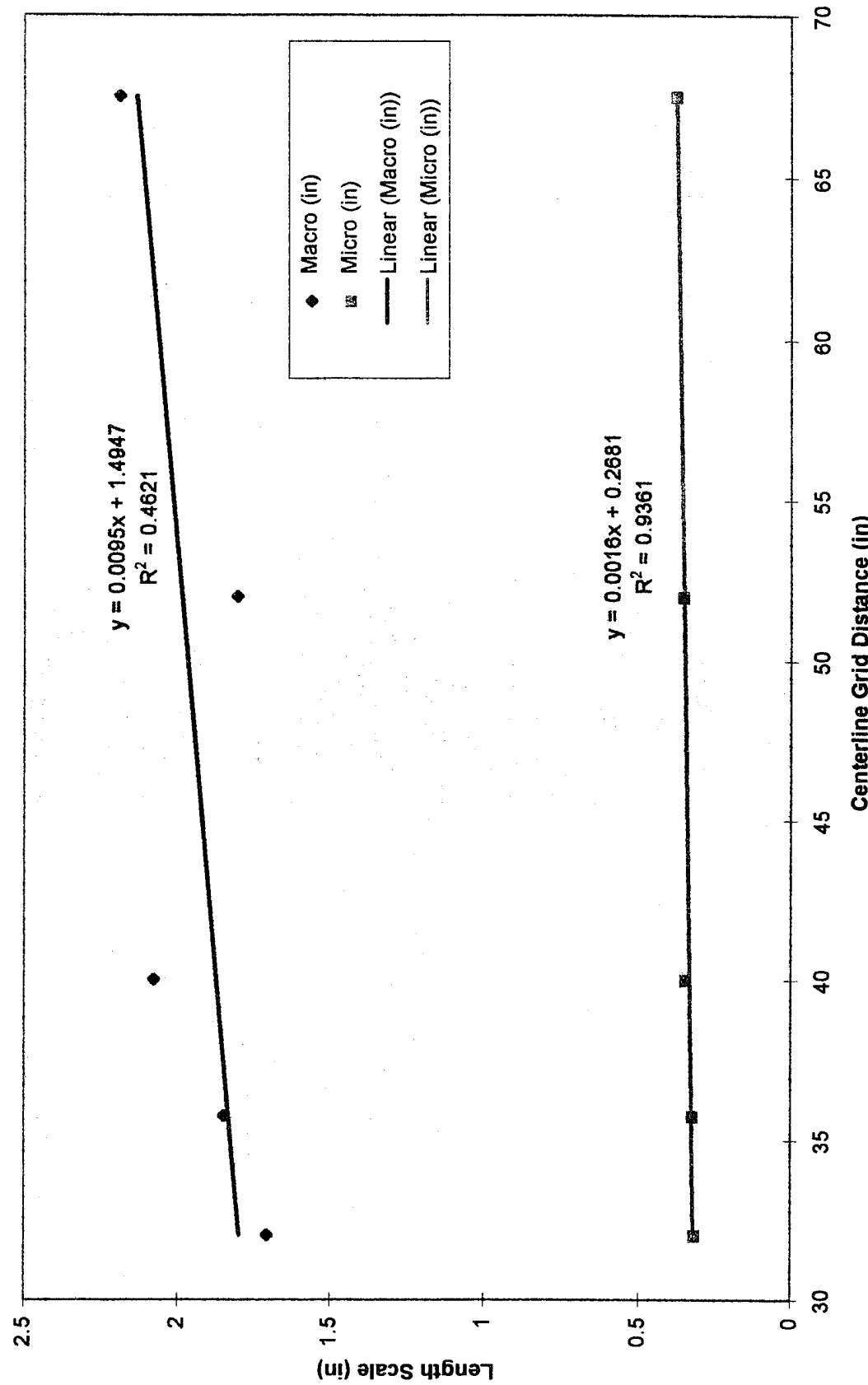


Turbulence Intensity Calculation Method Comparison - Air ON



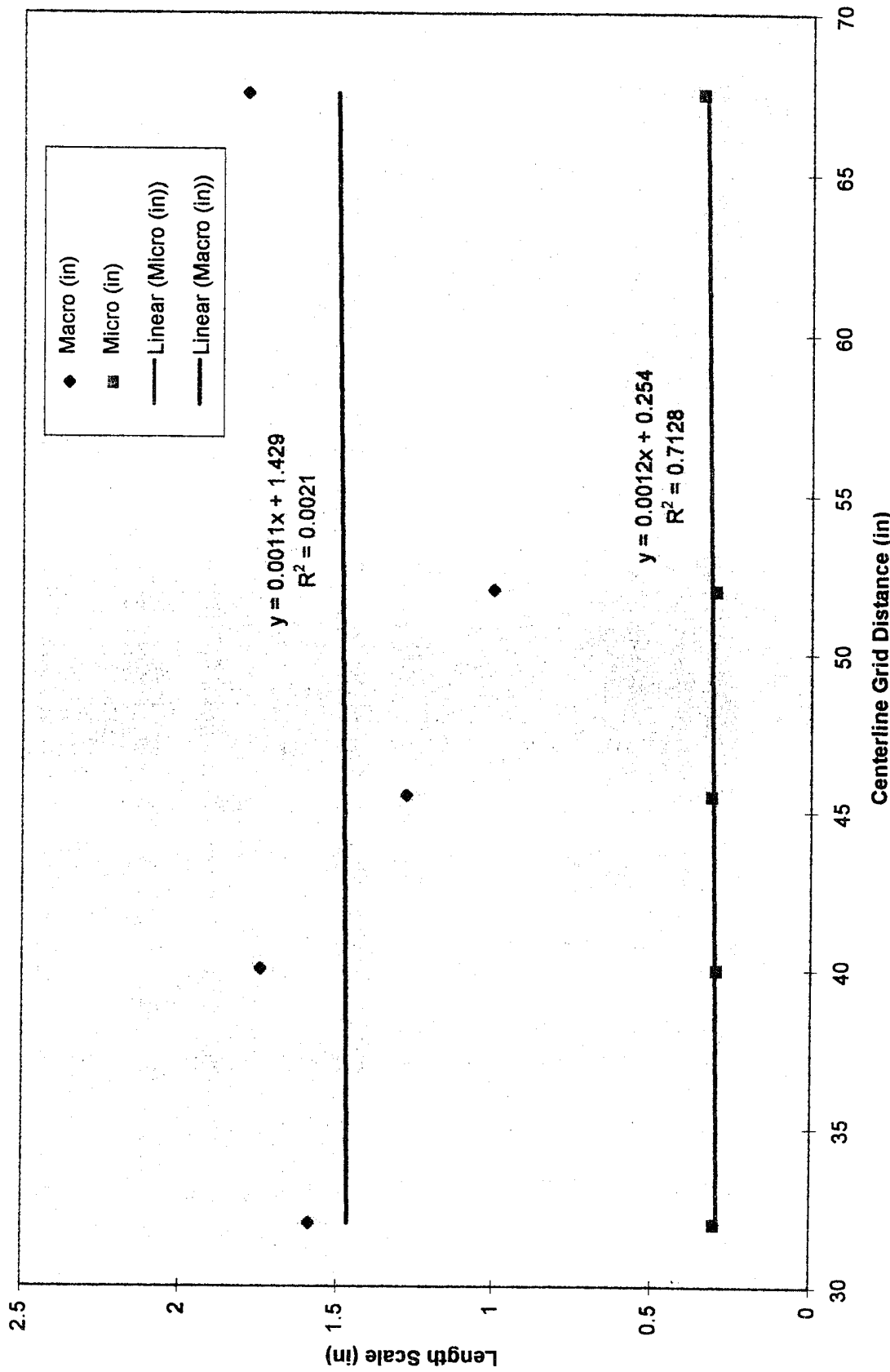
APPENDIX I:

Length Scale Variation with Distance

Length Scale Variation with Distance - Air ON

L_{soft}

Length Scale Variation with Distance - Air OFF



Instrument Identification

The serial number is located on the rear label (see Figure 8-1) on both models.

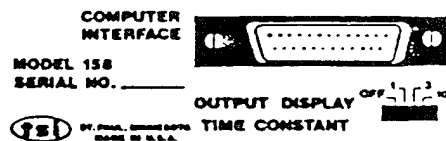


Figure 8-1.

8.3. Model 150

Amplifier:

Typical Input Voltage Noise: 1:1 Bridge Position: $1.85 \text{ nV}/\sqrt{\text{Hz}}$
Standard and Hi Pwr bridge Position:
 $2.5 \text{ nV}/\sqrt{\text{Hz}}$

Typical Equivalent Input Drift: $0.35 \mu\text{V}/^\circ\text{C}$ on 5:1 bridge
 $0.6 \mu\text{V}/^\circ\text{C}$ on 1:1 bridge

Maximum Common Mode Input Voltage: 6 volts for the 1:1 Bridge position;
10 volts for the Standard and Hi Pwr bridge positions

Output Impedance: 50 ohm (Resistance in series with output)

Output Voltage Range: 0-12 Volts
Maximum Bridge Current: 1.2 A

Amplifier Gain: $>1 \times 10^6$

8. SPECIFICATIONS

8.1. Model 158

Number of Channels: 4 (allows control of up to 16 channels)

Test Signal Specifications - Model 158:

Type of Signal:	Square wave
Frequency Range:	0.3-30 kHz
Amplitude Range:	0-4.5 volts

Display Specifications - Model 158:

Number of digits:	4½
Resolution:	1 mV
Accuracy:	±2 digits
Sample Rate:	2.5 readings per second
Time Constant accuracy:	20%
Temperature Stability:	40 ppm typical

Output Impedance - Model 158: 100 ohm

Accessories:	1.8 m (6 ft) RS232 cable
	1.8 m (6 ft) RG 58A/U output cable

APPENDIX J:

Sample Data Output and Reduction Spreadsheets

SAMPLE DATA REDUCTION - ITERATED CORRELATION

LENGTH SCALES FOR AIR JETS ON - POSITION 1

FACTOR FOR 7500 Hz
CENTERLINE HOT WIRE

Lag	Time	R	Rbar*delta t
1	0.000133	0.976	0.000127
2	0.000267	0.924	0.00012
3	0.0004	0.87	0.000113
4	0.000533	0.824	0.000108
5	0.000667	0.79	0.000104
6	0.0008	0.766	0.000101
7	0.000933	0.747	9.85E-05
8	0.001067	0.731	9.65E-05
9	0.0012	0.716	9.45E-05
10	0.001333	0.701	9.25E-05
11	0.001467	0.687	9.07E-05
12	0.0016	0.673	8.88E-05
13	0.001733	0.659	8.69E-05
14	0.001867	0.645	8.51E-05
15	0.002	0.632	8.34E-05
16	0.002133	0.619	8.17E-05
17	0.002267	0.607	8.01E-05
18	0.0024	0.595	7.87E-05
19	0.002533	0.585	7.73E-05
20	0.002667	0.575	0.000076
21	0.0028	0.565	7.46E-05
22	0.002933	0.554	7.31E-05
23	0.003067	0.542	7.13E-05
24	0.0032	0.528	6.95E-05
25	0.003333	0.515	6.78E-05
26	0.003467	0.502	6.62E-05
27	0.0036	0.491	6.49E-05
28	0.003733	0.482	6.37E-05
29	0.003867	0.473	6.25E-05
30	0.004	0.465	6.14E-05
31	0.004133	0.456	6.02E-05
32	0.004267	0.447	5.89E-05
33	0.0044	0.437	5.76E-05
34	0.004533	0.427	5.62E-05
35	0.004667	0.416	5.48E-05
36	0.0048	0.406	5.34E-05
37	0.004933	0.395	5.19E-05
38	0.005067	0.384	5.05E-05
39	0.0052	0.374	4.92E-05
40	0.005333	0.364	0.000048
41	0.005467	0.356	4.69E-05
42	0.0056	0.348	4.58E-05
43	0.005733	0.339	4.47E-05
44	0.005867	0.331	4.35E-05
45	0.006	0.322	4.23E-05
46	0.006133	0.313	4.12E-05
47	0.006267	0.305	4.03E-05
48	0.0064	0.299	3.96E-05
49	0.006533	0.295	3.93E-05

50	0.006667	0.294	3.91E-05
51	0.0068	0.293	3.89E-05
52	0.006933	0.291	3.85E-05
53	0.007067	0.287	3.81E-05
54	0.0072	0.284	3.76E-05
55	0.007333	0.28	3.71E-05
56	0.007467	0.276	3.65E-05
57	0.0076	0.272	3.59E-05
58	0.007733	0.267	3.53E-05
59	0.007867	0.262	3.45E-05
60	0.008	0.256	3.37E-05
61	0.008133	0.25	0.000033
62	0.008267	0.245	3.22E-05
63	0.0084	0.238	3.13E-05
64	0.008533	0.231	3.02E-05
65	0.008667	0.222	0.000029
66	0.0088	0.213	2.78E-05
67	0.008933	0.204	2.67E-05
68	0.009067	0.196	2.57E-05
69	0.0092	0.189	2.48E-05
70	0.009333	0.183	0.000024
71	0.009467	0.177	2.31E-05
72	0.0096	0.17	2.22E-05
73	0.009733	0.163	2.13E-05
74	0.009867	0.157	2.05E-05
75	0.01	0.151	1.98E-05
76	0.010133	0.146	1.91E-05
77	0.010267	0.141	1.85E-05
78	0.0104	0.137	1.79E-05
79	0.010533	0.132	1.72E-05
80	0.010667	0.126	1.64E-05
81	0.0108	0.12	1.56E-05
82	0.010933	0.114	1.48E-05
83	0.011067	0.108	1.42E-05
84	0.0112	0.105	1.38E-05
85	0.011333	0.102	1.35E-05
86	0.011467	0.1	1.33E-05
87	0.0116	0.099	1.31E-05
88	0.011733	0.097	1.27E-05
89	0.011867	0.094	1.24E-05
90	0.012	0.092	1.21E-05
91	0.012133	0.09	1.19E-05
92	0.012267	0.088	1.15E-05
93	0.0124	0.084	1.09E-05
94	0.012533	0.08	1.03E-05
95	0.012667	0.075	9.67E-06
96	0.0128	0.07	9.13E-06
97	0.012933	0.067	8.73E-06
98	0.013067	0.064	8.33E-06
99	0.0132	0.061	7.93E-06
100	0.013333	0.058	7.47E-06

101	0.013467	0.054	6.87E-06
102	0.0136	0.049	6.13E-06
103	0.013733	0.043	5.4E-06
104	0.013867	0.038	4.8E-06
105	0.014	0.034	4.4E-06
106	0.014133	0.032	4.2E-06
107	0.014267	0.031	4.07E-06
108	0.0144	0.03	3.87E-06
109	0.014533	0.028	3.6E-06
110	0.014667	0.026	3.2E-06
111	0.0148	0.022	2.73E-06
112	0.014933	0.019	2.27E-06
113	0.015067	0.015	1.8E-06
114	0.0152	0.012	1.47E-06
115	0.015333	0.01	1.33E-06
116	0.015467	0.01	1.33E-06
117	0.0156	0.01	1.27E-06
118	0.015733	0.009	1.07E-06
119	0.015867	0.007	7.33E-07
120	0.016	0.004	

LENGTH SCALES

macro (m)	macro (in)
0.043348	1.706624

sum = 0.00466

micro (m)	micro (in)
0.008007	0.315226

Vmean = 9.303
Std Dev = 1.586

Tu = 0.170483

101	0.013467	0.054	6.87E-06
102	0.0136	0.049	6.13E-06
103	0.013733	0.043	5.4E-06
104	0.013867	0.038	4.8E-06
105	0.014	0.034	4.4E-06
106	0.014133	0.032	4.2E-06
107	0.014267	0.031	4.07E-06
108	0.0144	0.03	3.87E-06
109	0.014533	0.028	3.6E-06
110	0.014667	0.026	3.2E-06
111	0.0148	0.022	2.73E-06
112	0.014933	0.019	2.27E-06
113	0.015067	0.015	1.8E-06
114	0.0152	0.012	1.47E-06
115	0.015333	0.01	1.33E-06
116	0.015467	0.01	1.33E-06
117	0.0156	0.01	1.27E-06
118	0.015733	0.009	1.07E-06
119	0.015867	0.007	7.33E-07
120	0.016	0.004	

LENGTH SCALES
macro (m) macro (in)
0.043348 1.706624

sum = 0.00466

micro (m) micro (in)
0.008007 0.315226

Vmean = 9.303
Std Dev = 1.586

Tu = 0.170483

References:

- Acum, W.E.A., et al. Subsonic Wind Tunnel Wall Corrections. Aerodynamics Division, National Physical Laboratory: Teddington. 1966.
- Baughn, James W., et al. "An Experimental Investigation of Heat Transfer, Transition and Separation on Turbine Blades at Low Reynolds Number and High Turbulence Intensity." (unpublished), 1995.
- Han, J.C. and Zhang, L. "Influence of Mainstream Turbulence on Heat Transfer Coefficients From a Gas Turbine Blade." Transactions of the ASME. November 1994.
- Langston, L.S., et al. "Three-dimensional Flow Within a Turbine Cascade Passage." Journal of Engineering Power. Jan 1997.
- Moffat, Robert J. and Sahm, Michael K. "Turbulent Boundary Layers with High Turbulence: Experimental Heat Transfer and Structure on Flat and Convex Walls." Stanford University. Jan 1992.
- Pope, Alan and William H. Rae, Jr. Low-Speed Wind Tunnel Testing. John Wiley & Sons: New York. 1984.
- Roach, P.E. "The Generation of Nearly Isotropic Turbulence by Means of Grids." Heat and Fluid Flow. Rolls Royce Ltd, 1986.
- Schlichting, Hermann, Dr. Boundary-Layer Theory. McGraw-Hill Publishing Company: New York. 1979.